THE VERIFICATION OF DIFFERENT MODEL CONFIGURATIONS OF THE UNIFIED ATMOSPHERIC MODEL OVER SOUTH AFRICA

by

DAWN DUDUZILE MAHLOBO

Submitted in partial fulfillment of the requirements for the degree

MASTER OF SCIENCE

in the

Faculty of Natural and Agricultural Sciences

University of Pretoria

April 2013

Declaration

I hereby declare that the dissertation that I hereby submit for the degree MSc (Meteorology) at the University of Pretoria is my own work, and that it has not been previously submitted by me for degree purposes at any other university. I also declare that all the sources I have quoted have been indicated and acknowledged by complete references.

Signature Date

The Verification of Different Model Configurations of the Unified Atmospheric Model over South Africa

Dawn Duduzile Mahlobo

Promoter: Prof. C.W.deJ. Rautenbach

Department: Department of Geography, Geoinformatics and Meteorology

Faculty: Faculty of Natural and Agricultural Sciences

University: University of Pretoria

Degree: Master of Science

Summary

In 2006 a Numerical Weather Prediction (NWP) model known as the Unified Model (UM) from the United Kingdom Meteorological Office (UK Met Office) was installed at the South African Weather Service (SAWS). Since then it has been used operationally at SAWS, replacing the Eta model that was previously used. The research documented in this dissertation was inspired by the need to verify the performance of the UM in simulating and predicting weather over South Africa. To achieve this aim, three model configurations of the UM were compared against each other and against observations. Verification of rainfall as well as minimum and maximum temperature for the year 2008 was therefore done to achieve this. 2008 is the first year since installation, where all the configurations of the UM used in the study are present. For rainfall verification the model was subjectively verified using the eyeball verification for the entire domain of South Africa, followed by objective verification of categorical forecasts for rainfall regions grouped according to standardized monthly rainfall totals obtained by cluster analysis and finally objective verification using continuous variables for selected stations over South Africa. Minimum and maximum temperatures were subjectively verified using the eyeball verification for the entire domain of South Africa, followed by objective verification of continuous variables for selected stations over South Africa, grouped according to different heights above mean sea level (AMSL). Both the subjective and objective verification of the three model configurations of the UM (for both rainfall as well as the minimum and maximum temperatures) suggests that 12km UM simulation with DA gives better and reliable results than the 12km and 15km UM simulations without DA. It was further shown that although there was no significant difference between the model outputs from the 12km and the 15km UM without DA, the 15km UM simulation without DA, proved to me more reliable and accurate than the 12km UM simulation without DA in simulating minimum and maximum temperatures over South Africa, on the other hand the 12km UM simulation without DA is more reliable and accurate than the 15km UM simulation without DA in simulating rainfall over South Africa.

ACKNOWLEDGEMENTS

The author wishes to express her appreciation to the following persons and institutions who have contributed immensely towards the success of this research work.

- The South African Weather Service for allowing me the opportunity and resources to do this research.

- Prof. C.J. deW. Rautenbach for his advice and mentorship during the course of this study.

- My husband Khumbuza for his never ending love, encouragement, understanding and support during the course of this work.

- My children Nolizwi, Makabongwe and Zethembiso for the compromise they had to take during the course of the study.

- My mother Esther and my late father Robert, for their support.

- Thembi Meni, Bawinile Mgedesi, Lindiwe Albrektsen, Bhekinkosi Hlatshwayo and Zodwa Dlamini for their belief in me.

- Dr Winifred Jordaan and Ms Elsa de Jager for their guidance and support.

- Ms Maryjane Bopape, for her encouragement and assistance especially to modeling issues.

- My utmost gratitude goes to the almighty God, my Helper, Teacher, Councilor and Advocate. This would not have been possible without Him.

"It is not by my own mind, nor by my own power but by his Spirit"

Zechariah 4:6

TABLE OF CONTENTS

LIST OF ABBREVIATIONS

ACC	Anomaly Correlation Coefficient
AMSL	Above Mean Sea Level
AOH	Atlantic Ocean High
AWS	Automatic Weather Station
CAPE	Convective Available Potential Energy
CRM	Cloud Resolving Model
DA	Data Assimilation
DAFF	Department of Agriculture, Forestry and Fisheries
ECMWF	European Center for Medium Range Weather Forecasts
FAR	False Alarm Rate
GCM	Global Circulation Model
GDP	Gross Domestic Product
IOH	Indian Ocean High
ITCZ	Inter-Tropical Convergence Zone
LAM	Limited Area Model
LB	Lateral Boundary
LBC	Lateral Boundary Conditions
MAE	Mean Absolute Error
ME	Mean Error
MRF	Medium Range Forecast
NC	Now Casts
NCEP	National Centers for Environmental Prediction
NEC	Nippon Electronic Company
NEC SX-8	Super Computer with a UNIX-like operating system developed by NEC

NH	Northern Hemisphere
NWP	Numerical Weather Prediction
OI	Optimum Interpolation
PC	Percent Correct
QPF	Quantitative Precipitation Forecasts
RMSE	Root Mean Square Error
SAST	South African Standard Time
SAWS	South African Weather Service
SRF	Short Range Forecast
TC	Tropical Cyclone
TTT	Tropical Temperate Troughs
UK Met Office	United Kingdom Meteorological Office
UM	Unified Model
VSRF	Very Short Range Forecast
WMO	World Meteorological Organization
3D VAR	Three Dimensional Variational
4D VAR	Four Dimensional Variational

LIST OF FIGURES

LIST OF TABLES

CHAPTER 1

BACKGROUND

1.1 INTRODUCTION

It is known that weather conditions influence human behaviour and even the choices people make. Various decision makers make use of weather information to make better decisions for their day to day commitments, for example travellers, transport service operators, infrastructure owners, church attendance, and even stock market returns, are all affected to a varying extent by weather conditions. Weather can also affect many sectors directly or indirectly (e.g. agriculture, insurance, tourism, transport and health). However, the greatest impact of weather conditions is on the livelihood of the poorest and most vulnerable communities. The South African Weather Service (SAWS), in particular, has an integral role to play in assisting the South African government in minimising the impact of weather related natural disasters in South Africa (SAWS, 2006).

Weather plays an integral role in the economy of any country (Zavala, 2009). According to Nurmi et al. (2012) it implies changes in the production cost or revenues, and in some cases causing loss of capital due to physical damage of infrastructure, agriculture etc. The better preparedness resulting from weather information (e.g. forecasts) received and better informed decisions attenuate extreme weather induced cost and price effects, which is in principle a common benefit to all market parties (Nurmi et al., 2012). Weather forecasts also affect production and consumption activities in society (Nurmi et al., 2012).

Weather plays an important role in agricultural production. As a matter of fact there is no aspect of agriculture that is not affected by weather (Coiffier, 2004). Cultivated areas cover 82% of South Africa, and the agriculture industry employs 16.5% of South Africa's economically active population (Schulze, 1997). Agriculture therefore plays a major role in the economy of South Africa (Harrison, 1984) and contributes 44% of the Gross Domestic Product (GDP) (Schulze, 1997); the percentage rises to about 13% of the GDP after processing and adding value have been considered. Rainfall forecasting is therefore important for agricultural production and water resource management, and consequently the GDP of the country (Harrison, 1984; Matarira and Jury, 1992; Jury, 2002). It is important to note that the Department of Agriculture, Forestry and Fisheries (DAFF) uses the rainfall variable as an indicator to declare drought in the agriculture in South Africa.

There have been numerous weather related incidents in South Africa that have claimed a lot of lives and caused damage to agriculture, infrastructure and therefore have affected the economy of the country. Figures 1.1 and 1.2 indicate the number of heavy rain and flood events, respectively, that caused havoc and destroyed lives and property in South Africa. The definition of heavy rainfall varies for different places. It can refer to rainfall from a station or an average rainfall for an area. Harnack et al. (1999) defined heavy rainfall as rainfall of more than 51mm on one to two days over an area of 10000km^2, whereas, the definition of Teixeira and Satyamurty (2007), is rainfall of more than 50mm in a 24-hour period over an area of 10000km^2. Chen et al. (2007) defined heavy rainfall as rainfall of more than 50mm in 24 hours at one or more stations. Heavy rainfall may also last for days. Floods damage may result when rainfall occurs over long periods or is of short duration and is accompanied by hail and strong winds (Teixeira and Satyamurty, 2007).

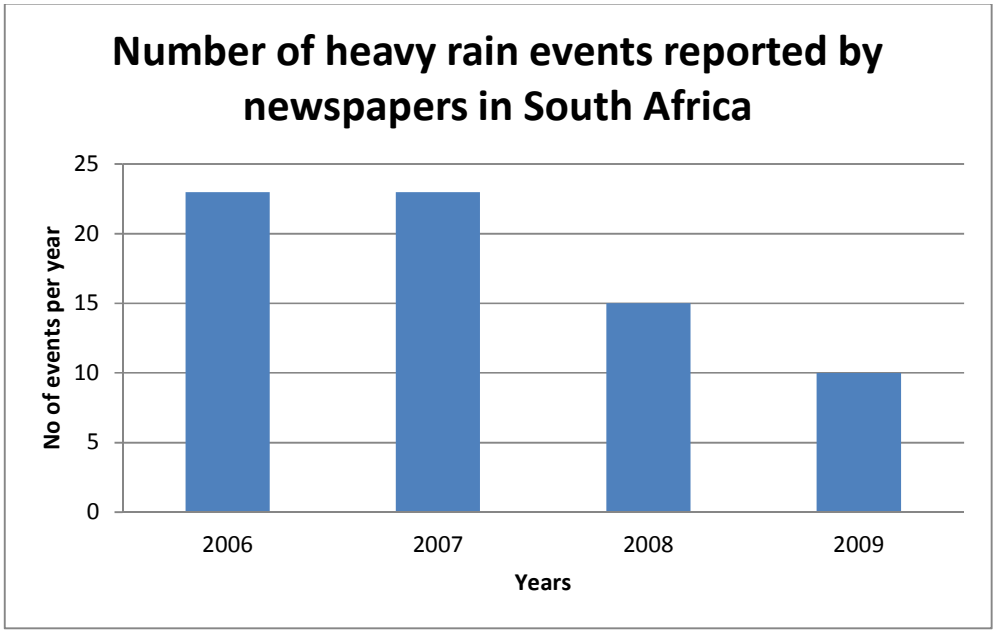

Figure 1.1:

The number of heavy rain events reported by newspapers for the period 2006-2009.

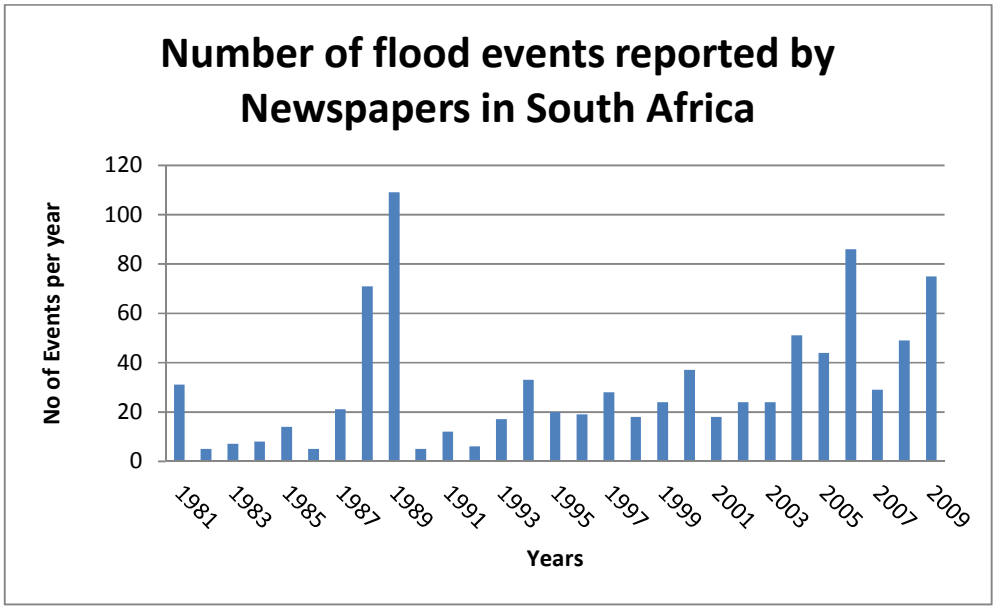

Figure 1.2:
The number of flood events reported by newspapers for the period 1981-2009.

Recent notable weather related events that affected the economy of South Africa tremendously are: (1) R22.5 million damages that was reported in Klerksdorp on 13 November 2006 (Sapa, 2006), (2) R20 million on 21-22 December 1999 in Tulbagh, (3) damages in Ashton estimated to be R12 million on 25 March 2003 (Thiel and Gosling, 2003; von Lieres, 2003). Events that have caused damage to infrastructure leaving people homeless include:(1) 3500 people that were left homeless due to floods that occurred on 3 to 9 July 2001 in Cape Town (Strydom and Arendse, 2001), (2) more than 122 families were left homeless when 68 shacks were destroyed in Durban due to floods that occurred on the 27 November 2003 (Sapa, 2003), (3) houses of 300 families were washed away in Giyani on 24 February 2004 (Louw, 2004), (4) on the 16 December 2004 floods caused extensive damage to property in Heidelberg, Kynsna, Laangeberg, Port Elizabeth, Riverdale, Robertson and Swellendam (Richter and Taljaard, 2004). When these extreme weather conditions occur, warnings need to be issued so that preventive measures could be taken against possible damage and loss of lives. Forecasting technologies and skill should then also be improved continuously in order for early warnings to be improved and issued regularly. Such early warnings could save lives.

1.2 NUMERICAL WEATHER PREDICTION

Numerical Weather Prediction (NWP) is defined as the process of producing a weather forecast with the aid of a set of equations (Holton, 2012) that describe the evolution in time of variables that define the state of the atmosphere (Schulze, 2007). NWP models are computer programmes that solve these equations and may give insight about the dynamical and physical processes behind many atmospheric phenomena. Sound understanding of the abilities and limitations of the model is suggested to everyone who makes use of a NWP model (Stenrud, 2007).

The first NWP models used were simplified versions of the complete set of equations of motion and were applied over relatively small portions of the globe (Stenrud, 2007). For example, a one day weather forecast was produced using a one layer barotrophic model in 1949 (Charney et al., 1950). Since then NWP models have been improved resulting in multi-layer primitive equations models with a capacity to even predict cyclone development (Stenrud, 2007). Weather forecasters make use of NWP models for guidance, but these models first need to be evaluated against observational data in order to verify if the initialization process of a NWP is correct and to determine the skill of such a forecast model.

NWP models may be classified according to the size of their resolution which affects the details and accuracy of the state of the atmosphere. For example, the finer the resolution, the more details are captured in the model simulations and the more accurately it can take into account the topography and other lower boundary conditions of the concerned area (Roeber et al., 2004). Models for NWP include (1) General Circulation Models (GCMs), (2) Meso-scale models and (3) Cloud Resolving Models (CRMs).

GCMs are a primary tool used in representing the processes governing the global climate systems (AMS, 2001; Kendon et al., 2010). Most GCMs have a resolution of about a few hundreds of kilometers (McGregor et al., 1993; Robertson et al., 2004; Kendon et al., 2010). GCMs are capable of running in higher resolutions, but computer power is to be drastically increased for this to be achieved (Ji and Verneker, 1996; McGregor et al., 1993; Giorgi and Mearns, 1991; Ploshay and Lau, 2010). It was found that most GCMs are performing well in simulating the main characteristics of the global general circulation over South Africa e.g. (Joubert et al., 1999). Since severe weather in South Africa is often associated with localized

meso-scale features (Tyson and Preston-Whyte, 2000) ; GCMs are not always regarded as the best tool to simulate these features due to computational requirements (McGregor et al., 1993). However, GCMs could provide valuable lateral boundary values to models that are designed to address meso-scale processes.

Meso-scale models were developed with the principle objective to forecast meso-scale weather events (Brooks et al., 1992). These models have the potential to capture meso-scale features since they have finer resolutions and better parameterization of cloud related processes than GCMs, but also coarser resolution than CRMs (Su et al., 1999) and might lead to more accurate forecasts of weather (Colle et al., 2003; Molinari and Dudek, 1992). Meso-scale models have resolutions which are selected to be computationally viable for operational forecasting (Done, 2002). Design field experiments with the aid of meso-scale models, for example, showed that the structure of lake effects storms is strongly influenced by horizontal symmetries, and that the location and intensity of convective cloud activity and subsequent precipitation are controlled by meso-scale disturbance (Cotton and Pielke, 1976). A three dimensional meso-scale model was developed by Pielke (1976) to demonstrate the paternity of showers over a region as a function of sea breeze convergence zones. Studies that resulted from this model showed that meso-scale models could predict the local circulation and convergence patterns over the area of study. The circulation and convergence patterns particularly indicate that topographic influences may result in a significant impact on the climatology of precipitation (Cotton and Pielke, 1976; Snook and Pielke, 1995).

CRMs, which address even more localized circulation and physical processes, provide another avenue to study the interaction of convection with its large scale environment to produce precipitation, latent heat, eddy fluxes of heat, moisture and momentum (Su et al., 1999). These models could simulate deep convection very well, and hence a more realistic cloud-scale structure with higher precipitation maxima could be achieved (Mass et al., 2002; Moeng et al., 2010). The use of CRMs is, however, limited by computational requirements because of its fine grid (Su et al., 1999; Done, 2002; Wu et al., 2007; Moeng et al., 2010).

1.3 WEATHER FORECASTING AT THE SAWS

According to its mandate the SAWS is responsible for producing national weather forecasts to the South African public. End users of weather forecasts in South Africa include the

general public, media, marine, agriculture, aviation, event planners and others. Weather forecasts could either be short-term or long-range (SAWS, 2011). Long-range forecasts are classified as extended range forecasts which are two weeks ahead in time and seasonal predictions which are three months and more ahead in time (Das et al., 2010). Seasonal predictions are often compiled with the aid of statistical and dynamical prediction models and are used to aid farmers with crop estimation and the prediction of possible future droughts (Das et al., 2010).

Short-term forecasts include Now Casts (NCs), Very Short Range Forecasts (VSRFs), Short Range Forecasts (SRFs) and Medium Range Forecasts (MRFs). The time span is zero to two hours for NCs, beyond two to twelve hours in advance for VSRFs, beyond twelve to 72 hours for SRFs, and beyond three to seven days in advance for MRFs. Forecast confidence normally increases with decreasing lead time, e.g. from five days in advance towards initialisation (Das et al., 2010; SAWS, 2011). Remote sensing (weather satellites and weather radar) is used to aid forecasters in issuing forecasts. NCs and VSRFs are founded on analysis and extrapolation of trajectories that refer to a relatively wide set of products (e.g. radar maps, meteorological satellite images, NWP models, local and regional observations etc.) (Das et al., 2010). In SRFs and MRFs, the evolution of atmospheric variables is obtained from a NWP approach.

The skill of NWP models has improved so much over time that some centres have implemented automating routine forecasts which enable forecasters to focus on high-impact weather or areas where their forecasts may add significant value (Coiffier, 2004; Schulze, 2007). This might also lead to further improvements in forecast accuracy, since forecasters are in a position to give feedback to model developers on the prognostic performance of NWP models. The accuracy of mean sea-level pressure forecasts, for three (D+3), four (D+4) and five days (D+5) in advance, of the European Centre for Medium-Range Weather Forecasts (ECMWF) NWP model for the Southern Hemisphere has significantly increased since 1990 to 2003 (figure 1.3). Figure 1.3 further compares the (D+3) and the three day forecast for the Northern Hemisphere (D +3NH), and it is clear that the Northern Hemisphere three day forecasts are still more skilful that their corresponding Southern Hemisphere forecasts. The limited availability for skilful forecasts over longer periods in the Southern Hemisphere is due to the scarcity of surface and upper air observations over the large areas of the ocean (Schulze, 2007).

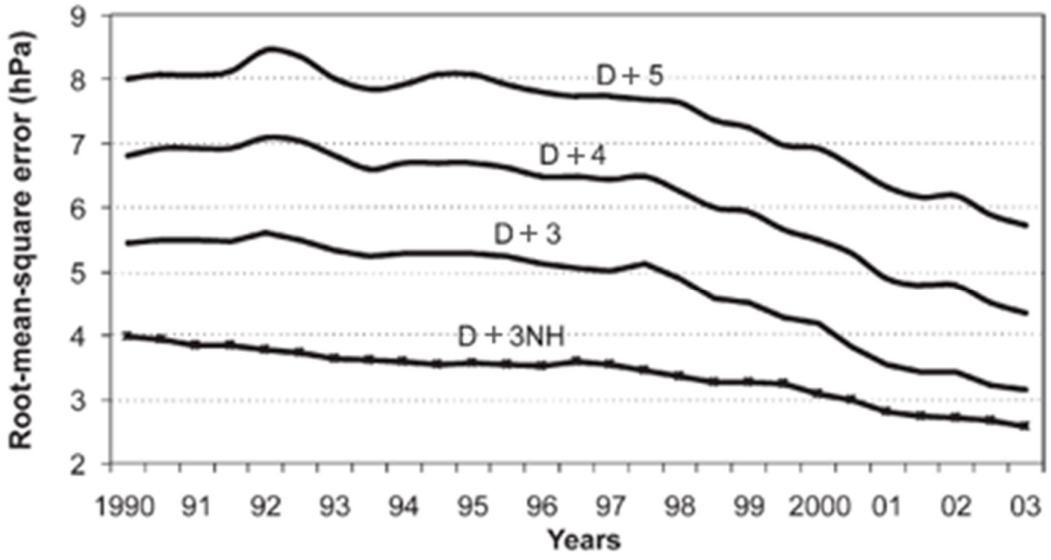

Figure 1.3:

The improvement of mean sea-level pressure predictions since 1990 to 2003, for three, four and five days in advance, of the ECMWF model for the Southern Hemisphere (Schulze, 2007).

1.4 MOTIVATION FOR THE RESEARCH

Weather forecasting is regarded as very important for South Africa. Meteorological organizations make use of NWP models to assist forecasters in coming up with accurate, relevant and reliable forecasts, thus ensuring the safety and well-being of life and property. However, De Coning (1997) showed that there is still a need for the improvement of forecasting tools in South Africa and that NWP models are of great assistance as contributing in forecasting the weather. Dyson and van Heerden (2002) used an NWP tool called Model for the Identification of Tropical Weather Systems (MITS) to aid forecasters in identifying tropical systems and Riphagen et al. (2002) did improvements in the then operational NWP model, namely Eta (Mesinger et al.,1988; Janjic,1994), used in SAWS.

In 2006 a NWP model known as the Unified Model (UM) from the United Kingdom Meteorological Office (UK Met Office) was installed at the SAWS. Since then it has been used operationally at SAWS, replacing the Eta model that was previously used. The verification of the UM is imperative for SAWS and essential for the model's continuous

improvement. It serves to identify systematic errors and forecasting uncertainties (e.g. which parameters are difficult to forecast in which regions).

The research in this dissertation was inspired by the need to verify the UM. In future, the UM implemented at SAWS will also be used to supply initial and boundary conditions to other models used in southern Africa. The verification results and conclusions found in this study will therefore contribute to a better understanding of the performance of the UM, not only in South Africa, but also to southern Africa.

1.5 THE OBJECTIVES OF THE RESEARCH

The aim of this research is to verify the performance of the UM in simulating and forecasting weather over South Africa. This will be achieved by addressing the following objectives:

OBJECTIVE 1

To compare three model configurations of the UM

For this study three configurations of the UM were selected. These configurations are (1) data assimilation at a 12km resolution, (2) no data assimilation at a 12km resolution and lastly (3) no data assimilation at a 15km resolution. The question to be addressed is: will the different configurations of the UM give different model outputs? In other words is the UM sensitive to domain size, change in horizontal resolution and the data ingest through data assimilation?

OBJECTIVE 2

To verify model outputs from the three model configurations against observations

The performance of an NWP model is measured by its ability to resolve features at the limit of its grid. NWP models need to be continuously improved in order to resolve atmospheric features as accurate as possible. An increase of the amount of input data by data assimilation, a change of the domain or the resolution of the model may improve the performance of a model**.** The model output from the three configurations of the UM will be verified against observations. The questions to be addressed are: does the skill and accuracy of the model improve by configuring the model differently? and which of the model configurations has more skill in reproducing reality?

1.6 ORGANIZATION OF THE REPORT

CHAPTER 2 is sub-divided into two sections. The first section gives an overview of the climate of South Africa and discusses various system that affect the climate of south, and the second section gives an insight into the meso-scale modeling of the South African climate.

CHAPTER 3 gives a detailed description of the UM. The UM, observational data as well as verification scores used in this study are also described.

In CHAPTER 4 results for subjective and objective rainfall verification of the UM are discussed.

The subjective and objective verification results of the UM in predicting minimum and maximum temperatures over the whole of South Africa are described in CHAPTER 5.

The summary of the study as well as concluding remarks are outlined in CHAPTER 6.

CHAPTER 2

CLIMATE AND MESO-SCALE MODELLING OF CLIMATE OVER SOUTH AFRICA

2.1 INTRODUCTION

This chapter is divided into two sections. The first section gives an overview of the climate of South Africa and discusses various system that affect the climate of south, and the second section gives an insight into the meso-scale modeling of the South African climate.

2.2 THE CLIMATE OF SOUTH AFRICA

2.2.1 GEOGRAPHICAL LOCATION AND TOPOGRAPHY OF SOUTH AFRICA

South Africa is located on the southern domain of southern Africa with its northern boundary at approximately 22^0S and the southern most point at approximately 35^0S. Namibia, Botswana and Zimbabwe form the northern borders of South Africa and Mozambique and Swaziland form the borders to the east, while Lesotho is an enclave surrounded by the South African territory (Schulze, 1965) as depicted by figure 2.1.

The topography of South Africa also indicated in figure 2.1, plays a major role in its climate and weather. The topography could be described as a high plateau centered at about 1000m above mean sea level (AMSL) increasing to heights of 1500m AMSL along the great escarpment in the east. The plateau reaches over 3000m AMSL in Lesotho. The escarpment is found at about 200-300km from the east and south coast line and consists of mountain ranges that encircle the central basin. The lowest area of the central basin is found in the north-eastern Botswana. From the escarpment to the eastern and southern coastline there is a descent of land in a series of abrupt grades (Schulze, 1965). Towards the west the escarpment is not prominent, however, higher-lying mountainous areas are found in Namakwaland and Richtersveld (Kruger, 2004).

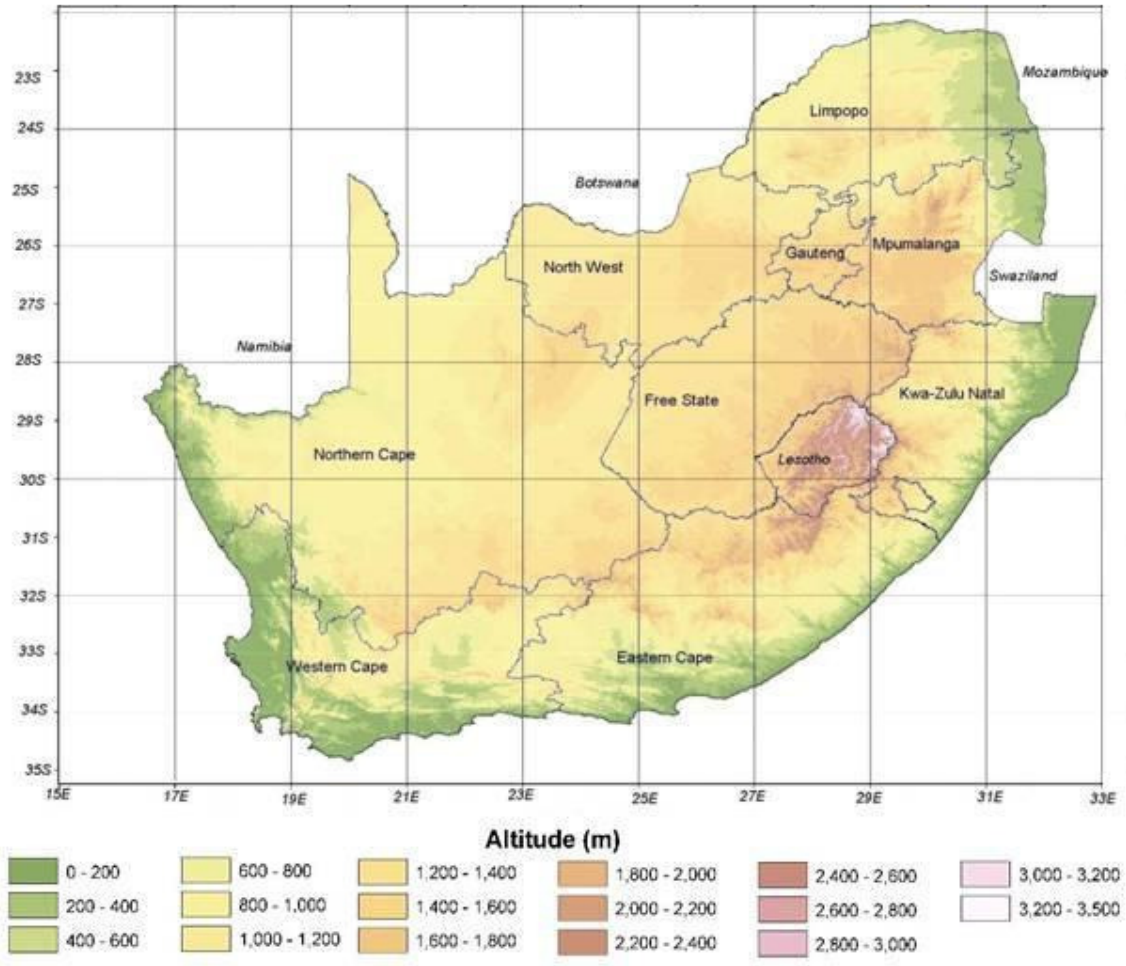

Figure 2.1:

The Provinces and topography of South Africa altitude in meters above mean sea level (SAWS).

2.2.2 CONTROLLS OF THE WEATHER AND CLIMATE OF SOUTH AFRICA

South Africa is situated in the subtropics; hence its climate and weather are affected by circulation systems that prevail in the tropics to the far north, subtropics as well as the temperate latitudes to the south (Tyson and Preston-White, 2000).

2.2.2.1 TROPICAL DISTURBANCES

Tropical disturbances over South Africa occur in summer as the Inter-Tropical Convergence Zone (ITCZ) propagates southwards to approximately 17°S (Taljaard, 1994). Cloud bands

associated with most of the late summer rainfall results from the presence of the ITCZ (Tyson and Preston-Whyte, 2000). Tropical systems over South Africa normally occur in the form of tropical easterly flow and the existence of easterly waves or lows, evident at the surface and replaced by a ridge of high pressure cells in the upper atmosphere because of the planetary scale meridional Hadley circulation. Easterly waves and lows are both characterised by low level convergence. The difference between the easterly waves and easterly lows is that upper air divergence is evident at 500hPa for the easterly wave, whilst, for the easterly low, divergence occurs at higher levels in the troposphere than in the case of easterly waves. Consequently surface divergence and upper air convergence is evident west of the surface trough formed by the easterly wave or low resulting in subsidence and clear skies (Tyson and Preston-Whyte, 2000), while rain occurs to the east of such a trough.

Easterly waves usually result in general rains that last for days and sometimes also thunder storms, whereas easterly lows also result in widespread rainfall over the central and eastern parts of South Africa (Tyson and Preston-Whyte, 2000). Although easterly waves and lows are the main cause of the summer rainfall in South Africa, there are, however, tropical systems resulting in extreme rainfall in South Africa, such as Tropical Cyclones (TCs) and Tropical-Temperate Troughs (TTTs).

TCs from the South West Indian Ocean are usually accompanied by torrential rains along the eastern coast (e.g. Reason and Keibel, 2004). TCs that had a significant effect on South Africa were TC Domonia in January 1984, TC Imboa in February 1984 and TC Eline in February 2000. The latter resulted in extreme flooding over Mozambique and the northern parts of South Africa where thousands of people died during the flooding and many were left homeless. Damages caused by TC Eline were more than R300 million in South Africa alone (Reason and Keibel, 2004; Du Plessis, 2002). TCs degenerate to tropical lows when landfall takes place or when moving over colder oceans. This might favour the large river valleys as they migrate westwards (Tyson and Preston-Whyte, 2000).

TTTs act as a link between tropical and temperate circulation systems (Tyson and Preston-Whyte, 2000). They are also known to be major rainfall producing systems over South Africa. Lindesay and Jury (1991) indicated that TTTs are characterized by a trough linking an area of convection over tropical or sub-tropical Africa with a temperate depression to the south of the subcontinent. The combination of a tropical system in the form of an easterly wave, or easterly low, and a westerly wave disturbance, or cut-off low, with convergence at

the surface and divergence aloft, will encourage vertical uplift to form extended cloud bands linking tropical and temperate systems (Tyson and Preston-Whyte, 2000). According to Harrison (1984) 39% of the mean annual rainfall in South Africa is due to TTTs.

2.2.2.2 SUB TROPICAL DISTURBANCES

The subtropical climate is characterized by high pressure system that dominates over South Africa and is split around the sub-continent into two near-surface high pressure systems (anticyclones) namely the Indian Ocean High (IOH) and the Atlantic Ocean High (AOH) during the austral summer months. These anticyclones are part of an irregular belt of high pressure cells in the subsidence region of the planetary Hadley cell, which encircle the Southern Hemisphere at 30^0 south. They oscillate northwards and southwards during the austral winter and summer, respectively (Tyson and Preston-White, 2000; Schulze, 1965). The high pressure system over the interior is associated with subsidence, fine clear conditions and little or no rainfall. During summer surface radiation allows for trough formation, which in turn, allows for moisture advection from the tropics to form rain over the east of South Africa. Winter subsidence inversions caused by the high frequency of high pressure system over the interior may cause adverse climate within the boundary layer bearing serious implication for air pollution dispersion (Taljaard, 1994), especially over the eastern highveld.

2.2.2.3 TEMPERATE DISTURBANCES

Temperate disturbance affects the rainfall of South Africa by means of eastward propagating waves in the westerlies. For example, the passage of cold fronts throughout the year (Tyson and Preston-Whyte, 2000). A front is defined as a zone of strong discontinuity and temperature gradients when two air-masses, with substantially different characteristics, come into contact (Tyson and Preston-Whyte, 2000). Cold fronts usually occur south of South Africa as the cold polar air and warm subtropical air come into contact. Cold fronts normally results in winter rainfall over the south western and south coast as they migrate northwards during winter (Tyson and Preston-Whyte, 2000).The passage of cold fronts is normally characterized by a significant drop in minimum temperatures.

Cold fronts always occur in the vicinity of westerly waves, depressions or cut-off lows. Most of the flood producing rains over South Africa results from cut-off-lows (Tyson and Preston-

Whyte, 2000). The development of the rainfall season caused by temperate disturbances in the summer rainfall region starts in September, from the south and south-west and progress northwards as far as the Mpumalanga Province in November. Some stations in the Mpumalanga even encounters two rainfall regimes superimposed, one resulting from tropical disturbance and the other from temperate disturbance (Schulze, 1965). For example a double rainfall maximum over Ermelo is indicated in November and January as shown in figure 2.2.

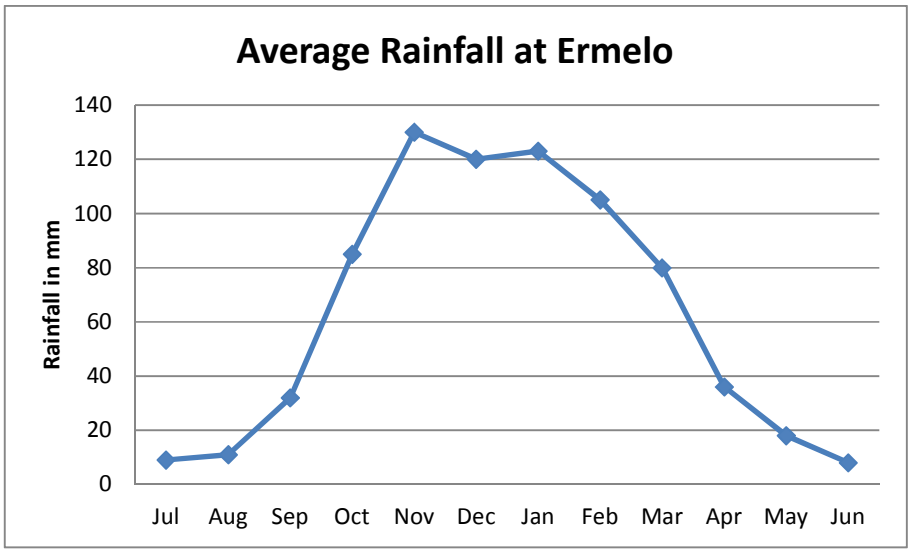

Figure 2.2:
Average rainfall (mm) for each month calculated from a 47 year record (1961-2008). Note the two peaks in November and January

2.2.3 RAINFALL OVER SOUTH AFRICA

Rainfall over South Africa is highly variable (Kruger, 2007) and is characterized by eight regions with similar inter-annual rainfall variability (Mason, 1998; Landman and Mason, 1999; Kgatuke et al, 2008); as shown in figure 2.3. The Western Cape Province receives most of its rainfall in winter, the south Eastern Cape Province receives its rainfall throughout the year and regions three to eight, although, they have different rainfall variability, they all form part of the summer rainfall zone. Similarly, Schulze and Maharaj (2007) also group the rainfall regions based on their seasonality, namely the winter rainfall region (south Western Cape Province), all-year rainfall (southern coast) and finally the summer rainfall region which

is further grouped into early-summer, mid-summer, late-summer and very late- summer (fig 2.4).

The summer rainfall zone receives much of its rainfall as a result of thunderstorms, and its rainfall is more frequent and of greater intensity than in the south Western Cape and the Eastern Cape Provinces. The winter rainfall over the western and the most southern parts is due to frontal systems (Schulze, 1965). Figures 2.5 and 2.6 illustrate the summer and the winter rainfall in South Africa as obtained from Schulze et al. (2008).

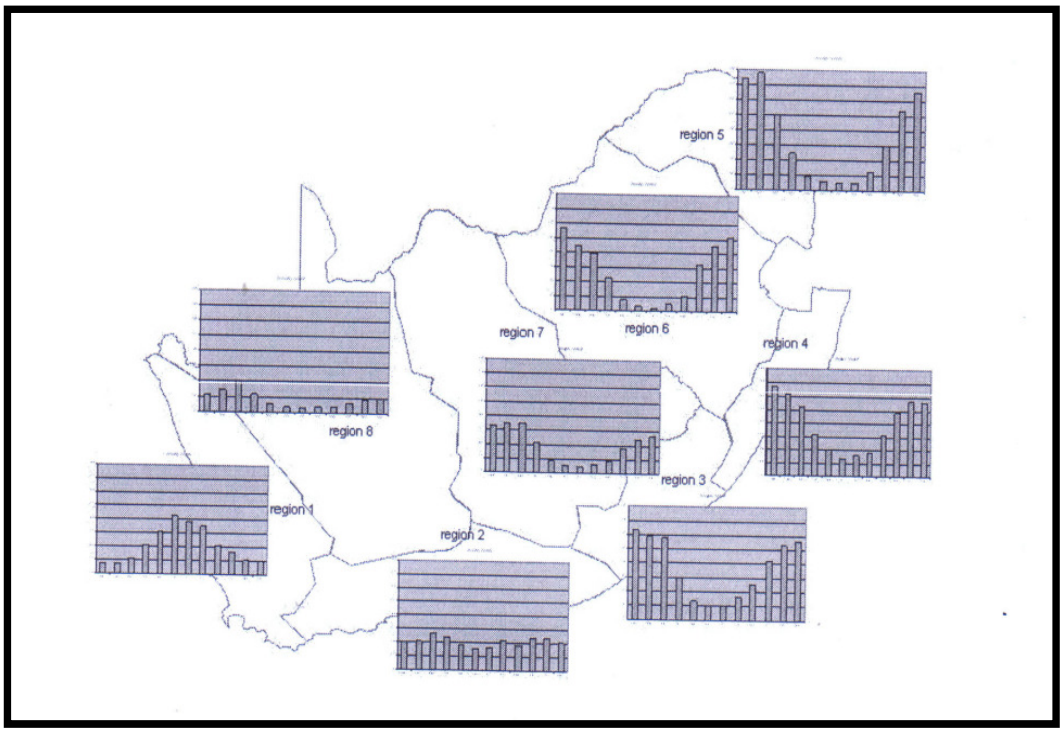

Figure 2.3:
South African Rainfall regions (Kgatuke et al, 2008)

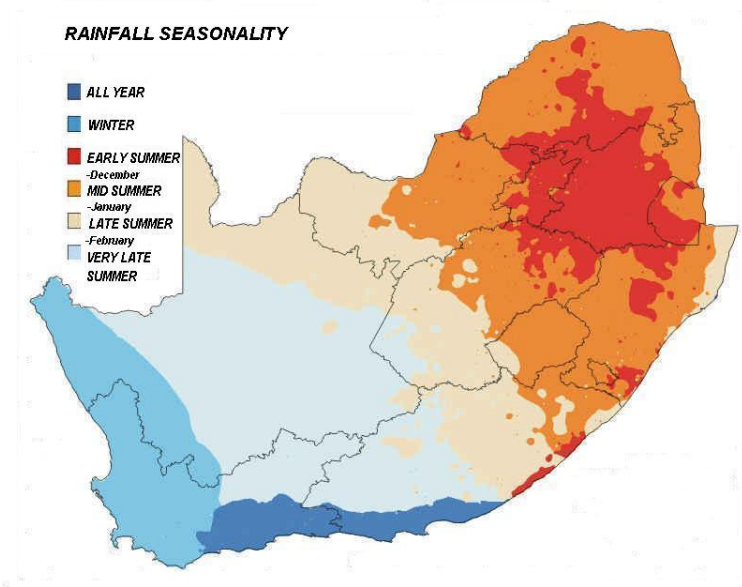

Figure 2.4:

Rainfall seasonality over South Africa per quaternary catchment (Schulze et al, 2008)

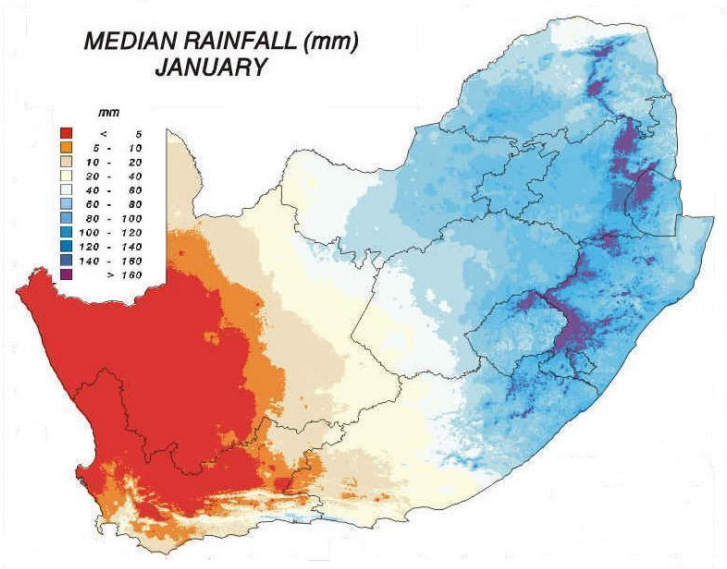

Figure 2.5:

The Median Rainfall for January over South Africa (Schulze et al, 2008)

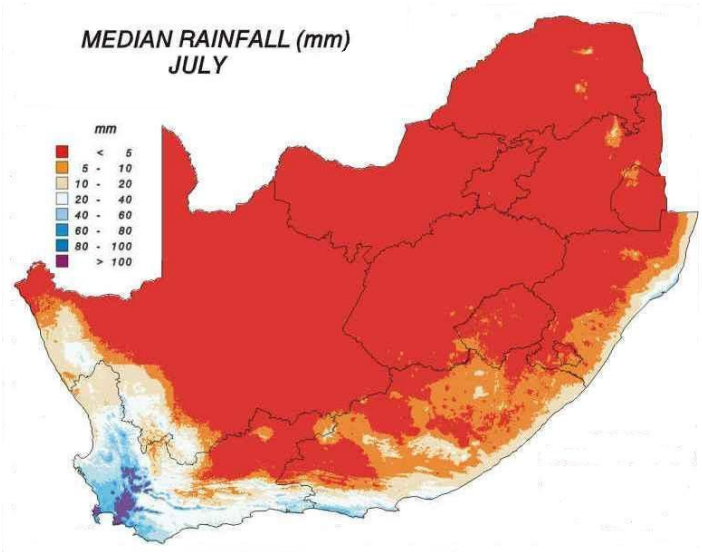

Figure 2.6:

The Median Rainfall for July over South Africa (Schulze et al, 2008)

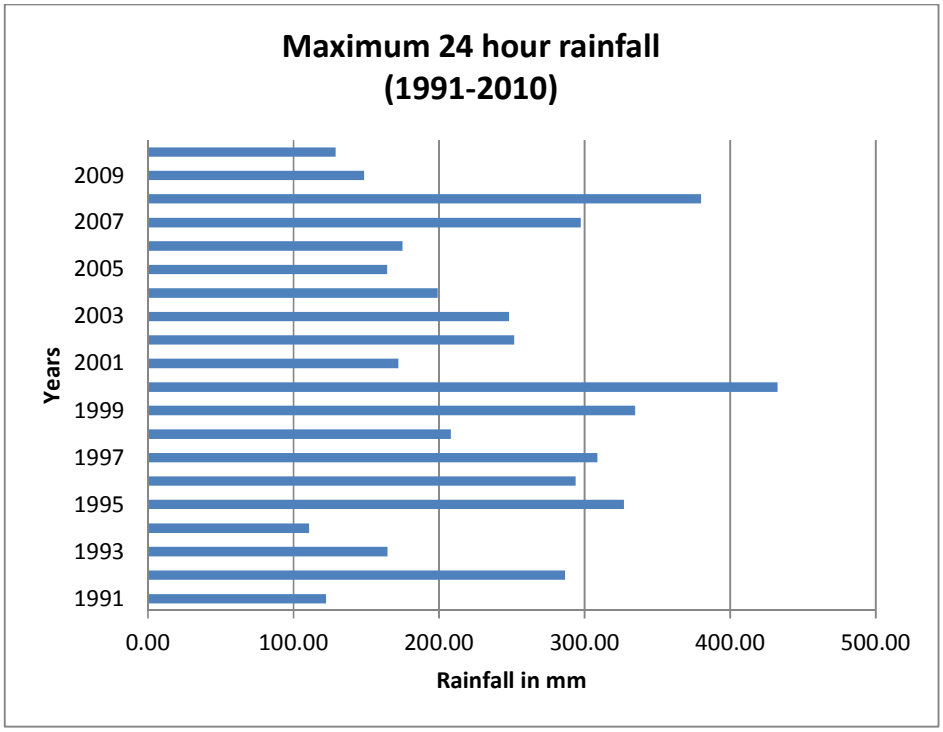

Figure 2.7:

Maximum 24hr rainfall (mm) in South Africa for the period 1991-2010.

The average of rainy days per month differs from place to place, due to the mean annual rainfall received, the rainfall seasonality and also the type of rainfall received. The western and southern coastlines receive most of their rainfall due to westerly wave frontal systems and hence rainfall may last for several days, whereas over the interior of South Africa most of the rainfall is due to thunderstorms and hence high amounts of rainfall is often received in a relatively short periods (Kruger, 2007). Therefore stations along the western and southern coastlines may indicate lower mean annual rainfall amounts, with a high number of rain days, while the opposite may occur over the eastern interior. Daily rainfall in South Africa may sometimes reach more than 400mm per day. The highest daily rainfall that recorded in South Africa was 597mm in St Lucia on 31 January 1984, due to the passage of TC Domonia. Figure 2.7 shows maximum 24 hour rainfall per year for the period 1991 -2010.

2.2.4 MINIMUM AND MAXIMUM TEMPERATURES OVER SOUTH AFRICA

Daily mean temperature is defined by Taljaard (1996) as the mean value of the 24 hourly values measured on a specific day. A number of factors are known to affect near-surface air temperature distribution on both short and longer time scales. These factors are topography, cloudiness, radiational control and advection, to name a few. In the following sections some of the most important temperature features of South Africa are discussed.

2.2.4.1 TOPOGRAPHICAL FACTORS

The topography of South Africa has the most important effect of temperature distribution over the country. The topography and the mean annual temperatures over South Africa almost follow the same spatial pattern. The lowest temperatures occur over the escarpment, while the highest temperatures are found in the low lying areas (Schulze, 1997; Taljaard, 1996; Kruger, 2008). However, in winter months changes in altitudes may also result in cold air drainage into valleys at night time, thereby posing a risk for the development of frost. Higher altitudes are linked with reduced atmospheric pressure, which might enhance the transimitivity of solar radiation, leading to an increment in the rate of vaporisation under clear skies. These factors might be reduced under conditions of cloud cover (Schulze, 1997).

The lowest temperature in January are found in the Drakenberg range, starting from the Limpopo Province , across Lesotho mountains (Figure 2.1), through the Eastern Cape Province and westwards to the Roggesveld ranges in the Northern Cape Province. The warmest temperatures are mostly found also in the valleys, like the Orange River Valley, Limpopo valley, Tugela River Valley and the eastern Low-veld. Schulze (1965) classified the Great Karoo, which is located in the southern parts of the Northern Cape Province and parts of Western and Eastern Cape Provinces, as hot during the summer months. A steep temperature gradient is found between the western coast of South Africa and the adjacent interior. From the main escarpment of the Eastern Cape Province to the sea belt, relative high temperatures are found. On a micro scale, different slopes and aspects that make up a landscape occur at different altitudes. These differences results in changes in solar receipts causing warm temperatures on north facing slopes and cooler temperatures on south facing slopes (Schulze,1997).

Topographic configuration also plays a role in the formation of berg winds. Berg winds are characterized by adiabatic warming of air as it descends from the inland plateau (Tyson and Preston-White, 2000; Taljaard, 1996). Berg winds usually occur in late winter and early spring; and normally results in the anomaly of highest maximum temperatures in winter on the east coast (Tyson and Preston-White, 2000). On the west coast the strong offshore berg winds results in visible plumes of dust extending out to the sea (Tyson and Preston-White, 2000).

2.2.4.2 CLOUDINESS

Cloudiness causes a reduction in the amount of solar radiation reaching the surface of the earth during daytime. When a cloud layer is present in the morning and persist throughout the day temperatures will remain below their normal cycle (Taljaard, 1996). However, if a cloud layer is present at night, it will transmit the solar radiation absorbed during the day, raising the minimum temperatures by several degrees (Taljaard, 1996). In January, cloud cover is profound over the interior of South Africa towards the eastern coast (Taljaard, 1996). In July, cloudiness decreases over South Africa, except for the south Western Cape Province where it increases as a result of the frequent passage of cold fronts (Taljaard, 1996).

2.2.4.3 LOCAL RADIATIONAL CONTROLS

Land use characteristics have a profound effect on air temperature. Assuming all factors to be equal in response to the same insolation, air over a drier surface warms up faster than air over a moist surface. When the surface is moist, most of the solar radiation energy absorbed is used for evaporation through absorption of latent heat (Moran and Morgan, 1994). If the surface is drier, the available heat will raise the temperature through conduction or turbulent mixing. The local radiation balance will result in air temperature to rise from a minimum around sunrise, to a maximum during the early or mid-afternoon. This could however change if an influx of cold air occurs over the same period (Moran and Morgan, 1994)

2.2.4.4 AIR MASS CONTROLS

Atmospheric advection is the horizontal movement of an air-mass from one location to another, which also has an effect on temperatures. Cold air-mass advection occurs when air moves from a colder area to a warmer area, and the opposite is true for the warm air- mass advection. If cold air-mass advection over a region is extreme, the air temperature is expected to drop significantly throughout the day in spite of bright sunny skies (Moran and Morgan, 1994). Air-masses with significantly different properties are found around the west, south and east coasts of South Africa. The influx of air-masses towards the land often results in temperature and moisture gradients over land (Taljaard, 1996).

2.3 MESO-SCALE MODELING

As discussed in the previous chapter, the critical advantage of meso-scale models is their ability to capture meso-scale weather. Meso-scale models may be improved by increasing the amount of initial and boundary input data by advanced data assimilation processes, the choice of physical parameterizations, resolution and model processing techniques (Roeber et al., 2004; Stenrud, 2007). The following sub-sections discuss the various alterations that could be made in meso-scale models in order to achieve better results from the model.

2.3.1 BOUNDARY CONDITIONS, DOMAIN SIZE AND NESTING

Nested meso-scale models are sensitive to where their Lateral Boundaries (LBs) are positioned. Choosing a smaller domain size may result in large errors. Hence tests should

be performed in order to locate the optimum positions of the LBs (Warner et al., 1997; Warner, 2011; Seth and Giorgi, 1998; Schmidli et al., 2011). LB conditions from a global model are imperative for the nesting of meso-scale models in order to achieve a desired result between small scale and large scale features (Dudhia, 1993; Ginis et al., 1997 and Kalnay, 2003). Roeber et al. (2004) showed that nested grids are normally used for high resolution modeling, but that the outer domain may affect the explicit precipitation forecasts within the inner nest negatively. Using nested grids, topographical, urban and coastal effects as well as deep convection may be resolved by simulating larger scale weather (Dudhia, 1993).

Most meso-scale models have an option of either one-way or two-way nesting across boundaries (Harris and Durran, 2010). However, one-way nesting is used in most applications (Kalnay, 2003; Harris and Durran, 2010). One-way nesting allows for most synoptic effects to be fed down to meso-scales. A two-way nesting approach implies that both the larger and smaller domains interact with each other (McGregor 1996; Ginis et al., 1997; Harris and Durran, 2010). According to McGregor et al., (1993) improved simulations may be achieved from two-way nesting. However, the challenge of two-way nesting is to provide compatibility in the overlapping zone of the two domains. The lack of compatibility in this zone may cause numerical instabilities that may have detrimental effects on the results of the entire domain (Ginis et al., 1997). The inconsistencies brought by lack of compatibility of the two domains may be avoided by matching grid resolutions from the two models at the LB area (Qian et al., 1999). A critical measure for the success of a nested NWP model is its ability to resolve features despite of the limits of its grid (Skamarock, 2004; Stenrud, 2007). NWPs can also be improved by increasing the amount of input data by advanced data assimilation processes (Roeber et al.2004). The choice of physical parameterizations and resolution might improve the performance of such a NWP model (Roeber et al., 2004; Stenrud, 2007).

2.3.2 RESOLUTION

Model resolution is defined as the horizontal and vertical scales dimensions in which a numerical model can resolve or reproduce atmospheric circulation and processes (Stenrud, 2007). A number of studies have shown that model simulations could be improved by increasing the grid resolution of the model (Anthes et al., 1983; Orlanski and Katzfey, 1987;

Colle et al., 2003). However, other studies demonstrated a degradation of skill when the grid resolution of the model was increased (Tustison et al., 2001; Gallus, 2002) that could be attributed to the complex nature of sub-mesoscale processes. As a matter of fact sensitivity studies done by Gallus (1999) showed that the response to change in horizontal resolution depends on the phenomena being simulated, and it also vary significantly with the choice of the parameterization scheme used, because physical parameterizations are formulated in such a way that they are suitable for a specific range of model grid lengths (Stenrud, 2007). Engelbrecht (2002) therefore recommends that the resolution of the model should at least be fine enough to capture the forcing and atmospheric circulation of interest.

2.3.3 DATA ASSIMILATION

Data Assimilation (DA) is a process whereby observations and forecast data are matched together mathematically in order to create a data field that is close as possible to reality. Such fields are usually used to initialize NWP models. The component fields should be in physical balance. Comprehensive studies were already done on assimilating observations to NWP model fields (Benjamin et al., 1991; Stauffer et al., 1991; Stauffer and Seaman, 1994; Seaman et al., 1995; Warner et al., 1997; Kalnay, 2003; Yussouf and Stenrud, 2010). These studies proved that employing DA in NWP model operation may improve the model's performance. The period of a pre-forecast DA may affect the LBCs negatively or positively whether continuous or intermittent assimilation techniques are used. The pre-forecast period enables LBC errors to move closer to the domain center by the start of the forecast, conversely the errors of the LBCs that are within the influence region of data will be partially corrected by DA (Warner et al., 1997).

The introduction of a three dimensional variational (3D VAR) DA in 1996 followed by four-dimensional variational (4D VAR) DA in 1997 led to improvements in NWPs. Daley and Puri (1980) defines the 4D VAR as the analysis technique that handles large amount of asynoptic data received from remote observing systems. The technique produces a time sequence of analysis which will reflect all observations available and be consistent where there are no observations (Daley and Puri, 1980).

The 4D VAR DA modifies the background error using the model dynamics over the assimilation period. The 4D VAR DA includes a time dimension to that of the 3DVAR DA i.e. all data within a 12-hour period are used simultaneously in one global estimation process

and the 12-hour forecast that best fits the available observation is generated and used (Schulze, 2007). Fisher (2002) did experiments to test sensitivity between the 4D VAR DA and the 3D VAR DA of the ECWMF model, and has found that the 4D VAR DA yielded better results than the 3D VAR DA. Other studies using the 4D VAR DA includes those of Stauffer et al., (1991); Stauffer and Seaman, (1994) and Seaman et al., (1995). A common finding of these studies is that model simulations are superior when the 4D VAR DA is incorporated in the model.

2.3.4 PARAMETERIZATION

Major components of a meso-scale NWP system require a high resolution and therefore a detailed physics, observing system which captures small scale features and a DA system which provides a balance amongst variables (Park and Zupanski, 2003; Leoncini et al., 2008). Studies by Molinari and Dudek (1992) and Marshal et al. (2003) showed that finer resolutions in models require that there should be more sophisticated physical parameterization in such models. Parameterization of cumulus cloud processes therefore has to be employed in NWP models to estimate cumulus convection (Molinari and Dudek, 1992; Frank, 1993; Stenrud, 2007).

Parameterization schemes are especially critical in the prediction of precipitation. Such schemes must therefore be comparable with the resolution of the model and with the phenomenon that is being studied (Stenrud, 2007). For example studies by Wang and Seaman (1997) showed that a convective parameterization scheme at 12km resolution improved rainfall forecasts as compared to the same convective parameterization scheme at 36km resolution, whereas, Gallus (1999) found a degradation of skill in rainfall forecasts as the model resolution was increased from 78km to12km . The same convective parameterization scheme was used in both cases.

Moliner and Dudek (1992), however, proved that convective parameterization schemes are successful in simulations of a resolution of approximately 10km, but seem to be lacking at smaller scales. This could be attributed to the lack of scale assumption at these lower grids. Changes in the microphysics of a model or the choice of convective parameterization schemes may result in greater variability in predictions (Stein and Alpert, 1993; Hamil, 1999; Jankovc et al., 2005). The average rainrate in NWPs is specifically affected by changes in convective treatment, whereas the total domain rain volume results from microphysics choices (Hamil, 1999).

The boundary layer parameterization is important in NWP because the potential of deep convection is closely tied to the boundary layer structure (Stenrud, 2007). Deep convection influences NWP from very short range forecasts to climate predictions (Stenrud, 2007). Boundary layer schemes not only influence the potential for deep convection, but also the type of deep convection to be expected is also influenced (Stenrud, 2007). However, more studies are still needed as there are still many unsolved issues pertaining to boundary layer parameterization (Marshal et al., 2003; Stenrud, 2007).

CHAPTER 3

DATA AND METHODS

3.1 INTRODUCTION

This chapter describes the data and methods used in order to meet the objectives of the study. These are divided into five sections: The first section following the introduction of this chapter gives a general description of the UM. Section 3.3 describes the UM and observational data used in this study, while the verification scores and methods used are described in section 3.4. Section 3.5 gives a short summary of the chapter.

3.2 DESCRIPTION OF THE UNIFIED MODEL

The UM is the suite of atmospheric and oceanic numerical modeling software developed and used at the UK Met Office (Dando, 2004). It targets multiple applications of earth system modeling, ranging from NWP through to long-term climate simulations. The UM became operational in 1992 (Dando, 2004).

A set of equations which include the equations of motion, the continuity equation, the energy equation and the equation of state (temperature, pressure and density) characterizes the UM dynamics. The hydrostatic approximations are used for large-scale flows. At the smallest scales horizontal diffusion is used to prevent the accumulation of energy. The UM is a grid-point model and has a hybrid sigma-pressure vertical coordinate that is based on an extended version of the traditional hydrostatic primitive equations (White and Bromley, 1995). The UM is formulated on a staggered Arakawa B-grid with split-explicit time integration using a forward-backward approach for the adjustment step and a Heun scheme for the advection step (Cullen and Davies, 1991).

Because of its wide range of temporal and spatial scale, the UM could be used for NWP and climate modeling, as well as for a variety of related research activities (Butchart and Austin, 1998; Dando, 2004; Williams and Brooks, 2008). The meso-scale boundary conditions for the UM are supplied by time-dependent data from the global model. LB conditions from the global model are imposed every six hours. One way nesting is used to ensure that

calculations on the meso-scale grid have no effect upon those at the global grid (Dando, 2004).

The modeling system is designed so that it can be run in atmosphere-only, ocean-only or in coupled mode. In each mode a run consists of an optional period of DA followed by a prediction phase. Predictions of a few days in advance are required for NWP while for climate modeling the prediction phase may be for tens, hundreds or even thousands of years (Dando, 2004).

3.2.1 RESOLUTION

Depending on the available computer capacity and a number of standard resolutions, the choice of horizontal and vertical resolution of the UM may be varied according to the needs of the user (Dando, 2004), for example see Austin et al. (1997); Butchart and Austin (1998); Scaife et al., 2002 and Warner et al. (2005). Since the advent of the non-hydrostatic version of the UM (Davies et al., 2005) a number of high resolution models have been feasible. Until early 2005 the highest resolution UM run operationally in the UK was the 12km resolution (Lean et al., 2008). There are a number of studies (Bornemann et al., 2005; Malcom and Roberts, 2005; Younger et al., 2006; Lean et al., 2008) that demonstrate improved representation of thunderstorms and squall lines in the UM as the grid-length is reduced.

3.2.2 PARAMETERISATION

The physical parameterizations are a critical component of the model performance, and represent those processes not explicitly governed by the equation set in the model dynamics. A comprehensive set of parameterizations are included in the model. A key issue in the UM is the convective parameterization. The 12km grid- length operational UM uses a mass flux convection scheme with Convectively Available Potential Energy (CAPE) closure (Gregory and Rowntree 1990), with additional downdraft and momentum transport parameterization. This scheme is designed on the assumption that there are many clouds per grid box (Lean et al., 2008).The boundary layer turbulent mixing is represented by a first order non-local K scheme with explicit entrainment parameterization, Lock et al. (2000). The radiation is parameterized by a two stream scheme, Edwards and Slingo (1996), using five spectral bands for long- wave and five for short- wave. The albedo of the Earth's surface depends on the vegetation type and is specified as an ancillary file. Long-wave fluxes

depend upon the amount and temperature of the emitting medium and its emissivity (Dando, 2004).

The UM includes a parameterized gravity wave drag, whereby flow over mountains in stable conditions stimulates waves. Stress exerted is proportional to the sub-grid scale difference of topography and the wind speed, and the waves allowed to propagate vertically, reducing static stability by ascent and increasing wind-shear. When "breaking" of the wave is diagnosed a drag is exerted, representing the outbreak of turbulence with the onset of shear instability (Gregory et al., 1996).

The parameterization of cloud and precipitation microphysics is performed by a mixed-phase scheme, Wilson and Ballard (1999) with advection by 3D winds of precipitation products. Fractional cloud cover which consists of separate values for cloud water and cloud ice mixing ratios is used. Precipitation occurs at a rate which is a direct simulation of growth by accretion and coalescence as a consequence of precipitation from a layer above and also includes the Bergeron-Findeisen process. Evaporation and melting of precipitation is allowed to take place. Dynamical ascent is the most important process but cloud may also be formed by radiative cooling and turbulent transport.

Other parameterizations included in the model are surface (Essery et al., 2001), and mixed-phase cloud microphysics (Wilson and Ballard, 1999). The soil and vegetation types are assigned to each land point. The characteristics associated with the soil and vegetation types are used to calculate the heat, moisture and momentum fluxes. Soils parameters are calculated in four separate levels. Temperature in the four levels varies according to the radiation balance at the soil surface. The moisture content of the soil also varies according to evaporation and precipitation. The moisture content of the soil varies according to the areas, soil types and also according to the local climatic conditions including evaporation and precipitation. Soil water is primarily lost though evaporation and transpiration through plants. Over the ocean the roughness length is increased with increasing wind speed to represent the interaction with waves (Dando, 2004).

3.2.3 THE UM AT THE SOUTH AFRICAN WEATHER SERVICE

The UM version 6.1 has been operational at SAWS since May 2006 and gives forecast guidance of up to two days in advance. The installations with the Ported UM (PUM) were

implemented on a Linux workstation. The Met Office 12km Limited Area Model, together with its DA was used as a benchmark to tender for a suitable supercomputer for SAWS. A supercomputer NEC SX8 system was then successfully installed to run 24-hour forecasts of the 12km UM over an actual time period of 35 minutes. 50% of the NEC SX8 computer peak performance was used during the run. DA at SAWS currently incorporates a 3-D VAR DA system, but there is an intention to upgrade it to 4D-VAR DA system at a later stage. The DA used for the UM is divided in continuous, intermittent and no DA. The continuous assimilation has input only from observations. Observations are supplied to the model at every six hours. This includes the latest satellite data. Data is supplied through an intermediate observation file provided by the UK Met Office on a daily basis (Tennant, 2008). Studies using the ETA model at SAWS showed a significant deterioration of skill without DA (Tennant, 2008). Similar results were also shown using the UM 2 week-statistics. Predictions generated from DA initial conditions showed a lower Bias, lower ACC, proved to be more stable computationally and were also able to capture temperature inversions (Tennant, 2008).

3.3 DATA

3.3.1 UNIFIED MODEL DATA

This study uses three UM configurations, namely the 12km horizontal resolution with DA, the 12km resolution without DA and the 15km resolution without DA. The domain size of the 12km resolution configuration is 601x 401 grid points. It covers an area of 0^0 to 44^0S and 10^0W to 56^0E and has horizontal resolution of 12km with 38 levels in the vertical. The 12km with DA runs twice a day and the 12km with no DA runs once a day. The 15km resolution has a smaller domain than the 12km resolution and covers South Africa. Its domain ranges from 22^0S to 35^0S and 15^0E to 34^0E and it has 138 x 101 grid points and runs only once a day. Figures 3.1 and 3.2 show the topography and domains of the 12 and 15km resolutions, respectively.

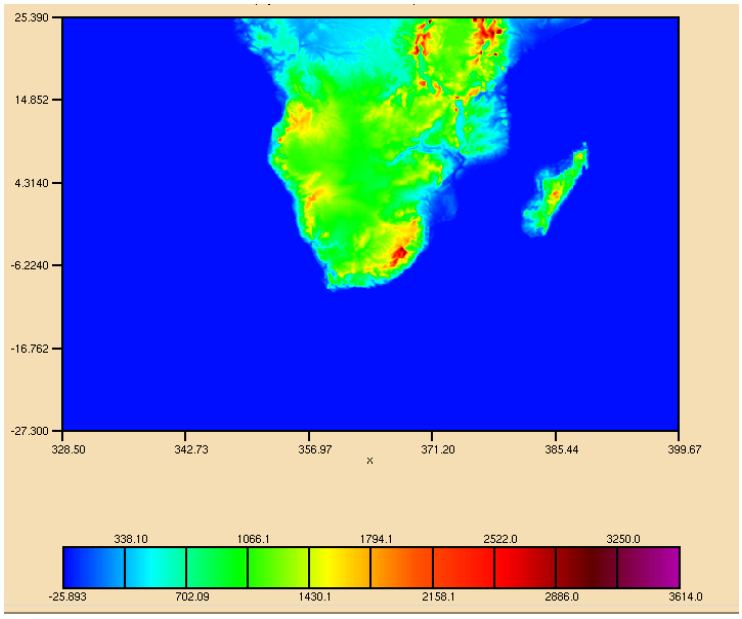

Figure 3.1:

Topography in meters above mean sea level and domain size of the 12km Unified Model (UM) configuration.

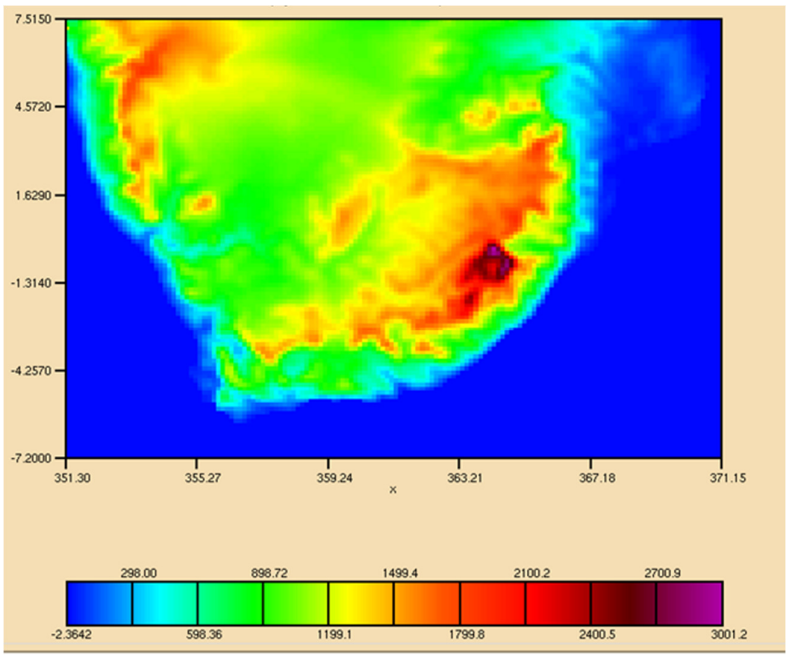

Figure 3.2:

Topography in meters above mean sea level and domain size of the 15km Unified Model (UM) configuration.

3.3.2 OBSERVATIONAL DATA

Observational data for the period 01 January 2008 to 31 December 2008 was extracted from the SAWS climate data base. The observational data include 24-hour rainfall totals and minimum and maximum temperatures. Observed rain is defined as 24hour precipitation total measured from 08:00SAST the given day until 08:00 in the morning. Minimum and maximum temperature for the day are also recorded on a daily bases. The data is quality controlled, as described in Kruger and Shongwe (2004). The rainfall data used was taken from a range of 1585 to 1624 stations all over South Africa. The observation network includes Automatic Weather Stations (AWSs) and manually operated stations. Stations used were chosen on the basis of completeness of records.

The objectives of the study involve comparing three different model configurations of the UM against each other and against observations. Rainfall minimum temperatures and maximum temperatures will be used as variables to achieve these objectives.

3.4 VERIFICATION SCORES AND METHODOLOGY

Verification of models is regarded as crucial in the weather industry. A reliable and accurate prediction of weather lies in continuous improvements of NWP Models. Model verification could therefore contribute to the reliability, skill and accuracy of model predictions. Verification methods involve measuring the relationship between a forecast and the corresponding observations (Banitz, 2001; Roeber et al., 2004).

A number of studies addressed verification methods used in meteorology (Kruzinga and Murphy, 1983; Murphy, 1991; Murphy, 1992; Murphy 1993; Murphy 1999). There have also been a growing number of studies verifying NWP models which has quantified the role of increased resolution and sensitivities to different microphysics (Gaudet and Cotton, 1998; Colle et al., 1999; Colle and Mass, 2000; Colle et al., 2003). Results from these studies showed an increased in model skill as the model resolution is increased. Brooks et al. (1992) states that some of NWP verification methods use event based verification techniques that are not well suited to the verification of strong temporal or spatial gradients. However, according to Colle et al. (2001), Case et al. (2004), Rife and Davis (2005), and Ma et al. (2010) using event-based verification techniques has some advantages. This can be

achieved by interpolating NWPs to locations of verifying observation (Colle et al., 2001; Rife and Davis et al, 2005; Ma et al., 2010) or by using spatial patterns, assisted by the very high density of observations available over the study area (Case et al., 2004). In the studies mentioned above, the model forecasts were first interpolated to observation points before the re-interpolation of both observations and forecast data onto the same verification grid.

In this study two types of verification methods are used. The guidelines for these verification methods are outlined in the World Meteorological Organization (WMO) technical document verification procedures sited in (WMO, 2000). The verification methods are classified as either subjective or objective. Subjective verification used in this study is eyeball verification. This is a method of looking at the forecast and observations side by side and uses one's own judgment to determine the forecast errors. Eyeball method may give a clear vision of the variable being investigated, however, it is not quantitative, and its interpretation may be Biased. It is therefore recommended that one should use it with caution in any formal verification procedure (WMO, 2000).

Objective verification could be classified as either verification of continuous variables or verification of categorical variables. Continuous variables are represented in numbers (WMO, 2000). The verification of forecasts for continuous variables measures how the values of the forecasts differ from the values of the observations (Stanski, 1989). Categorical forecasts consist of a statement that says that one and only one of a set of possible events will occur. It contains no expression of uncertainty (WMO, 2000; Banitz, 2001).

3.4.1 SUBJECTIVE VERIFICATION

Eyeball verification for the three model configurations was done for January (mid summer), July (mid winter), and for the transition months April and October representing autumn and spring respectively. The observational data was interpolated onto a 0.5^0 resolution grid and a visual comparison of the three model configuration with each other and with observations was then done

3.4.2 OBJECTIVE VERIFICATION

The study used continuous variables as well as categorical variables (only for rainfall), to do objective verification of the UM in predicting weather over South Africa. For the observations to be compared to the UM data, the UM value of the nearest grid point to the selected meteorological station was compared to the corresponding point station data.

3.4.2.1 CATEGORICAL VERIFICATION SCORES

Categorical error scores depend on a threshold value. Categorical prediction is verified by means of a contingency table. A contingency table may be built from a set of matched rainfall predictions (fi) and observations (oi) as indicated in table 3.3. An event identified when a predicted or the observed precipitation is below or above a threshold. The combination of different possibilities between observations and predictions defines the contingency table.

Rainfall stations were grouped into homogeneous rainfall regions based on standardized monthly rainfall totals obtained by cluster analysis. Figure 2.3 shows the different rainfall regions used in this study. Five rainfall thresholds; 0.1mm, 0.5mm, 2.0mm, 10.0mm and 50.0 mm per 24hour were selected to verify the three UM configurations in simulating rainfall over the different regions. The method used for selecting these rainfall thresholds is the same method as that used by Accadia et al. (2005).

For each rainfall threshold four categories of hits (a) , false alarms, misses and correct no rain predictions (a, b, c and d) were determined (WMO, 2000).

Table 3.1: *The contingency table for the analysis of categorical variables*

		Observation (o_i)	
		yes	**no**
Forecast (y_i)	**yes**	**a**	**b**
	no	**c**	**d**

The Bias, Percent Correct (PC) and False Alarm Rate (FAR) were then calculated. The Bias is the ratio of the number of times the event was predicted over the number of times it was observed. It accounts for the reliability of the model. The Bias ranges from zero to infinity. The perfect score is 1. Values less than 1 indicate under-prediction and values greater than I indicate over-prediction (WMO, 2000).

The Bias is given by the equation

$$\text{Bias} = \frac{a+b}{a+c} \qquad (1)$$

The PC gives a percentage of the correct prediction. It ranges from zero to 1, where 1 is the perfect score and 0 the worst score. PC accounts for the accuracy of the predictions.
The PC is given by the equation:

$$\text{PC} = \frac{a+d}{a+b+c+d} \qquad (2)$$

The FAR is defined as the ratio of the event predicted that did not occur. It also seen as a measure of accuracy and is given by the equation:

$$\text{FAR} = \frac{b}{a+b} \qquad (3)$$

3.4.2.2 CONTINUOUS VERIFICATION SCORES

Objective verification of the three model configurations of the UM was done for rainfall, minimum as well as maximum temperatures. Rainfall stations were randomly selected across the South African domain. Minimum and maximum temperatures data from stations grouped according to the height of the station above mean sea were also used as continuous variables to determine the performance of the UM.

Table 3.2: *The grouping of temperature stations according to altitude*

	Height range	No of stations used
Altitude 1	<20	3
Altitude 2	21 – 65	3
Altitude 3	70 -145	3
Altitude 4	146 -360	3
Altitude 5	361 – 800	3
Altitude 6	801 – 1190	3
Altitude 7	1191 -1500	3
Altitude 8	>1500	3

For a forecast (y_i) and its corresponding observation (o_i), where i represent the different days in the month and N is the total number of days for each month used in the study. The Mean Error (ME), Mean Absolute Error (MAE) and the Root Mean Square Error (RMSE) were calculated.

The ME is the gross measure of reliability. It is the difference between the average forecast and the average observation. Positive ME values indicate over-forecast and negative value indicate under-forecasting. ME is given by the equation:

$$ME = \frac{1}{N}\sum_{i=1}^{N}(y_i \cdot o_i) \quad (3)$$

$$MAE = \frac{1}{N}\sum_{i=1}^{N}|y_i \cdot o_i| \quad (4)$$

The RMSE is the average square root of the difference between the prediction and observation pairs. RMSE increases from zero for perfect forecasts through to larger values as the error increases. It could also be seen as a measure of accuracy.

The RMSE is given by the equation

$$\text{RMSE}= \sqrt{\frac{1}{N}\sum_{i=1}^{N}\left(y_i \cdot o_i\right)^2} \qquad (5)$$

3.5 SUMMARY

In this chapter the UM model has been described. The data as well as the verification scores and methods were also described. The verification results obtained by using the three model configurations of the UM are described in the next two chapters.

CHAPTER 4

RAINFALL VERIFICATION

4.1 INTRODUCTION

This chapter describes the verification results for rainfall as obtained using three different configurations of the UM over South Africa. The model configurations are firstly compared to each other and secondly against observations. In this study, rainfall verification is done in three ways. Firstly the model is subjectively being verified using eyeball verification for the entire domain of South Africa, followed by an objective verification of categorical forecasts for eight rainfall regions in South Africa (figure 2.3) and an objective verification using continuous variables for selected point stations over South Africa.

4.2 EYEBALL VERIFICATION

Eye ball verification is a method of looking at the forecast and observations side by side and then to use one's own judgment to determine the forecast errors by comparison. Such an eyeball method may sometimes give a clear vision of the variable being investigated, although the result is not quantitative, and the interpretation may be Biased (subjective). It is therefore recommended that one should use it with caution in any formal verification procedure (WMO, 2000). The eyeball verification for four months January, April, July and October for the year 2008 is illustrated in figures 4.1 to 4.4. January is considered as mid-summer with summer rainfall. Similarly July is considered as mid-winter with winter rainfall. April and October represent the autumn and spring, respectively.

Highest rainfall figures for January (figure 4.1a) occur over the northern Gauteng Province as well as over the southern parts of the Limpopo Province, north western parts of the Mpumalanga Province and the north eastern parts of the North-West Province. The central and south eastern parts of South Africa received rainfall of between 60mm and 200mm. Dry conditions (with monthly totals of below 15mm) have been recorded along the western parts of South Africa. January monthly totals represented by the 12km UM simulation with DA shows the closest resemblance to the observed data (figure 4.1c), especially over the western parts of South Africa. All three model configurations over-estimated monthly rainfall over the eastern parts of the country. Eye

ball verification of the three configurations shows that the 12km UM simulation with DA outperformed both the 12km and 15km UM simulations without DA.

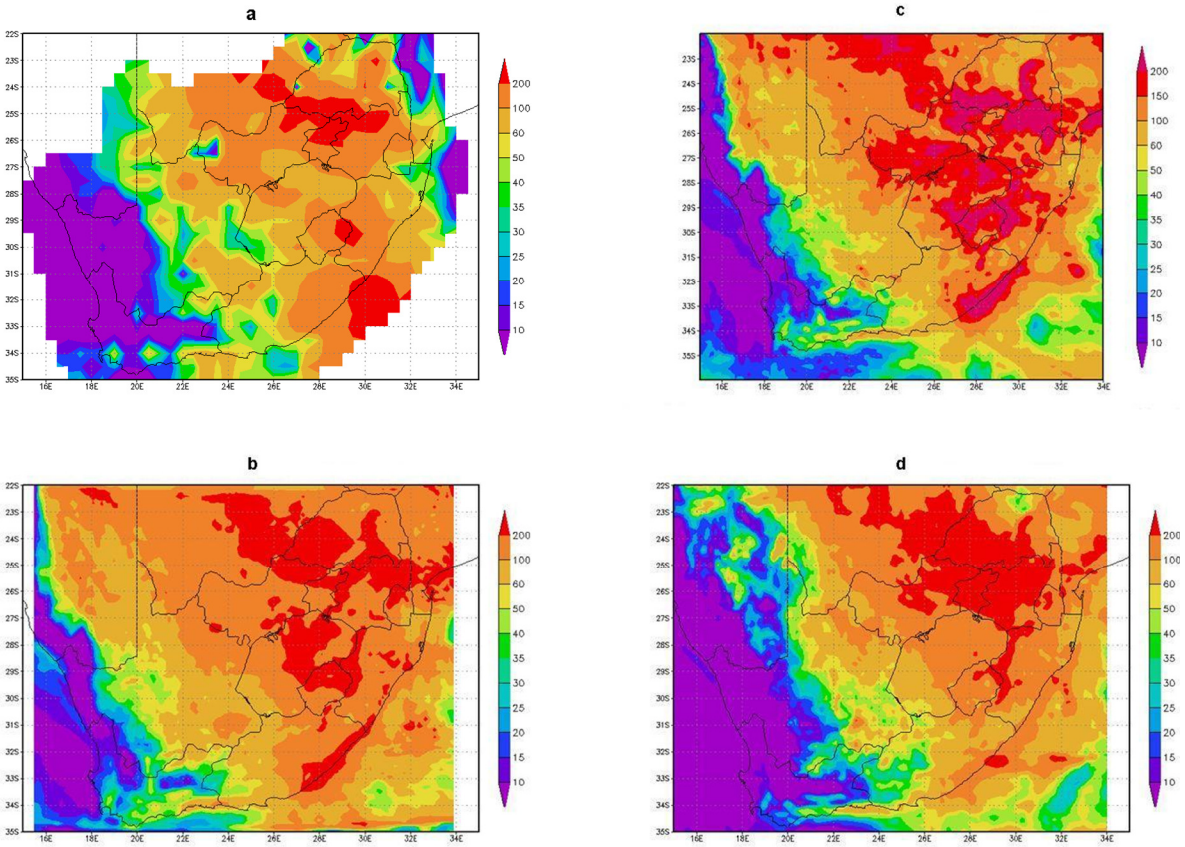

Figure 4.1:

January 2008 rainfall totals measured in mm from (a) observations, (b) 15km Unified Model (UM) without Data Assimilation (DA), (c) 12km UM without DA and (d) 12km UM with DA simulations.

Rainfall totals for April 2008 are displayed in figure 4.2. The highest rainfall figures for April occur over the far eastern parts of South Africa between latitudes 26^0S and 33^0S. Dry conditions (with monthly totals of below 15mm) have been recorded over northern Western Cape Province and the Northern Cape Province. The three model configurations reproduce this pattern but over-estimate rainfall over the country. For example, over Gauteng observations showed rainfall of below 20mm but the 12km UM simulation with DA showed rainfall totals of more than 40mm, the 12km and 15km UM simulations without DA showed rainfall totals of below 35 and 40mm respectively. Over the southern parts of Limpopo province and western parts of Mpumalanga province, the observed rainfall totals are less than 20mm, the simulated rainfall totals are above

50mm for the 12km UM simulation with DA, and just below 50mm for the 12km and 15km UM simulations without DA. The 12km and 15km UM simulations without DA are in good agreement with each other and show a closer resemblance to observations than the 12km UM simulation with DA.

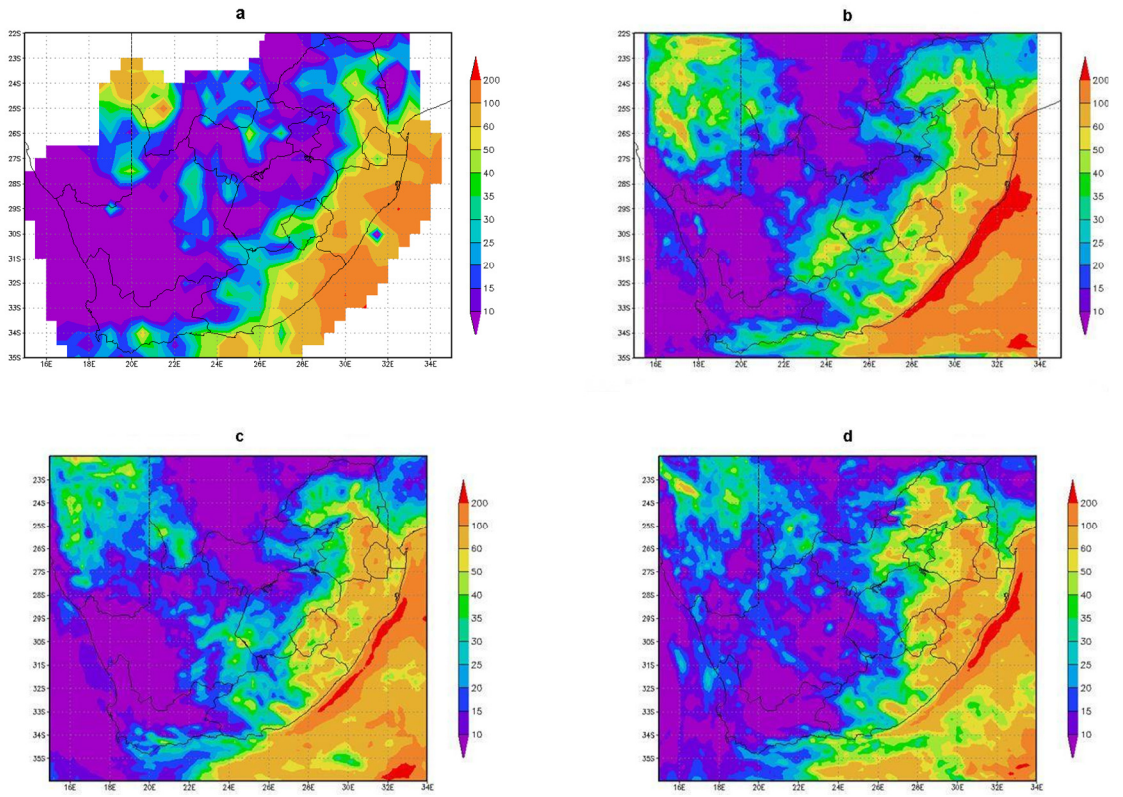

Figure 4.2:
April 2008 rainfall totals measured in mm from (a) observations, (b) 15km Unified Model (UM) without Data Assimilation (DA), (c) 12km UM without DA and (d) 12km UM with DA simulations.

Rainfall totals for July 2008 are displayed in figure 4.3. The highest rainfall figures (above 200mm) for July are evident in the Western Cape Province, which is simulated well by the three UM configurations. Dry conditions (with monthly totals of below 10mm) are evident over the eastern parts of South Africa. In spite of the simulated rainfall showing areas of more than 10mm over the eastern parts of the country, all three model configurations did well in simulating rainfall for July 2008.

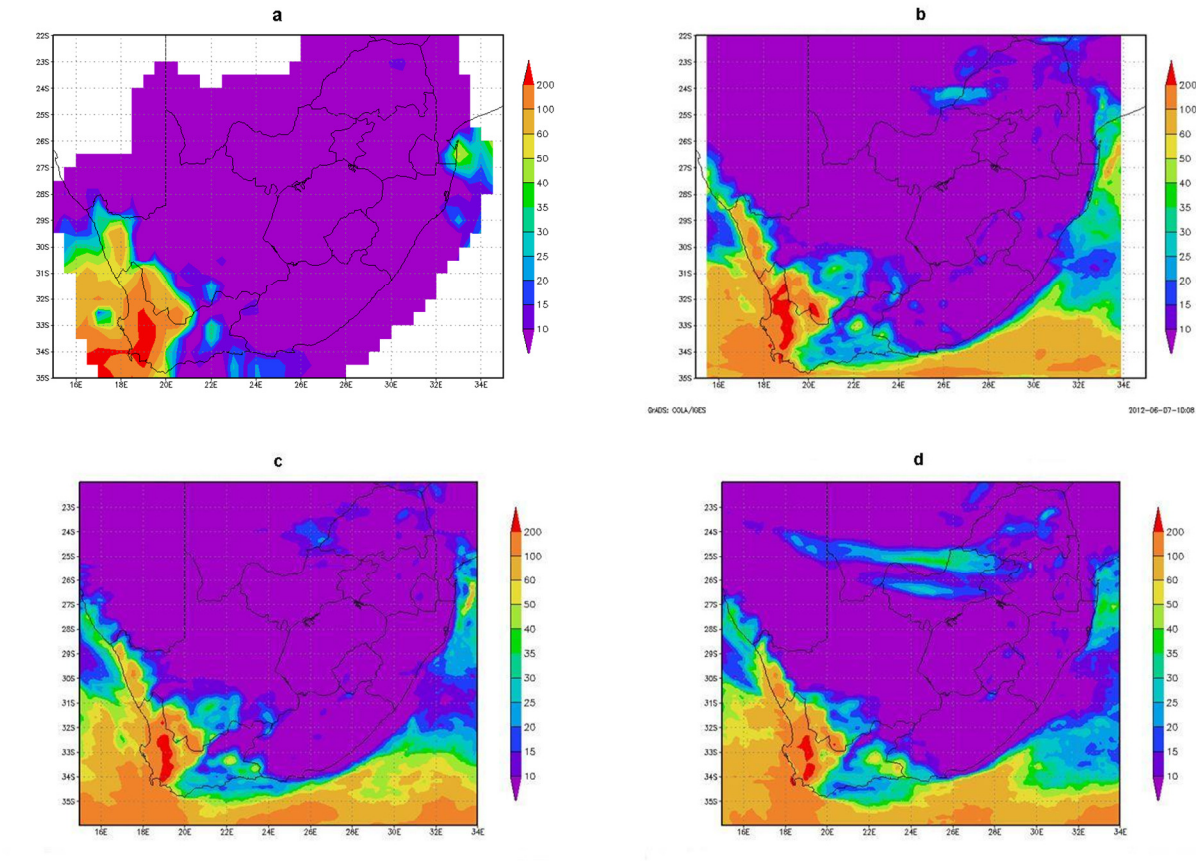

Figure 4.3:
July 2008 rainfall totals measured in mm from (a) observations, (b) 15km Unified Model (UM) without Data Assimilation (DA), (c) 12km UM without D A and (d) 12km UM with DA simulations.

Rainfall totals for October 2008 are displayed in figures 4.4. Highest rainfall figures for October occur over the south eastern parts of the Limpopo Province, north eastern half of the Mpumalanga Province and northern parts of the Free State Province, as well as the eastern and southern coasts of South Africa. Dry conditions (with monthly totals of below 15mm) have been recorded over the northern Western Cape Province and the Northern Cape Province. All three model configurations indicate an over-estimation of monthly rainfall over the country; however, eye ball verification of the three configurations shows that the 12km UM simulation with DA performed better than the 12km and 15km UM simulations without DA.

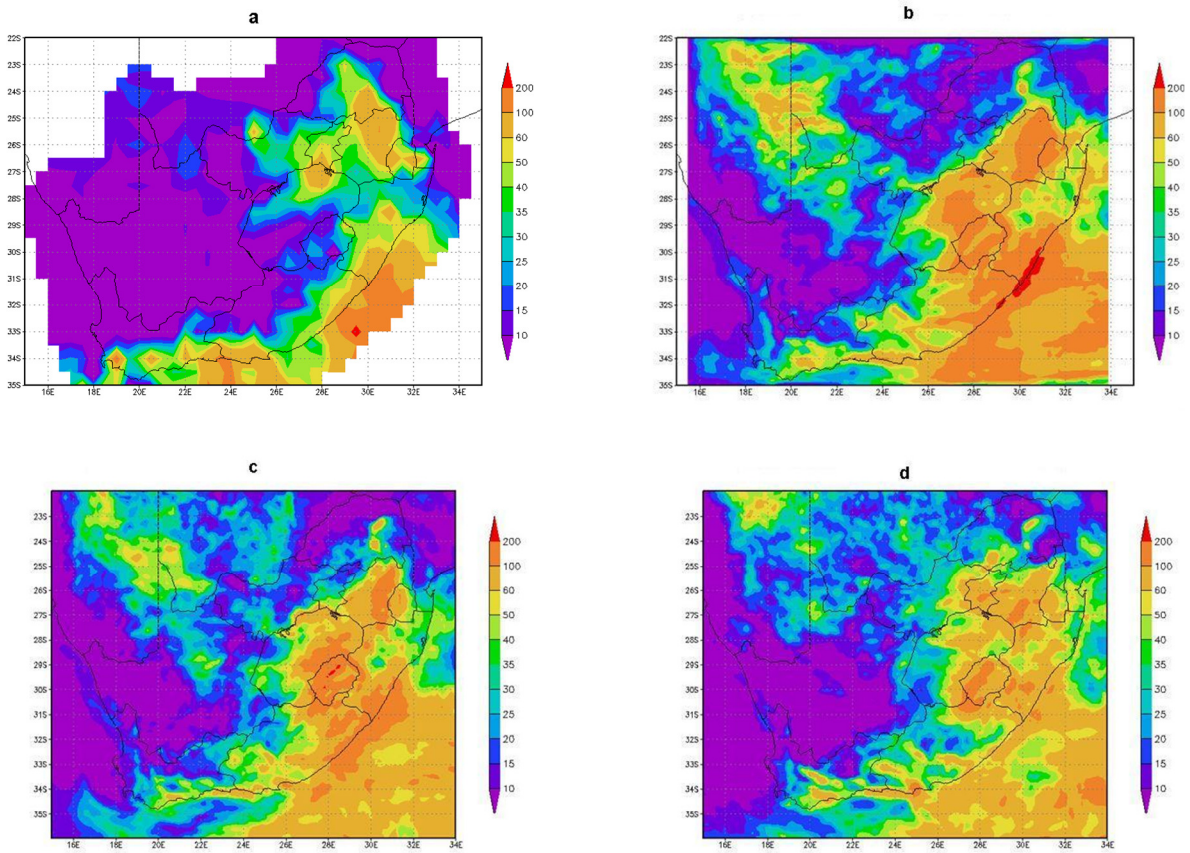

Figure 4.4:

October 2008 rainfall totals measured in mm from (a) observations, (b) 15km Unified Model (UM) without Data Assimilation (DA), (c) 12km UM without D A and (d) 12km UM with DA simulations.

4.3 CATEGORICAL VERIFICATION SCORES

The rainfall stations were group into eight homogeneous rainfall regions (figure 2.3) based on the standardized monthly rainfall totals obtained by cluster analysis. Mason (1998) grouped rainfall stations into regions with similar inter-annual rainfall variability. Five rainfall thresholds were selected to verify rainfall in the different regions, namely rainfall equal or above 0.1mm, 0.5mm, 2.0mm, 10.0mm and 50.0 mm per 24-hour. The PC, BIAS and FAR scores described in Chapter 3 were used in verifying UM rainfall simulation output for the eight different regions.

4.3.1 PERCENT CORRECT

The rainfall results of the PC scores (figures 4.5 and 4.6) show no significant difference in the PC scores of all three model configurations for the 0.1mm and 0.5mm rainfall thresholds. All the model configurations did well for all months (January to December) used in the study. The PC scores range from 0.97 to 1 for the 0.1mm rainfall threshold, and the highest PC scores are evident for July in all the rainfall regions, except for region 1 of figure 2.3. The 0.5mm threshold (figure 4.6) also showed the same pattern for the three model configuration and the PC scores range from 0.85 to 1. Region 1 had the highest PC scores for the January to March period, and the lowest scores for the June to September period. During the months April, November and December, region 8 had the best PC scores. The region with the lowest scores was region 5 (especially for January and November) and the highest scores are evident in July for all rainfall regions, except for region 1.

The PC scores for the 2mm rainfall threshold are shown in figure 4.7. The pattern is the same for all three UM configurations, but the 12km UM simulation with DA showed PC scores of 0.8 and above for the months of May to September; whereas the PC scores for the 12km and 15km UM simulations without DA where below 0.8 for the same months. On average, PC scores for the 12km UM simulation with DA were higher than those of the 12km and 15km UM simulations without DA for all months and regions used. Significant differences between model simulations and observations start to show from the 2mm rainfall threshold category, indicating that PC scores decrease with increasing rainfall threshold.

Results from the 10mm threshold indicated in figure 4.8 show that the 12km UM simulation with DA did better than the 12km and 15km UM simulations without DA. The lowest PC score for the 12km UM simulation with DA was 0.62 (for December), and those of the 12km and 15km UM simulations without DA were 0.6 and 0.59, respectively. During the months of May to September the PC scores for the 12km UM simulation with DA ranged from 0.8 to 0.98, while the range for the 12km UM simulation without DA was 0.63 to 0.9 and for the 15km UM simulation without DA was 0.6 to 0.95. The pattern is almost the same for all three configurations. Rainfall region 1 appears to have the worst scores during winter months, region 3 the worst scores during November to December and region 8 the best scores from October to December.

Results illustrated in figure 4.9 show PC scores for the 50mm rainfall threshold. A different pattern for the three configurations is evident, compared to previous thresholds. However, the 12km UM simulation with DA showed higher scores as compared to the 12km and 15km UM simulations without DA . The score range for the 12km UM simulation with DA from May to September was from 0.78 to 1. Similarly the PC score range was from 0.42 to 0.69 for the 12km UM simulation without DA and 0.45 to 0.93 for the 15km UM simulation without DA. The lowest PC scores were found over summer months, while the lowest PC score was 0.45 (for February) in the12km UM simulation with DA, 0.39 (for January) in the12km UM simulation without DA and 0.30 (for December) in the15km UM simulation without DA.

The three model configurations used in this study yielded almost the same pattern in PC scores for the lower rainfall thresholds (< 2mm threshold). As the rainfall thresholds increased, differences were noted from the three UM configurations. The difference in the PC scores is more pronounced in the 12km UM simulation with DA when compared to the 12km and 15km UM simulations without DA. The results further indicate the 12km UM simulation with DA is superior to the 12km and 15km UM simulations without DA.

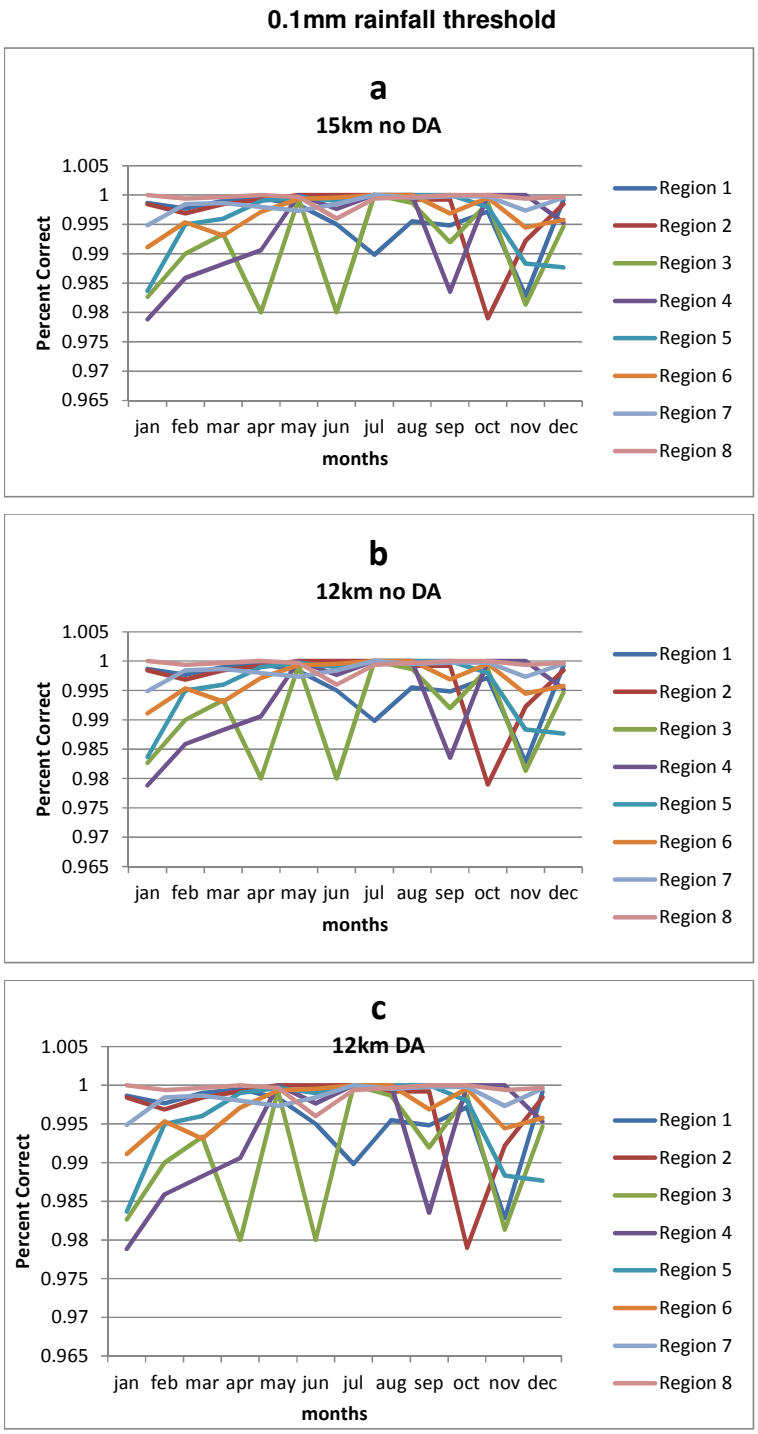

Figure 4.5:

Percent Correct (PC) scores for the 0.1mm rainfall threshold for days during 2008 from (a) the 15km Unified Model (UM) simulation without Data Assimilation (DA), (b) the 12km UM simulation without DA and (c) the 12km UM simulation with DA.

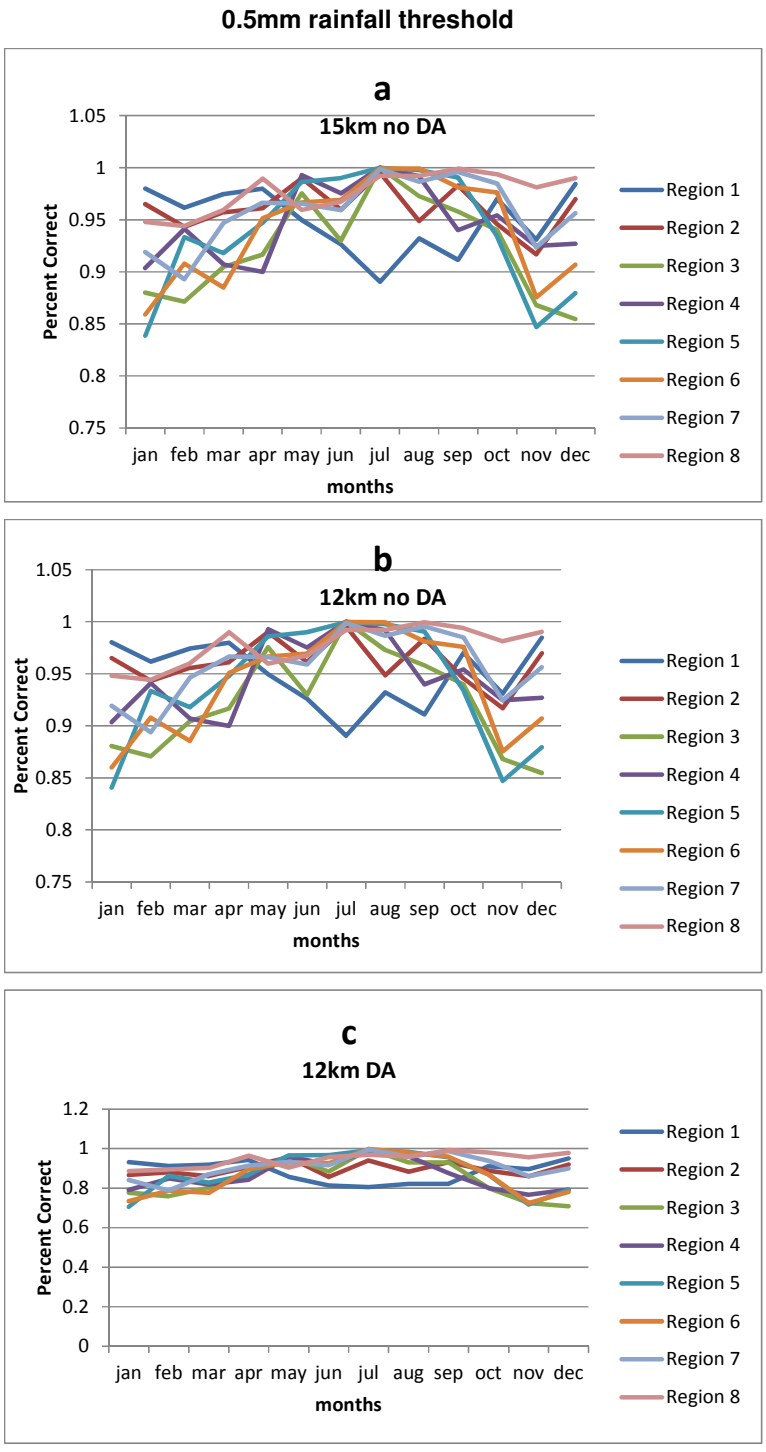

Figure 4.6:

Percent Correct (PC) scores for the 0.5mm rainfall threshold for days during 2008 from (a) the 15km Unified Model (UM) simulation without Data Assimilation (DA), (b) the 12km UM simulation without DA and (c) the 12km UM simulation with DA.

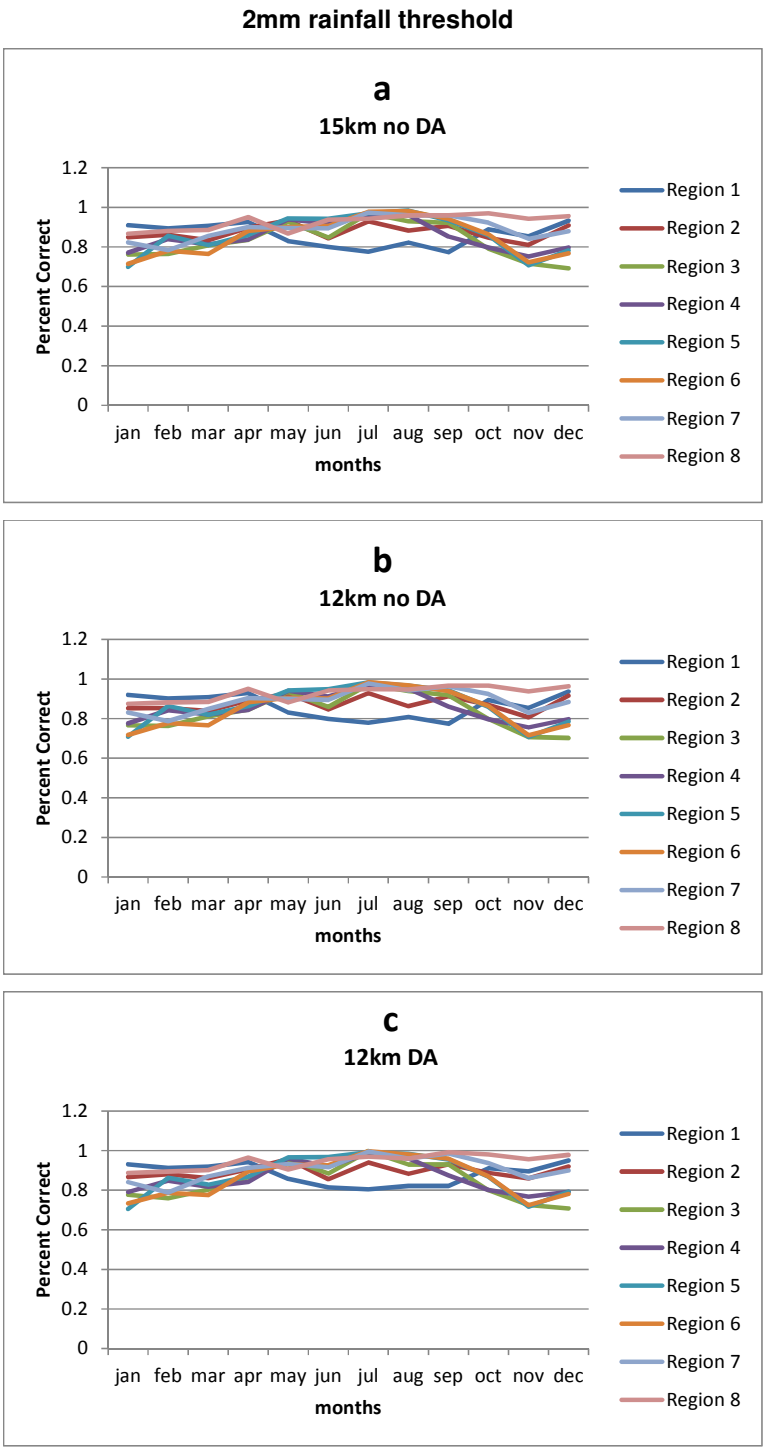

Figure 4.7:

The Percent Correct (PC) scores for the 2mm rainfall threshold for days during 2008 from (a) the 15km Unified Model (UM) simulation without Data Assimilation (DA), (b) the 12km UM simulation without DA and (c) the 12km UM simulation with DA.

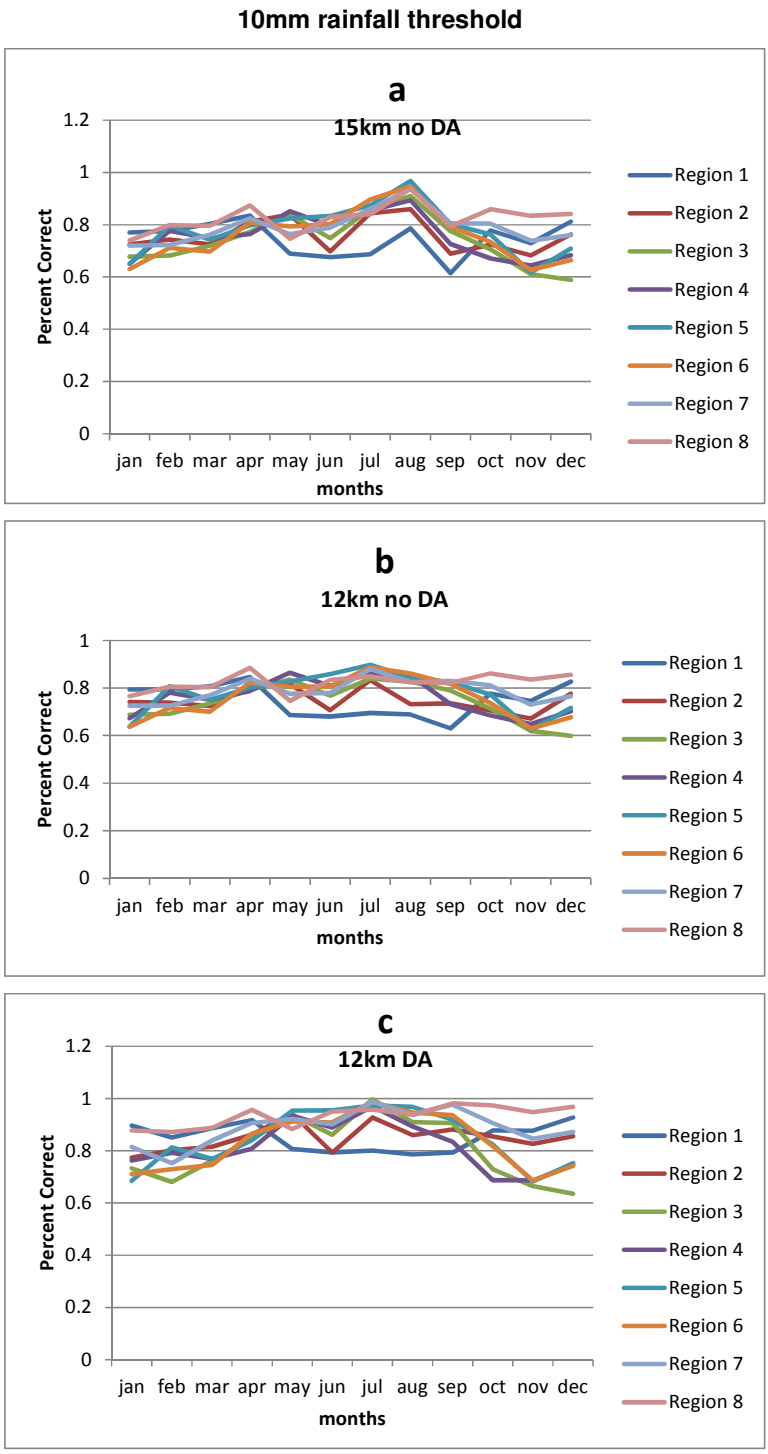

Figure 4.8:

The Percent Correct (PC) scores for the 10mm rainfall threshold for days during 2008 from (a) the 15km Unified Model (UM) simulation without Data Assimilation (DA), (b) the 12km UM simulation without DA and (c) the 12km UM simulation with DA.

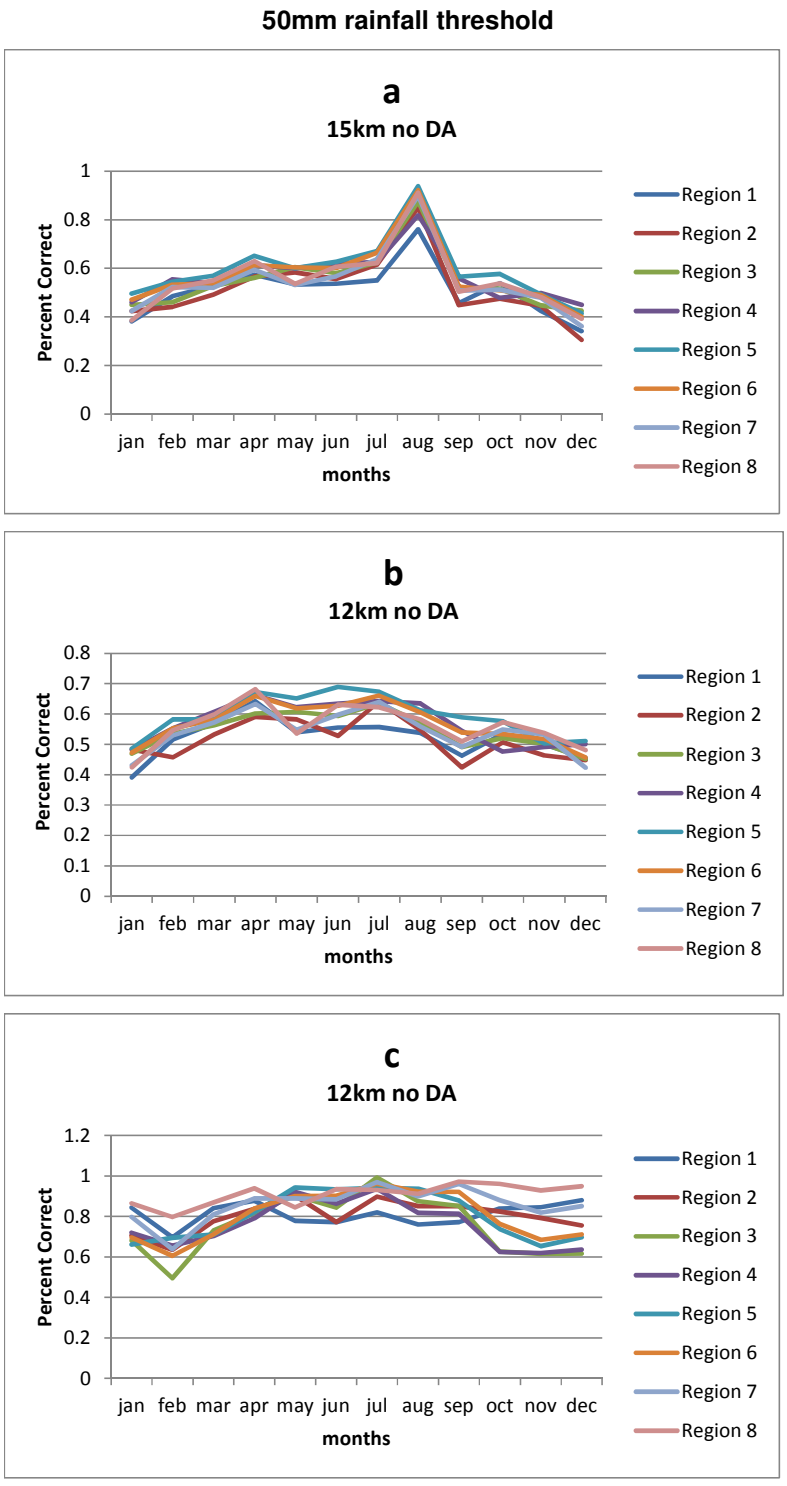

Figure 4.9:

The Percent Correct (PC) scores for the 50mm rainfall threshold for days during 2008 from (a) the 15km Unified Model (UM) simulation without Data Assimilation (DA), (b) the 12km UM simulation without DA and (c) the 12km UM simulation with DA.

4.3.2 BIAS

BIAS score results from rainfall simulated by the three UM configurations are shown in figures 4.10 and 4.11. Extremely small BIASes are evident in all three model configurations for the 0.1mm and 0.5mm rainfall threshold. The BIAS scores show an increase with rainfall threshold value. Figure 4.12 indicate the BIAS scores for the 2mm rainfall threshold. The BIAS scores for 12km UM simulation with DA is smaller when compared to the 12km and 15km simulations without DA. The maximum BIAS of 0.6mm (September) occur in the 12km UM simulation with DA. A maximum BIAS of 4mm (September) and 4.5mm (July) are similarly evident for the 12km and 15km UM simulations without DA, respectively.

BIAS scores for the 10mm rainfall threshold are denoted by figure 4.13. The figure shows that the 12km UM simulation with DA outperformed the 12km and 15km UM simulation without DA. The highest BIAS for the 12km UM simulation with DA is 1.4mm (July), 7.8mm (July) for the 12km UM simulation with DA and 8mm (July) for the 15km UM simulation without DA. The results for BIAS scores for the 50mm rainfall threshold are illustrated in figure 4.14. The 12km UM simulation with DA performed better than the 12km and 15km UM simulations without DA. The 12km and 15km UM simulations without DA had the largest errors for the 50mm rainfall threshold, with the highest BIAS of 9 for the 12km UM simulation without DA and 9.1 for the 15km UM simulation without DA.

In summary, all three model configurations indicate extremely small BIASes for the 0.1mm rainfall threshold analyses. A more obvious BIAS starts to become evident beyond the 0.1mm rainfall threshold. The BIAS scores for the three model configurations further show a general overestimation of rainfall beyond the 0.5mm rainfall threshold, especially during winter months. The 12km UM with DA, had lesser BIASes for almost all rainfall thresholds in all regions; implying more accuracy than the 12km UM simulation and 15km UM simulation without DA. BIAS scores for the 12km UM simulation and 15km UM simulation without DA were almost the same, but with 12km UM simulation without DA yielding slightly lesser BIASes.

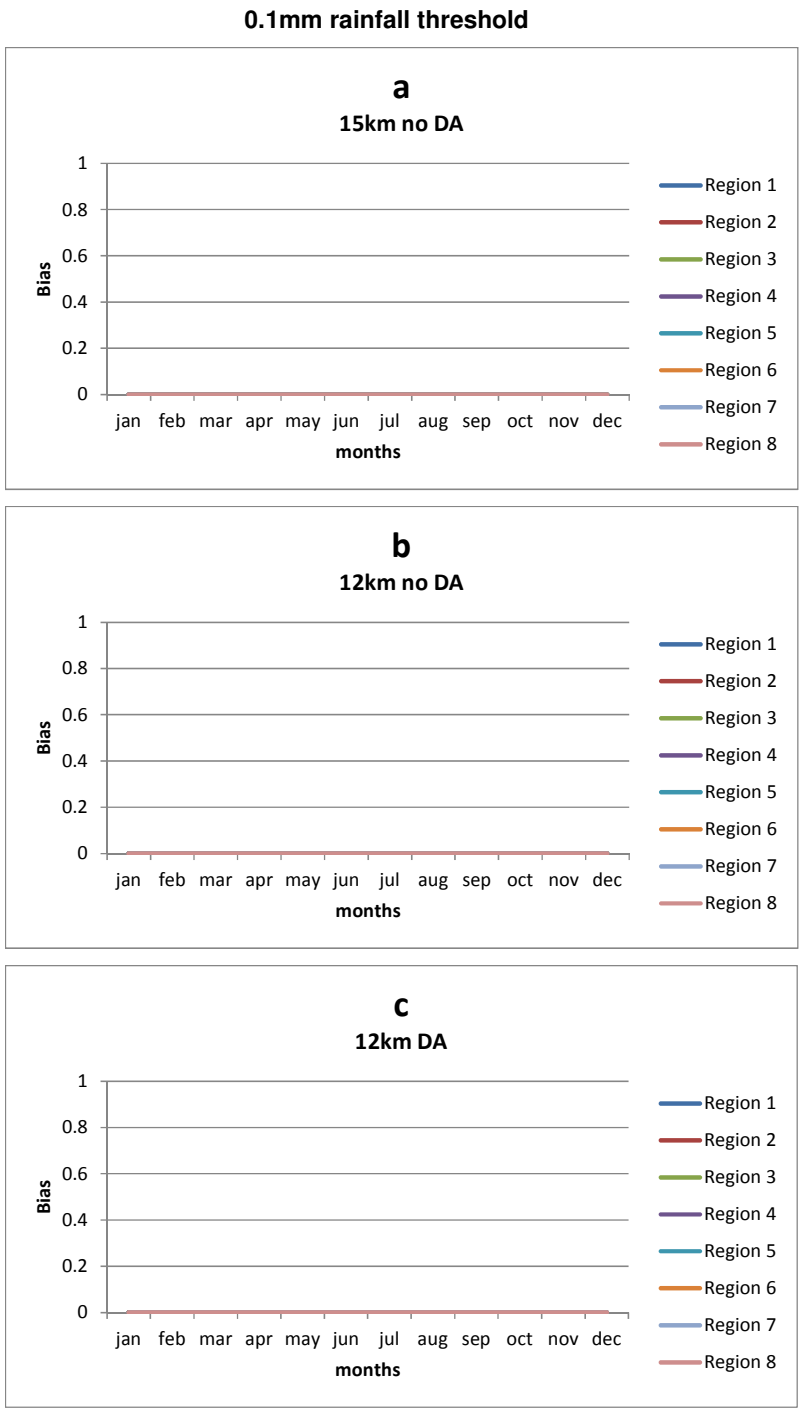

Figure 4.10:

BIAS scores for the 0.1mm rainfall threshold for days during 2008 from (a) the 15km Unified Model (UM) simulation without Data Assimilation (DA), (b) the 12km UM simulation without DA and (c) the 12km UM simulation with DA.

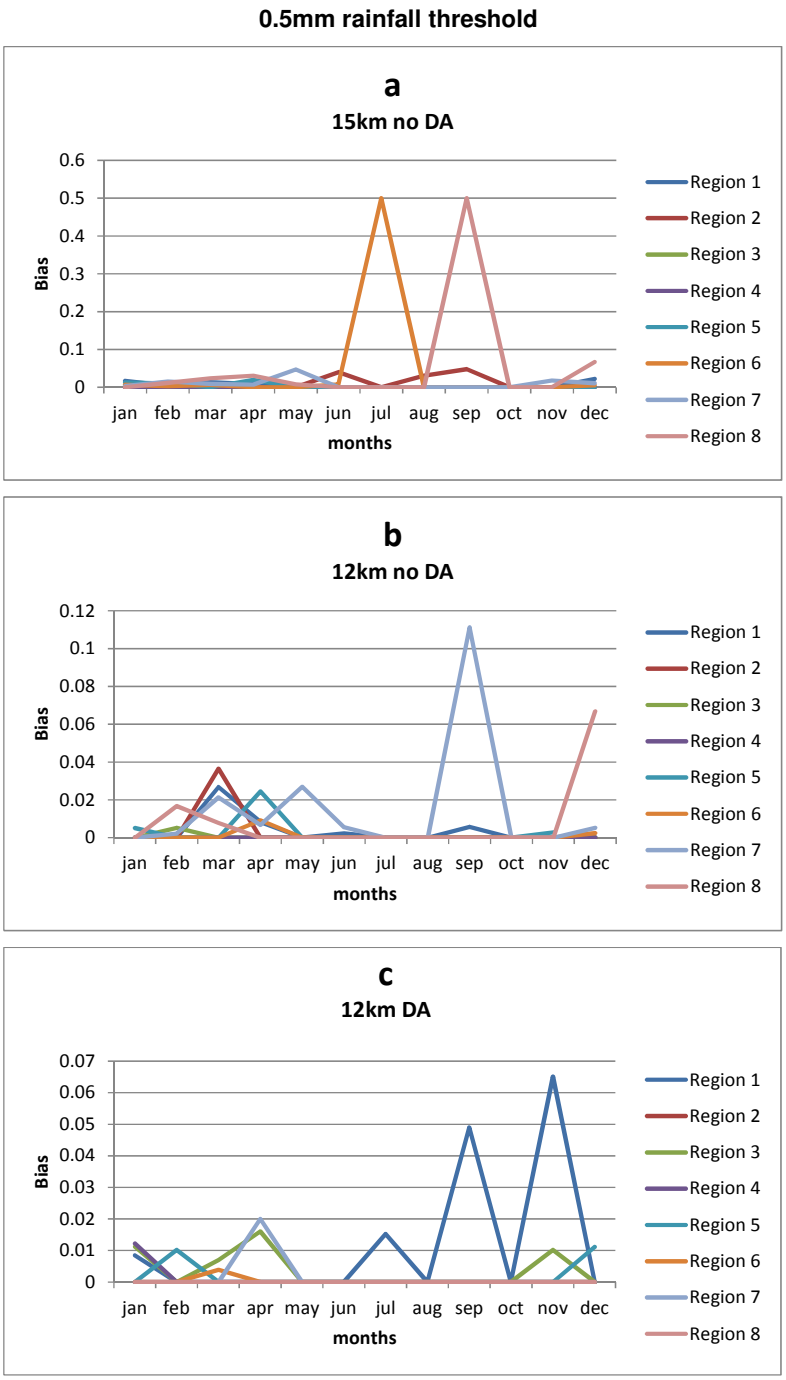

Figure 4.11:

BIAS scores for the 0.5mm rainfall threshold for days during 2008 from (a) the 15km Unified Model (UM) without Data Assimilation (DA), (b) 12km UM simulation without DA and (c) 12km UM simulation with DA.

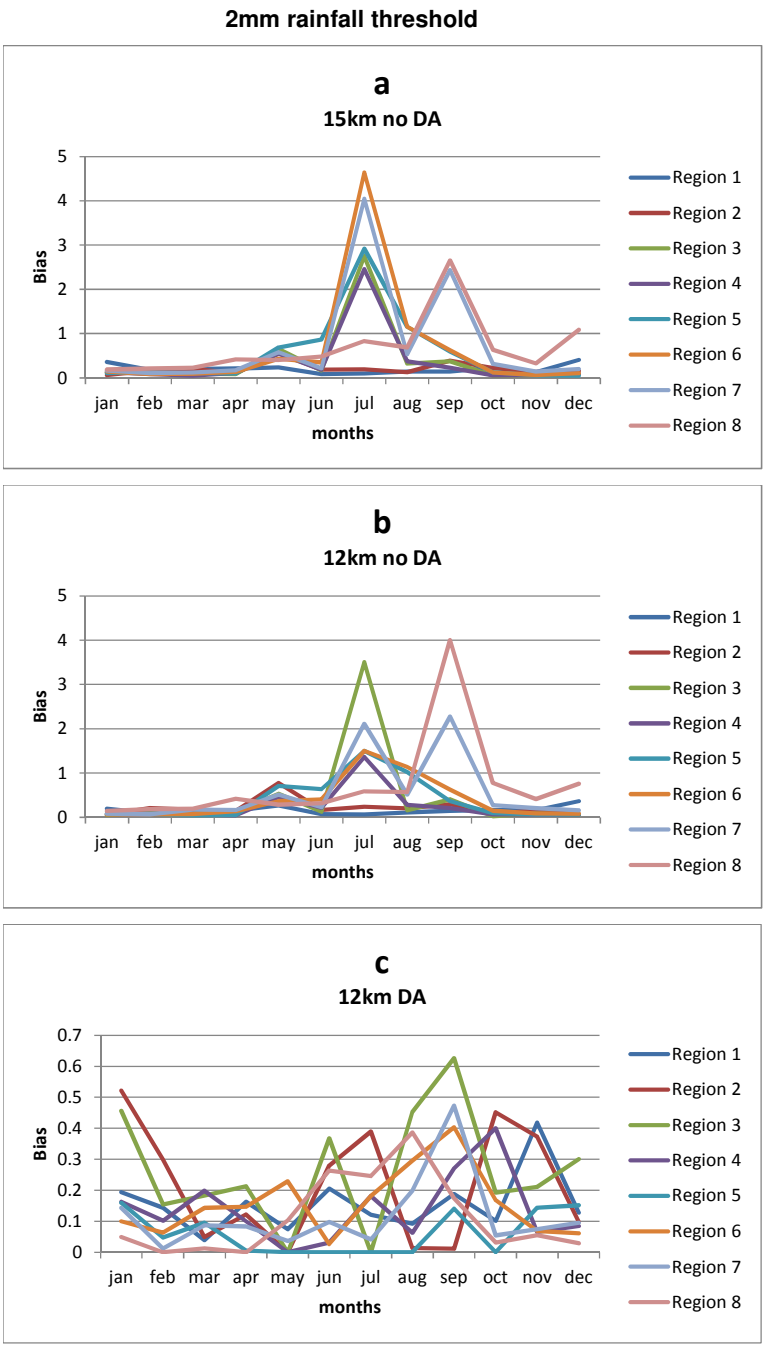

Figure 4.12:

BIAS scores for the 2mm rainfall threshold for days during 2008 from (a) the 15km Unified Model (UM) without Data Assimilation (DA), (b) 12km UM simulation without DA and (c) 12km UM simulation with DA.

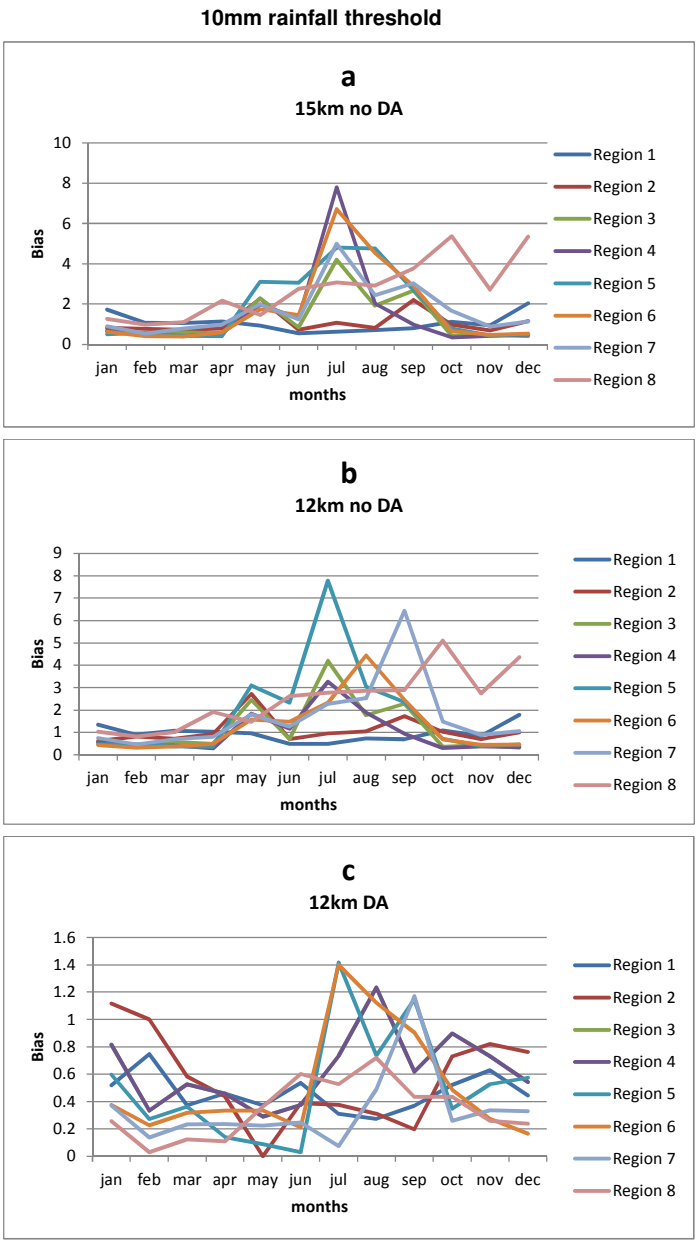

Figure 4.13:

BIAS scores for the 10mm rainfall threshold for days during 2008 from (a) the 15km Unified Model (UM) without Data Assimilation (DA), (b) 12km UM simulation without DA and (c) 12km UM simulation with DA.

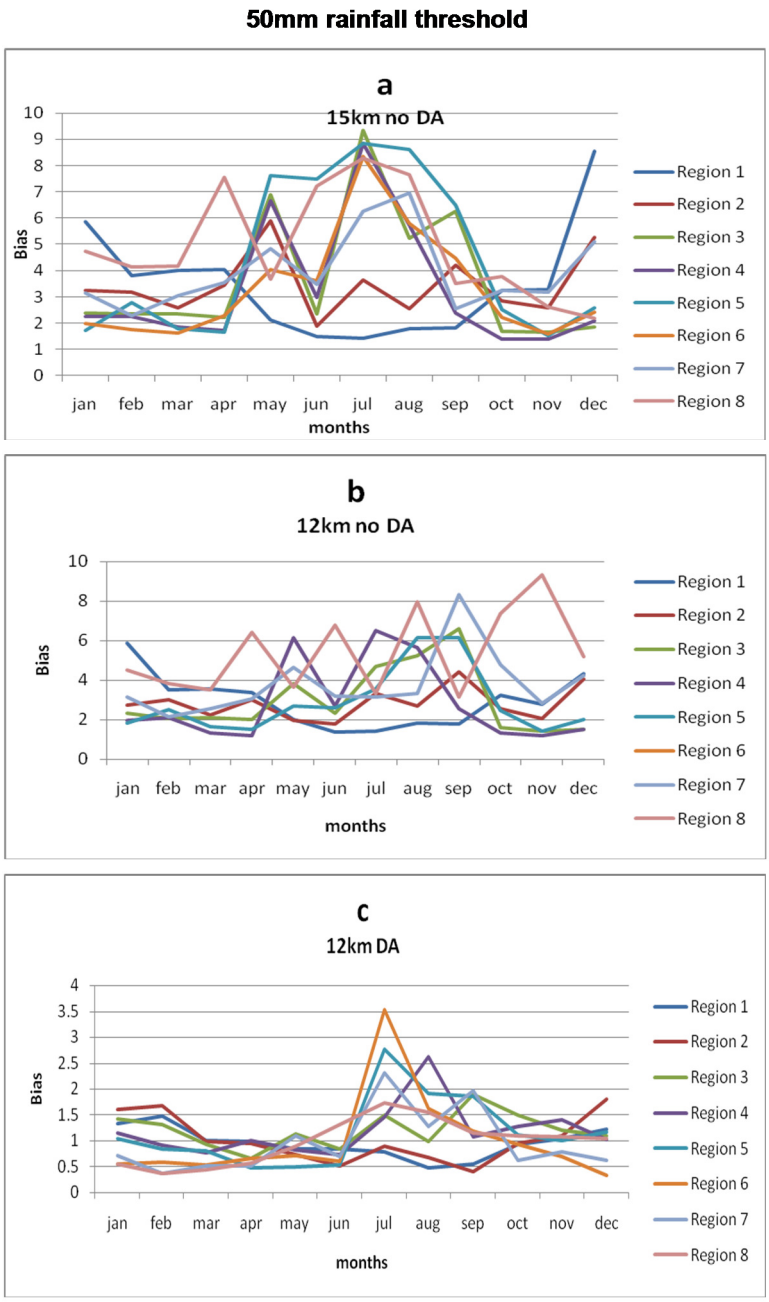

Figure 4.14:

BIAS scores for the 50mm rainfall threshold for days during 2008 from (a) the 15km Unified Model (UM) without Data Assimilation (DA), (b) 12km UM simulation without DA and (c) 12km UM simulation with DA.

4.3.3 FALSE ALARM RATE

The FAR scores for rainfall simulated by the three configurations of the UM are shown in figures 4.15 to 4.19. All three UM simulations show extremely small FAR values for the 0.1mm rainfall threshold for all the months (figure 4.15). These results are consistent with the low BIASes and high PC scores recorded for this threshold, confirming that the UM can be used as a reliable indicator in forecasting the occurrence of rainfall for smaller thresholds.

A noticeable increase in the FAR scores for the 0.5mm rainfall threshold as compared to the 0.1mm rainfall threshold for all three UM simulations is demonstrated in figure 4.16. The 12km and 15km UM simulations without DA indicate a FAR value of 1 for the entire year, while the 12km UM simulation with DA shows a FAR value of 1 only for the months January to March. The results prove that the 12km UM simulation with DA is more reliable in predicting rainfall of 0.5mm and higher as compared to the 12km and 15km UM simulations without DA.

FAR results for the 2mm rainfall threshold indicated in figure 4.17, are generally high for the 12km and 15km UM simulations without DA for all months. Although there is some regions with a FAR value of 1 for the 12km UM simulation with DA, most of the regions indicate a FAR value of zero for most of the months. FAR scores for the 10mm rainfall threshold (figure 4.18) show a similar pattern but higher FAR scores than those of the 2mm rainfall threshold. All three model configurations show a tendency to overestimate daily rainfall of 2mm and higher as well as 10mm and higher for all the months and regions, but of all the three model configurations, the 12km UM simulation with DA proved to be more reliable

The 12km and 15km UM simulations without DA generally show high FAR scores for the 50mm rainfall threshold for all the months and all regions used (figure 4.19). The 12km UM simulation with DA also indicates high FAR scores but lower than those of the 12km and 15km UM simulations without DA. This shows that the three UM simulations overestimates the occurrence of 50mm rainfall events, but the 12km UM simulation with DA performs better.

All three UM simulations show an increase in FAR values, when examining progressively larger rainfall thresholds for all months and regions. The FAR values are higher for the 12km and 15km UM simulations without DA and lower for the 12km UM simulation with DA. This results confirms

that the 12km UM simulation is more reliable than the 12km and 15km UM simulations without DA.

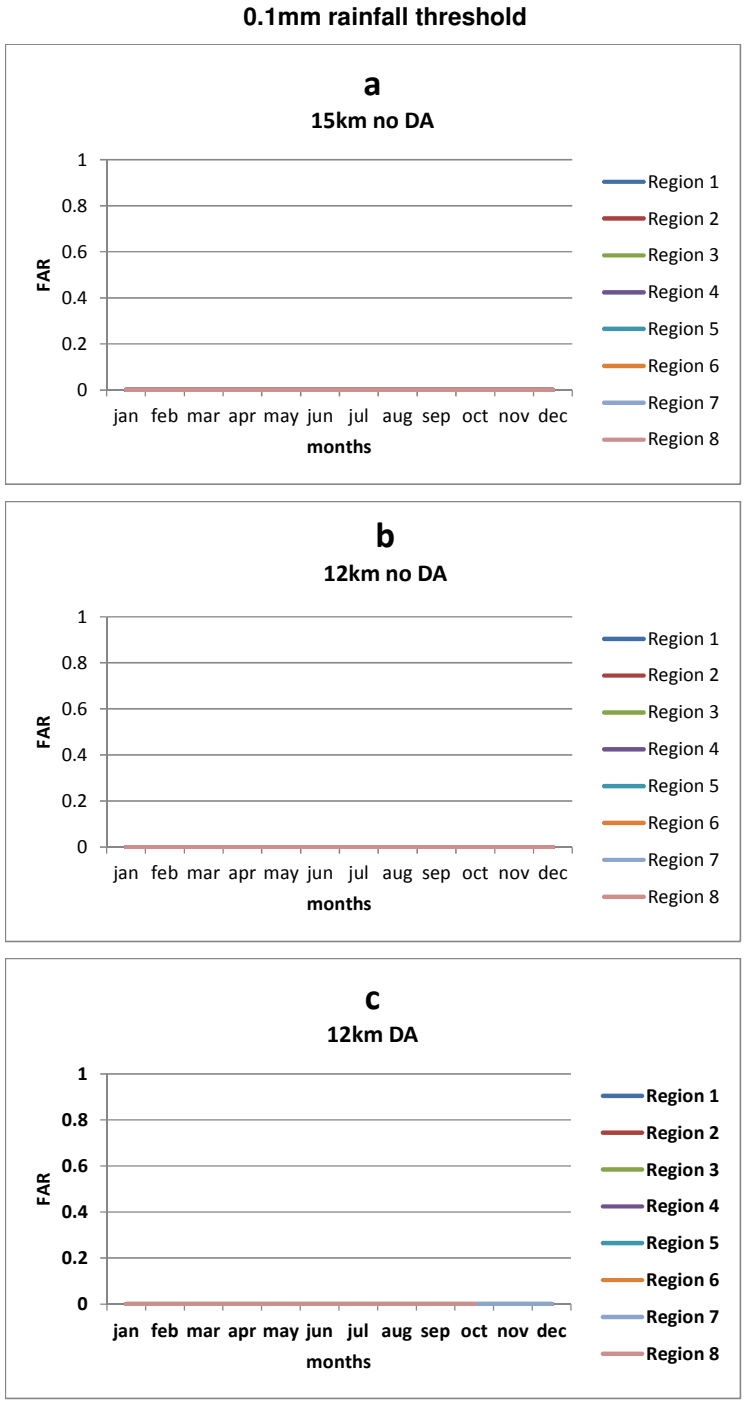

Figure 4.15:

False Alarm Rate (FAR) scores for the 0.1mm rainfall threshold for days during 2008 from (a) the 15km Unified Model (UM) simulation without Data Assimilation (DA), (b) the 12km UM simulation without DA and (c) the 12km UM simulation with DA.

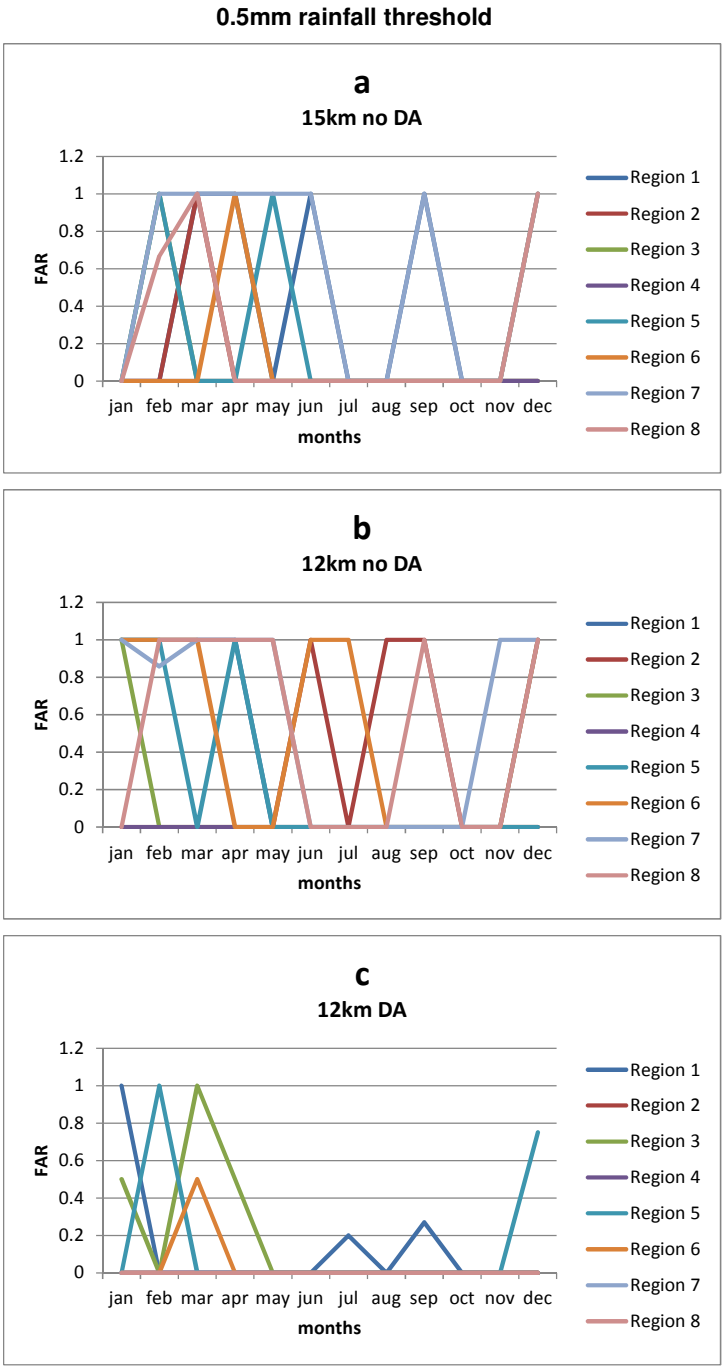

Figure 4.16:

False Alarm Rate (FAR) scores for the 0.5mm rainfall threshold for days during 2008 from (a) the 15km Unified Model (UM) simulation without Data Assimilation (DA), (b) the 12km UM simulation without DA and (c) the 12km UM simulation with DA.

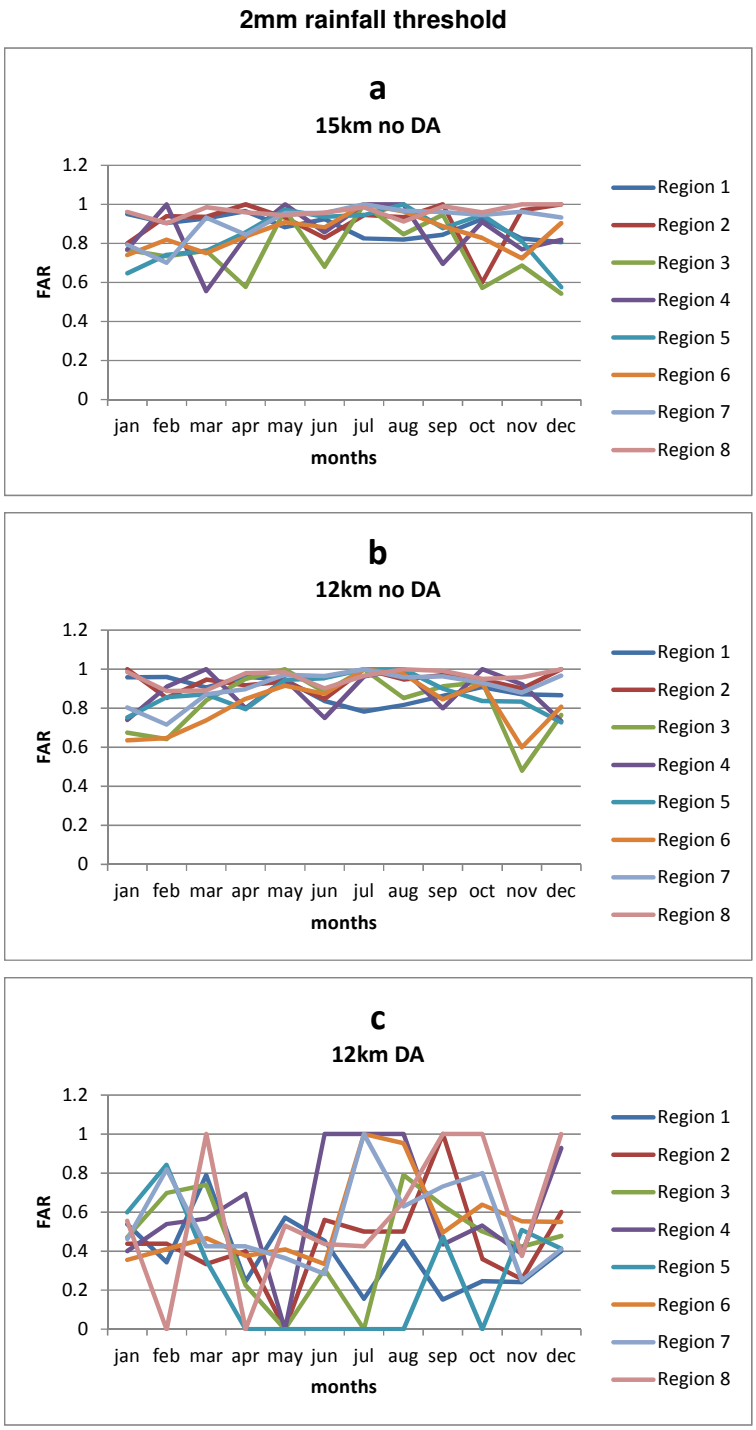

Figure 4.17:

FAR scores for the 2mm rainfall threshold for days during 2008 from (a) the 15km Unified Model (UM) simulation without Data Assimilation (DA), (b) the 12km UM simulation without DA and (c) the 12km UM simulation with DA.

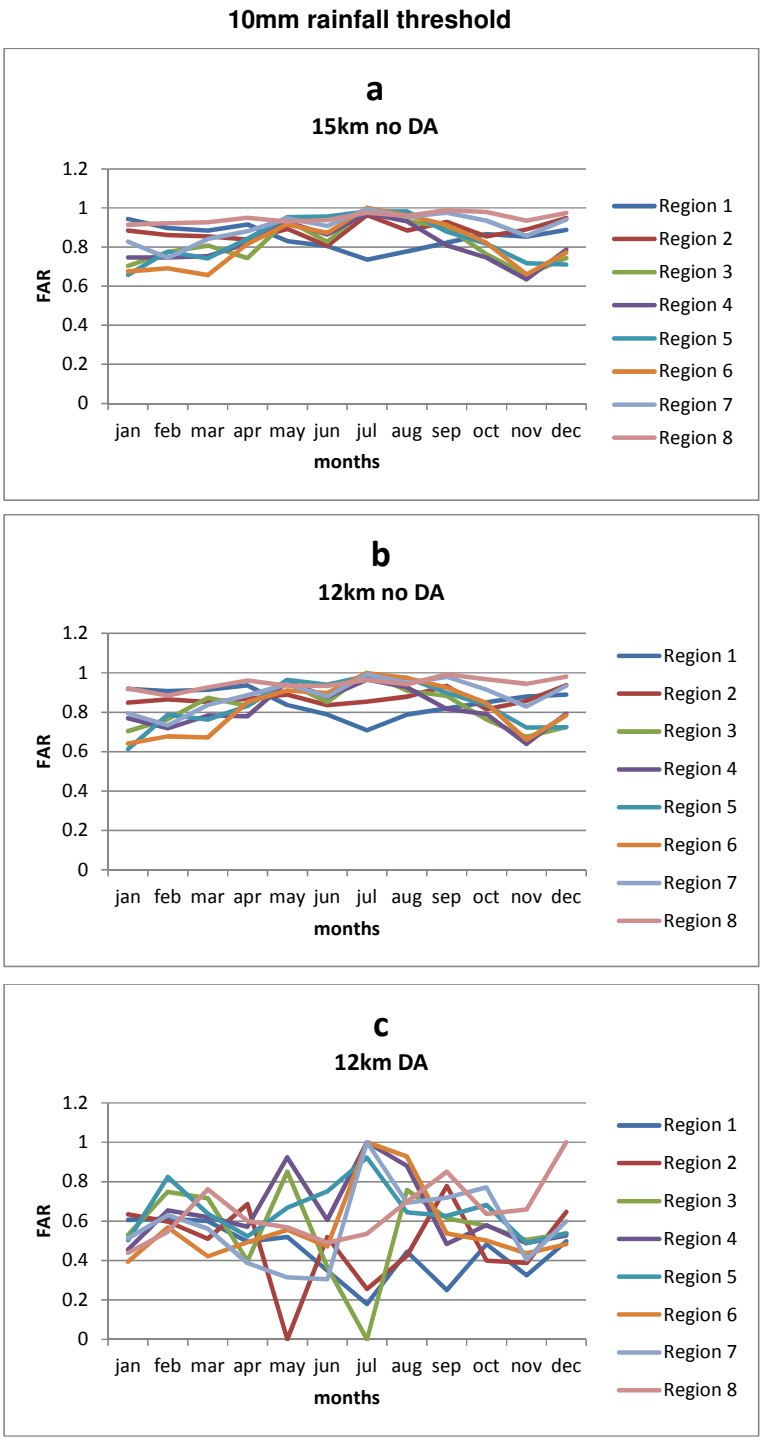

Figure 4.18:

False Alarm Rate (FAR) scores for the 10mm rainfall threshold for days during 2008 from (a) the 15km Unified Model (UM) simulation without Data Assimilation (DA), (b) the 12km UM simulation without DA and (c) the 12km UM simulation with DA.

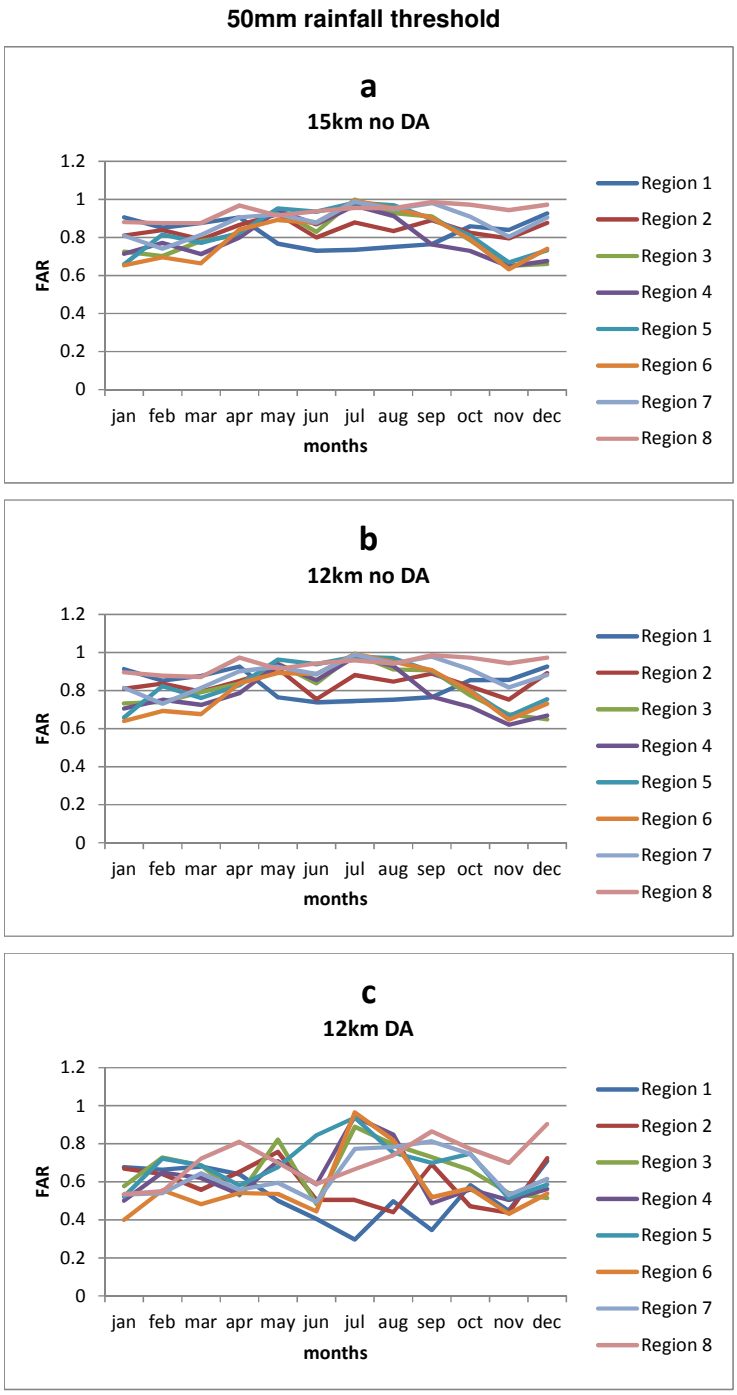

Figure 4.19:

False Alarm Rate (FAR) scores for the 50mm rainfall threshold for days during 2008 from (a) the 15km Unified Model (UM) simulation without Data Assimilation (DA), (b) the 12km UM simulation without DA and (c) the 12km UM simulation with DA.

4.4 VERIFICATION SCORES FOR CONTINUOUS VARIABLES

Different point stations were selected across the South African domain to verify rainfall at different locations (figure 4.20). The monthly average MAE and RMSE scores for the 24-hour rainfall for the selected stations was investigated and results are discussed.

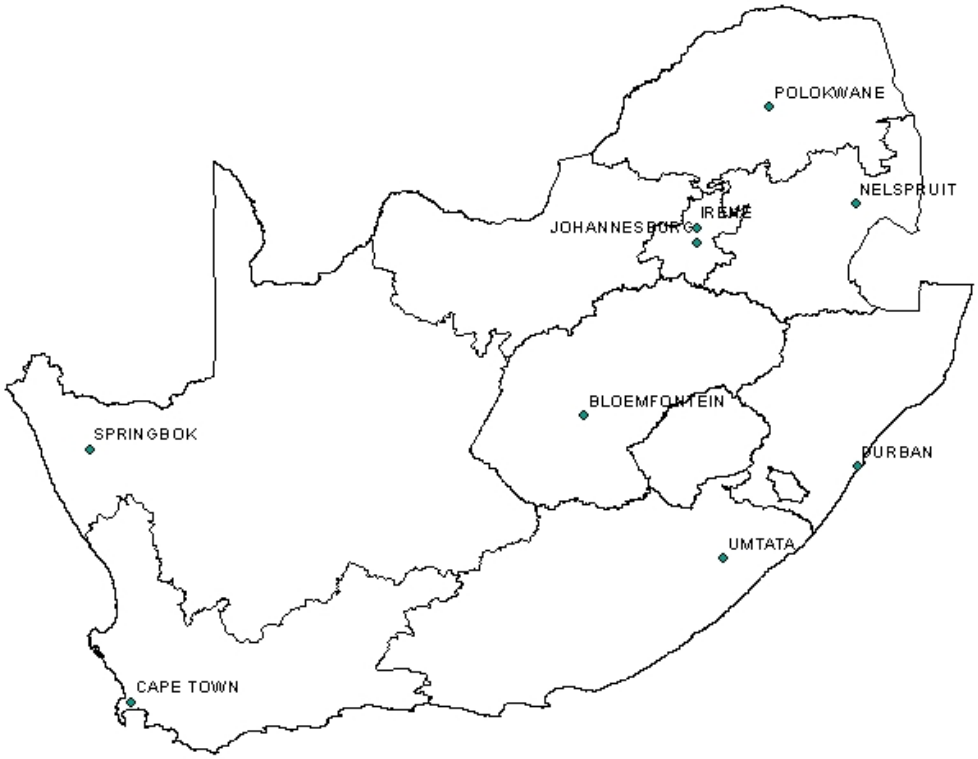

Figure 4.20:
Location of weather stations used for the verification of continuous variables.

4.4.1 MAE

Figure 4.21 demonstrates the MAE results from rainfall simulated by the three UM configurations for several stations across South Africa. All three configurations show small MAE scores for July and August for Durban, Nelspruit, Polokwane, Irene, Johannesburg, Umtata and Bloemfontein.

High MAE scores for these stations are evident during the summer months. This could be atributed to the fact the these stations fall within summer rainfall regions (Mason,1998; Schulze and Maharaj, 2007). Springbok although had highest MAE during July, its MAE scores are less throughout the entire period ranging from 0.1 in April to 2.4 in July. This may be due to the fact that Springbok falls within an arid region of South Africa. Cape Town has less MAE scores for the months December to April as well as in the month of October, and bigger MAE score during the months of June to September as well as the November month. This may be the result of the Mediterranean climate experienced over Cape Town.

The MAE results further show the differences for the three simulations. The 12km UM simulation with DA outperformed the other configurations in most of the months and for all stations used in this study. There is however months where the 12km UM simulation with DA performed the worst; this is evident over Johannesburg and Bloemfontein for the months January and February respectively. The three model configurations showed similar scores for Durban during July, Nelspruit during February, Polokwane in January, Cape Town in August and Bloemfontein in January. The MAE scores the 12km and 15km UM simulations without DA were similar but the 15km UM simulation performed better than the 12km UM simulation without DA in most of the months and for all the stations used in the study.

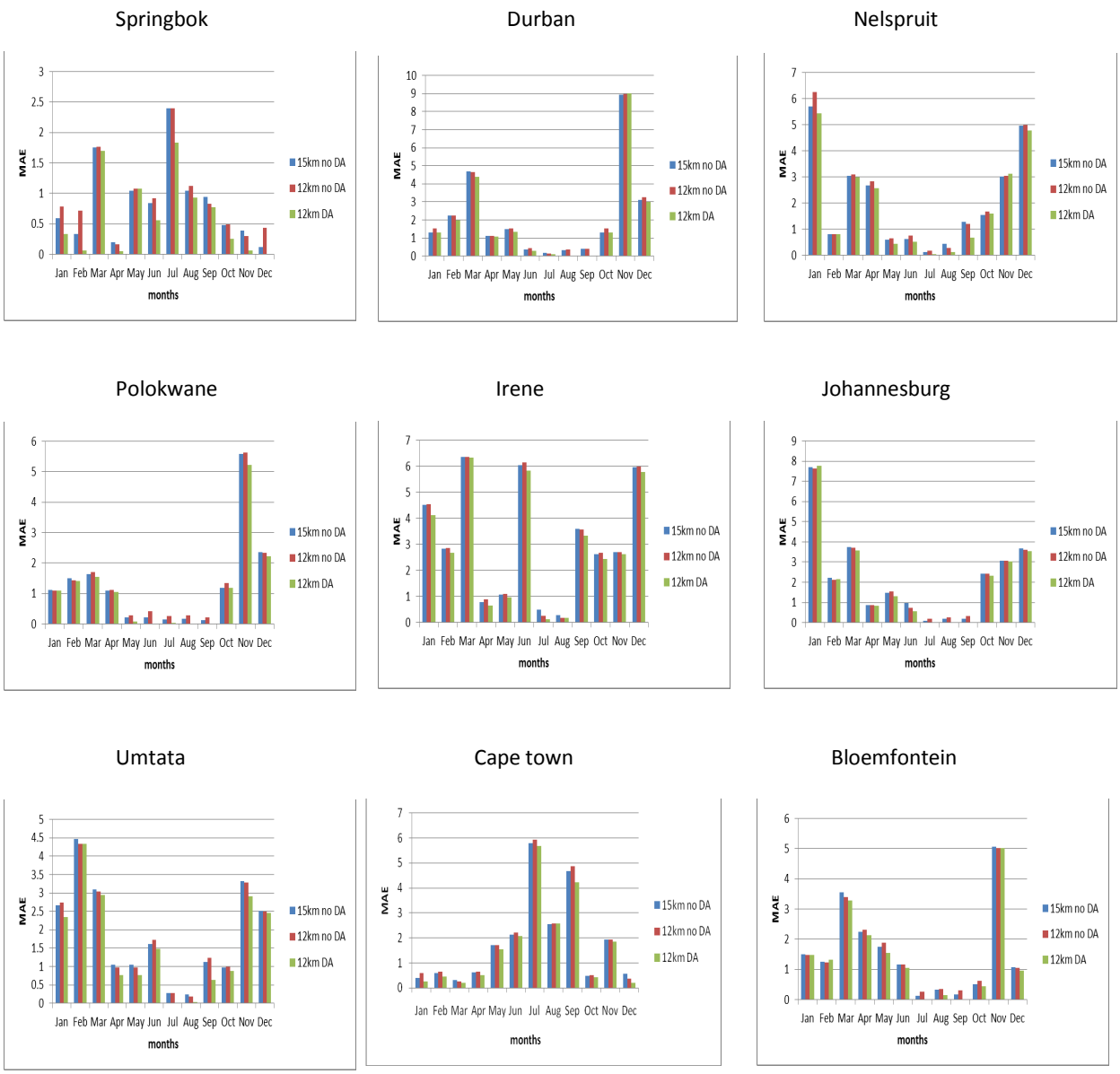

Figure 4.21:

The Mean Absolute Error (MAE) verification scores of daily rainfall during 2008 for the three Unified Model (UM) configurations, at selected weather stations across South Africa.

4.4.2 RMSE

The RMSE results from rainfall simulated by the three UM configurations for several stations across South Africa are illustrated in figure 4.22. The three UM configurations show a similar pattern in simulating rainfall for selected stations across South Africa. All three simulations show lower RMSE scores for winter months especially July and August for all the stations, except Springbok and Cape Town; and higher RMSE scores for summer months for the very same stations. The RMSE scores for Cape Town and Springbok show less error for the months December and bigger RMSE scores in July.

Although the three UM simulations showed a similar pattern for the RMSE scores for all the months and all stations, the 12km UM simulation with DA outperformed the 12km and 15km UM simulations without DA for most of the months and for all stations used in the study. The RMSE scores the 12km and 15km UM simulations without DA were similar but the 15km UM simulation without DA outscored the 12km UM simulation without DA in most of the months for all the stations used in the study.

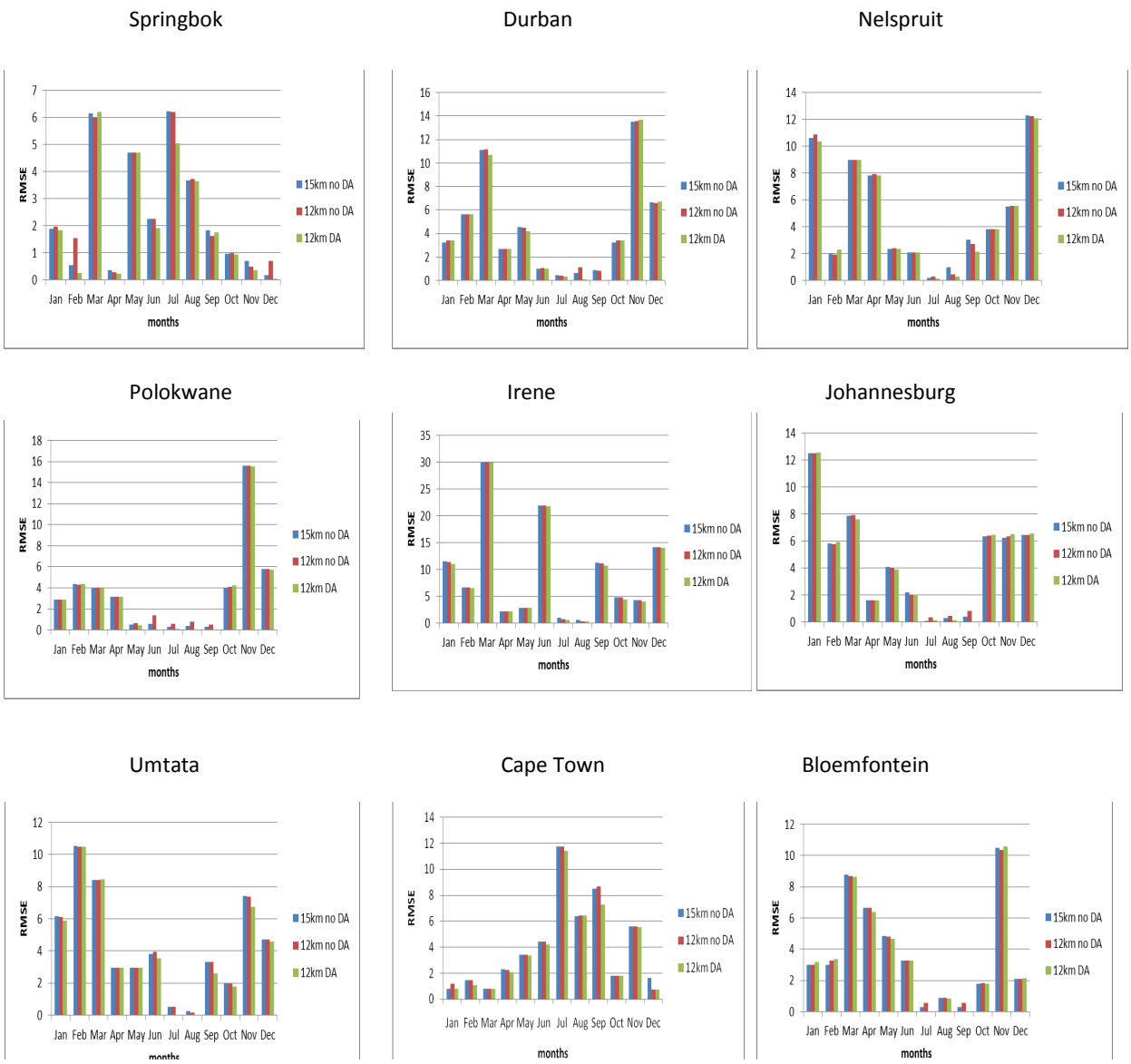

Figure 4.22:

The Root Mean Square Error (RMSE) verification scores of daily rainfall during 2008 for the three Unified Model (UM) configurations, at selected weather stations across South Africa.

4.5 SUMMARY

The verification of daily rainfall for three configurations of the UM has been presented. Three types of verification were done, namely (1) eye ball verification (2) verification of categorical variables and finally verification of continuous variables. Verifications scores from the three model configurations used in this study were consistent to each other and indicate a general overestimation of rainfall throughout the country. The results further indicate an ability of the three

configurations of the UM in simulating rainfall for smaller rainfall thresholds and a general difficulty of in simulating rainfall for thresholds beyond 0.5mm. All three types of verification done in this study show that the sole additional information produced by DA, had a beneficial impact in simulating rainfall over South Africa, thus increasing the skill of the 12km UM simulation with DA over the 12km and 15km simulations without DA. The results further indicate that there is no significant difference between the 12km and 15km UM simulations without DA.

CHAPTER 5

MINIMUM AND MAXIMUM TEMPERATURES

5.1 INTRODUCTION

In Chapter 3 the methods used to meet the research objectives of this study are outlined. The objectives involve evaluating the performance of the UM which is operational at the SAWS. In this chapter the observed minimum and maximum temperatures for the period January to December 2008 are compared with the three configurations of the UM. Verification of temperature in this study is done in two ways. Firstly the model is subjectively verified using the eyeball verification for the entire domain of South Africa, followed by an objective verification of continuous variables for selected stations over South Africa.

5.2 EYEBALL VERIFICATION

Eyeball verification, as defined in Section 4.2, is also applied in verifying temperatures. The observed minimum and maximum temperatures used in this study are only limited to South African weather stations and may not give a true representation over Namibia, Swaziland and Lesotho. Eyeball verification results for four months, namely January (mid-summer), July (mid-winter) and the transition months April (autumn) and October (spring) for the year 2008 is illustrated in figures 5.1 to 5.8.

5.2.1 MINIMUM TEMPERATURES

Averaged minimum temperatures for January 2008 are displayed in figure 5.1. The minimum temperatures for January 2008 range from 12^0C to over 18^0C over the central interior of South Africa. Minimum temperatures below 14^0C are confined to the eastern escarpment, but there are also areas over the northern parts of the Western Cape and southern parts of the Northern Cape Provinces where temperatures below 14^0C were recorded. High minimum temperatures were observed over the Northern Cape and Limpopo Provinces as well as the eastern coasts. A similar pattern to the observed is evident from the three UM configurations used in this study, but recorded minimum temperatures below 14^0C over a

larger area than the observed. In spite of this the 12km UM simulation with DA showed a closer resemblance to the observed.

Average minimum temperatures for April 2008 are shown in figure 5.2. Observed minimum temperatures for April 2008 range from 0^0C to 12^0C for the interior of South Africa, although there are some parts over the Free State, Eastern Cape and Northern Cape Provinces where minimum temperatures are below 0^0C. The three UM configurations show a similar pattern, but the 12km and 15km UM simulations without DA indicate minimum temperatures of below 0^0C over a larger area than observed, and the 12km UM simulation with DA shows minimum temperature of below 0^0C over a smaller area than observed. The western coast is well-represented by the three UM configurations, but over the eastern coastline and adjacent interior minimum temperatures of above 14^0C were recorded. This feature has been captured well by the 15km UM simulation without DA; the difference being that the minimum temperatures above 14^0C starts from the northern parts extending down to 32^0S, but for the 15km UM simulation without DA these minimum temperatures (above 14^0C) extends over the whole of the eastern coasts down to the southern coast. In the 12km UM simulation without DA and the 12km UM simulation with DA these minimum temperatures extend down to about 34^0S, although only confined to the coastline. Over the north western parts of the Northern Cape Province, temperature of more than 14^0C were observed, but the three UM configurations did not capture this feature.

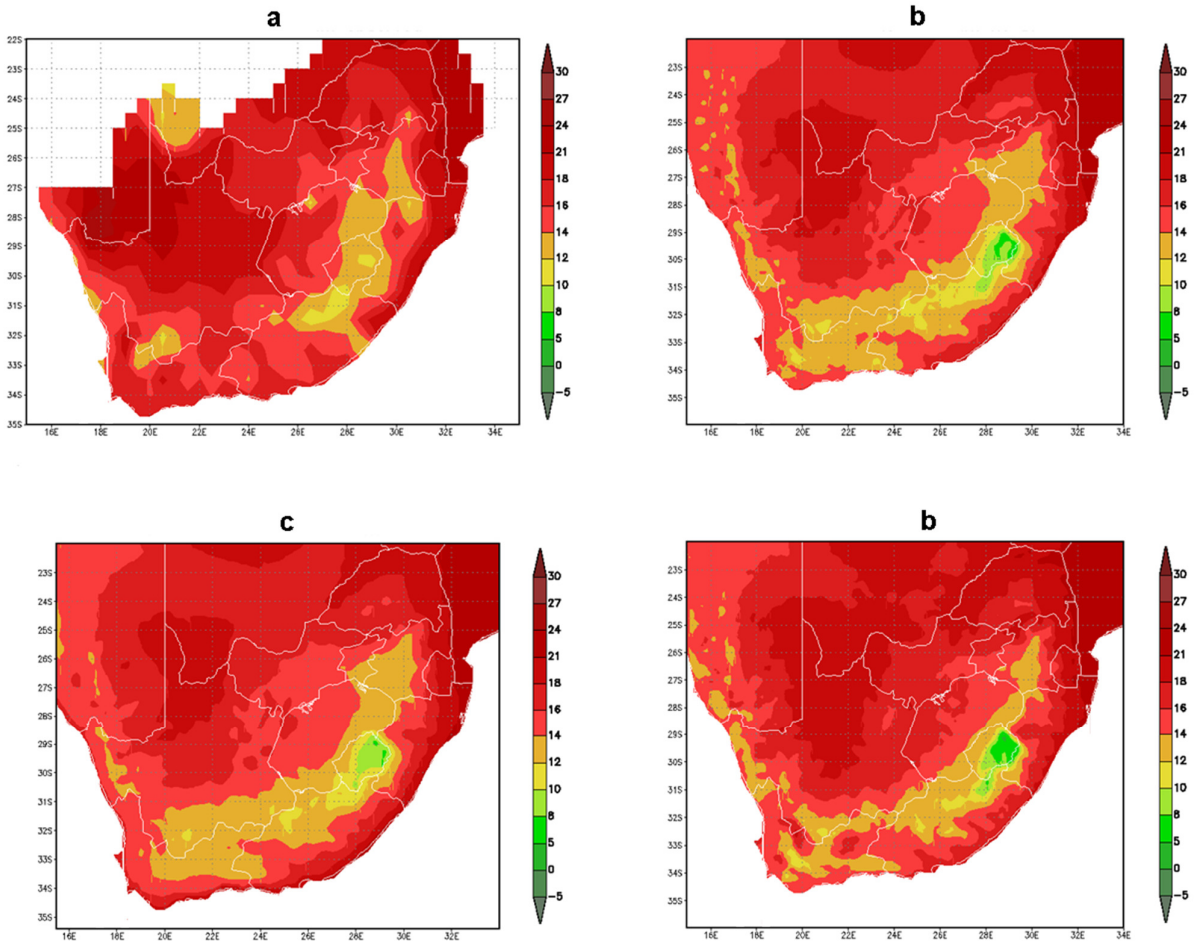

Figure 5.1:

January 2008 averaged minimum temperatures measured in ℃ from (a) observations, (b) 15km Unified Model (UM) without Data Assimilation (DA), (c) 12km UM without DA and (d) 12km UM with DA.

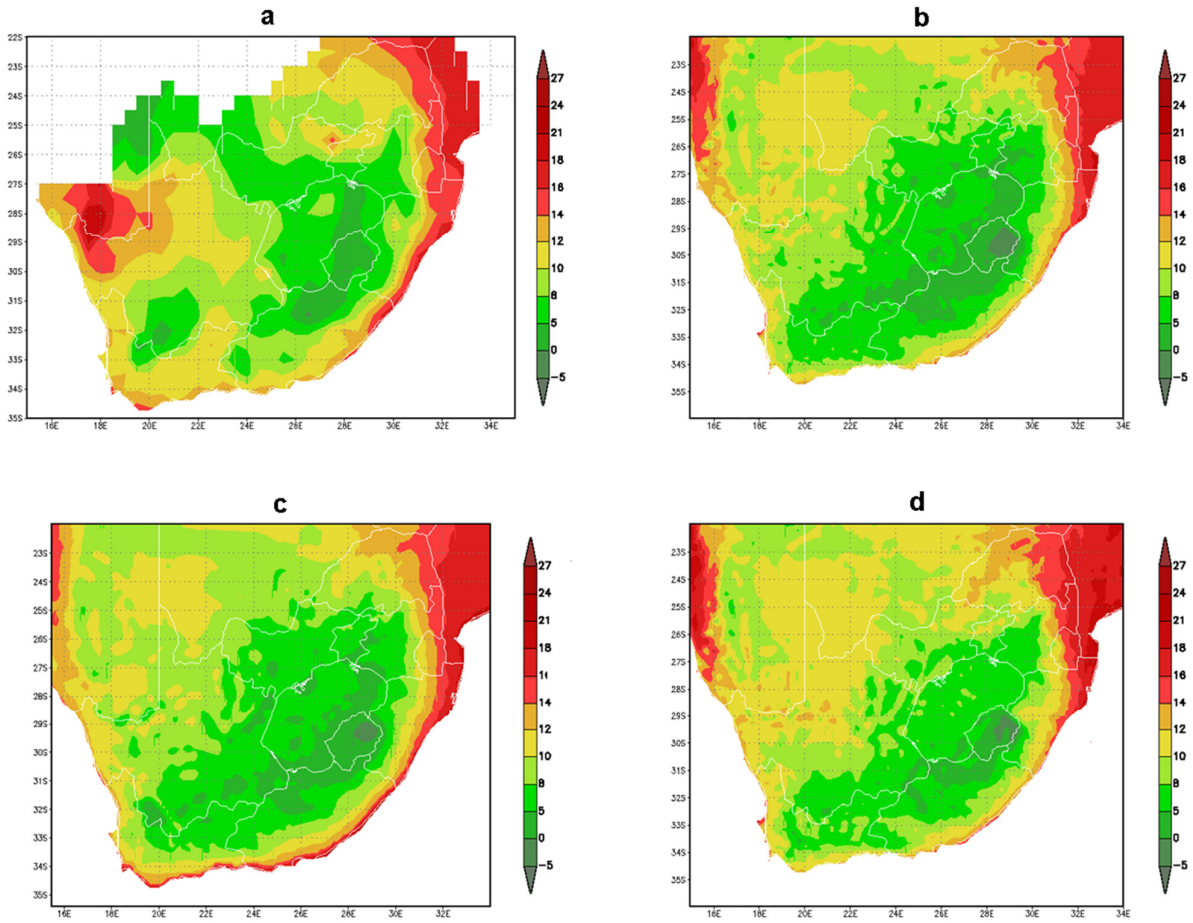

Figure 5.2:

April 2008 averaged minimum temperatures measured in ℃ from (a) observations, (b) 15km Unified Model (UM) without Data Assimilation (DA), (c) 12km UM without DA and (d) 12km UM with DA.

Average minimum temperatures for July 2008 are displayed in figure 5.3. Minimum temperatures for July 2008 range from 0^0C to 9^0C over the central parts of South Africa, and range from 10^0C to 14^0C over the eastern coastline, from where they decrease westwards to higher lying areas, from where they start to increase again. The pattern generated by the three UM configurations used in this study is similar to observations. The most obvious difference is that over the eastern interior of South Africa the 12km and 15km UM simulations without DA shows a larger area than observed with minimum temperatures of above -5^0C, while the 12km UM simulation with DA shows a smaller area than observed with minimum temperatures of above -5^0C. The observed data also indicate a small area over the Northern Cape Province with minimum temperatures of below -5^0C, a feature not shown by

the three UM configurations. Instead the 12km and the 15km UM simulations without DA show values of below -5^{0}C over a small area in the Western Cape Province. The 12km UM simulation with DA did not capture such a feature.

Average minimum temperatures for October 2008 are illustrated in figure 5.4. Observed minimum temperatures for October 2008 indicate lower minimum temperatures over the southern parts of South Africa, between latitudes 30^{0}S and 35^{0}S. Minimum temperatures of above 14^{0}C are evident over the north western parts of the Northern Cape Province, north eastern parts of the North West Province, northern parts of Gauteng Province, and most of the Limpopo Province. The 12km UM simulation with DA resembles observed fields well in these areas, but for the 12km and 15km UM simulations without DA, this feature is only confined to the Limpopo Province. Observed data also indicate minimum temperatures of 10^{0}C-14^{0}C over the central interior of South Africa and minimum temperatures of above 14^{0}C over the eastern coastline and adjacent interior. This feature has been captured well by the 15km UM simulation without DA; the difference is that the minimum temperatures above 14^{0}C starts from the northern parts extending down to 32^{0}S, but for the 15km UM simulation without DA these minimum temperatures (above 14^{0}C) extends for the whole of the eastern coasts down to the southern coast. The 12km UM simulation with DA and the 12km UM simulation without DA extend these minimum temperatures down to about 34^{0}S, but these are only confined to the coastline and do not extend to the adjacent interior.

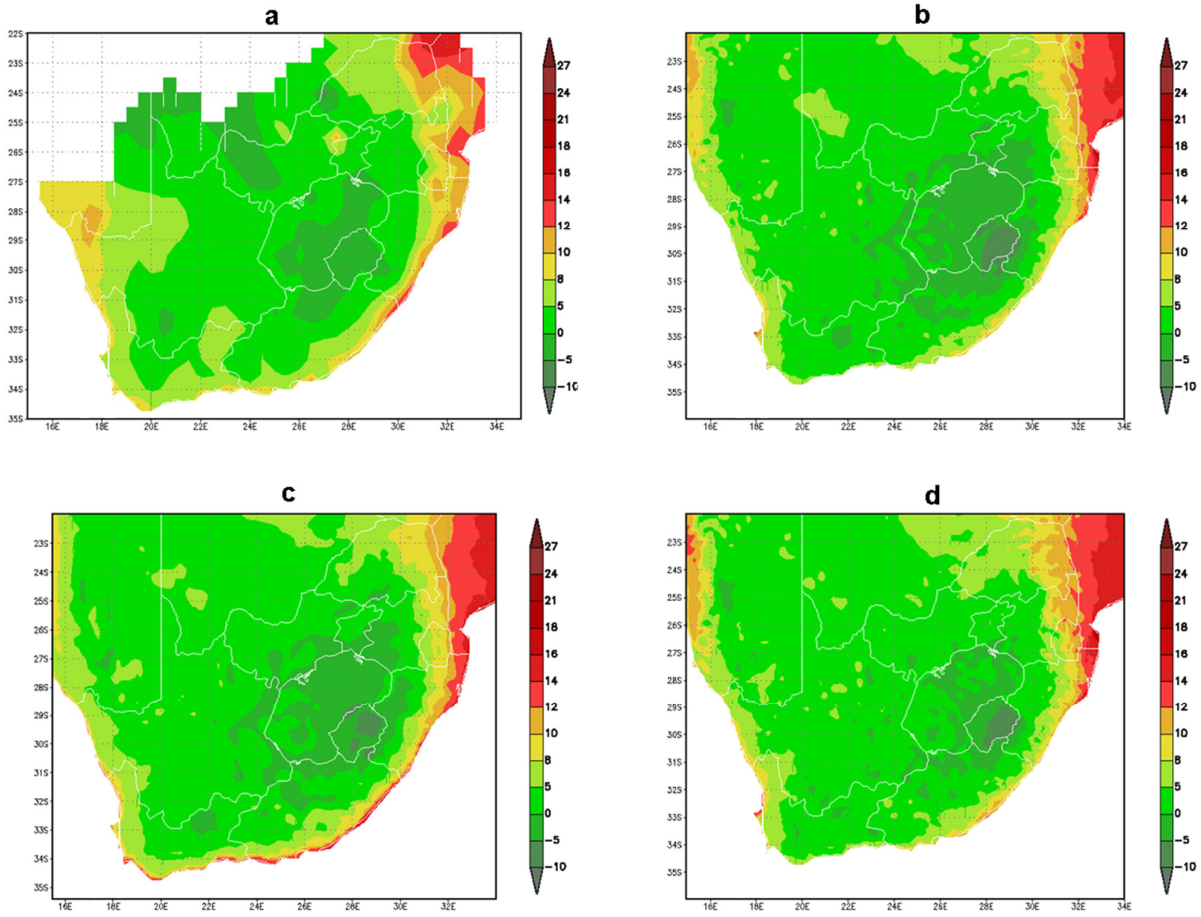

Figure 5.3:

July 2008 averaged minimum temperatures measured in ℃ from (a) observations, (b) 15km Unified Model (UM) without Data Assimilation (DA), (c) 12km UM without DA and (d) 12km UM with DA.

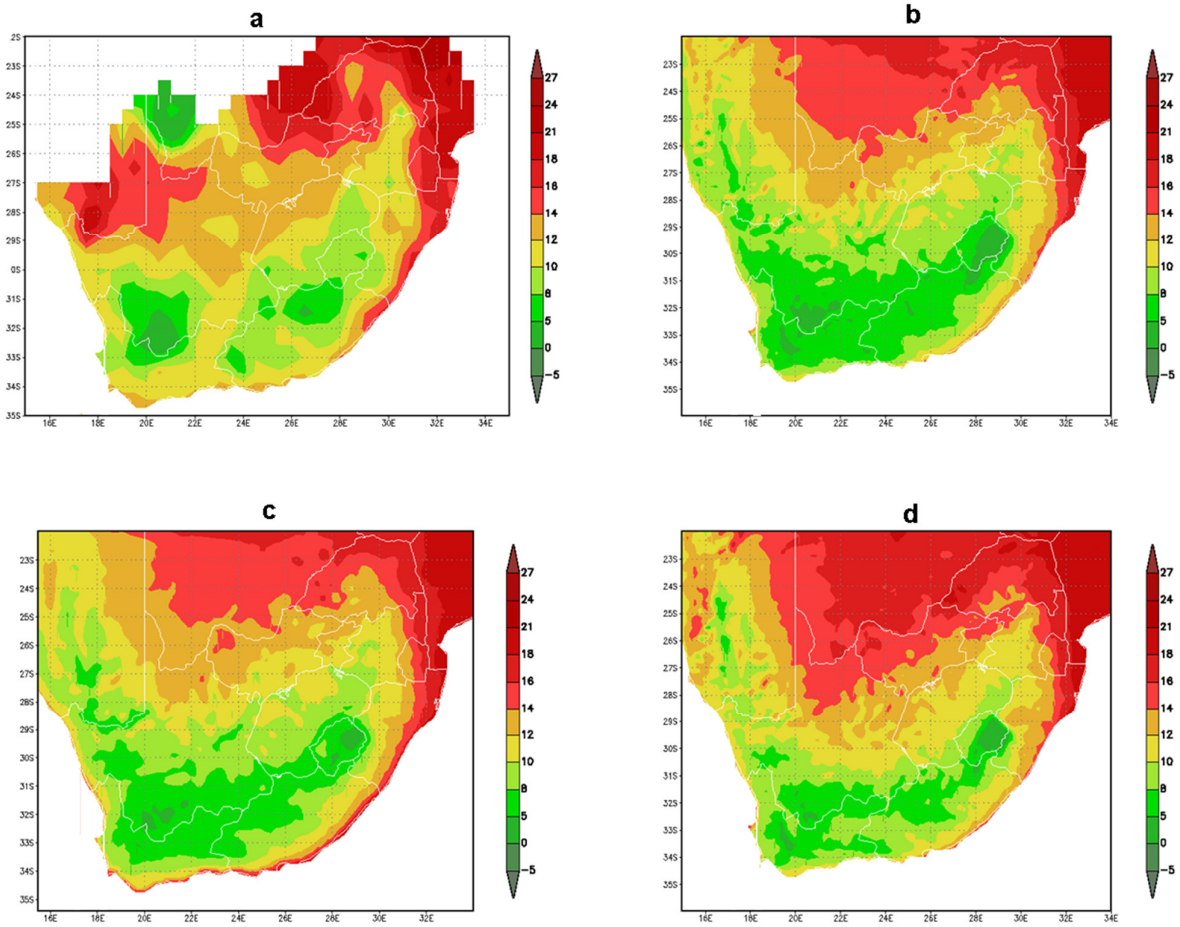

Figure 5.4:

October 2008 averaged minimum temperatures measured in ℃ from (a) observations, (b)15km Unified Model (UM) without Data Assimilation (DA), (c) 12km UM without DA and (d) 12km UM with DA.

5.2.2 MAXIMUM TEMPERATURES

January 2008 average maximum temperatures are displayed in figure 5.5. Highest observed maximum temperatures of below 20^{0}C are evident over Gauteng, Mpumalanga, eastern parts of the Free State Province, southwestern parts of KwaZulu-Natal and eastern parts of the Eastern Cape Province. The three UM configurations generated a similar pattern, but captured lower than observed maximum temperatures over the Limpopo Province and the western parts of the North West Province. The 15km UM simulation without DA resembles the observations well over the western and southern coasts, but over the interior, maximum

temperature simulations from the 12km and 15km UM without DA are lower than the observed maximum temperatures, whereas the 12km UM simulation with DA shows a close resemblance to the observed maximum temperatures.

Average maximum temperatures for April 2008 are shown in figure 5.6. Observed maximum temperatures for April 2008 range from 16^0C to 22^0C in the interior of South Africa; while the northern parts of the Northern Cape Province as well northern parts of the Limpopo Province has higher maximum temperatures (30^0C to 35^0C). Lower maximum temperatures (below 14^0C) are confined to the eastern escarpment, the three UM model configurations simulated these lower maximum temperatures over a broader area than observed. An obvious underestimation of maximum temperatures is evident from the three UM simulations throughout the country.

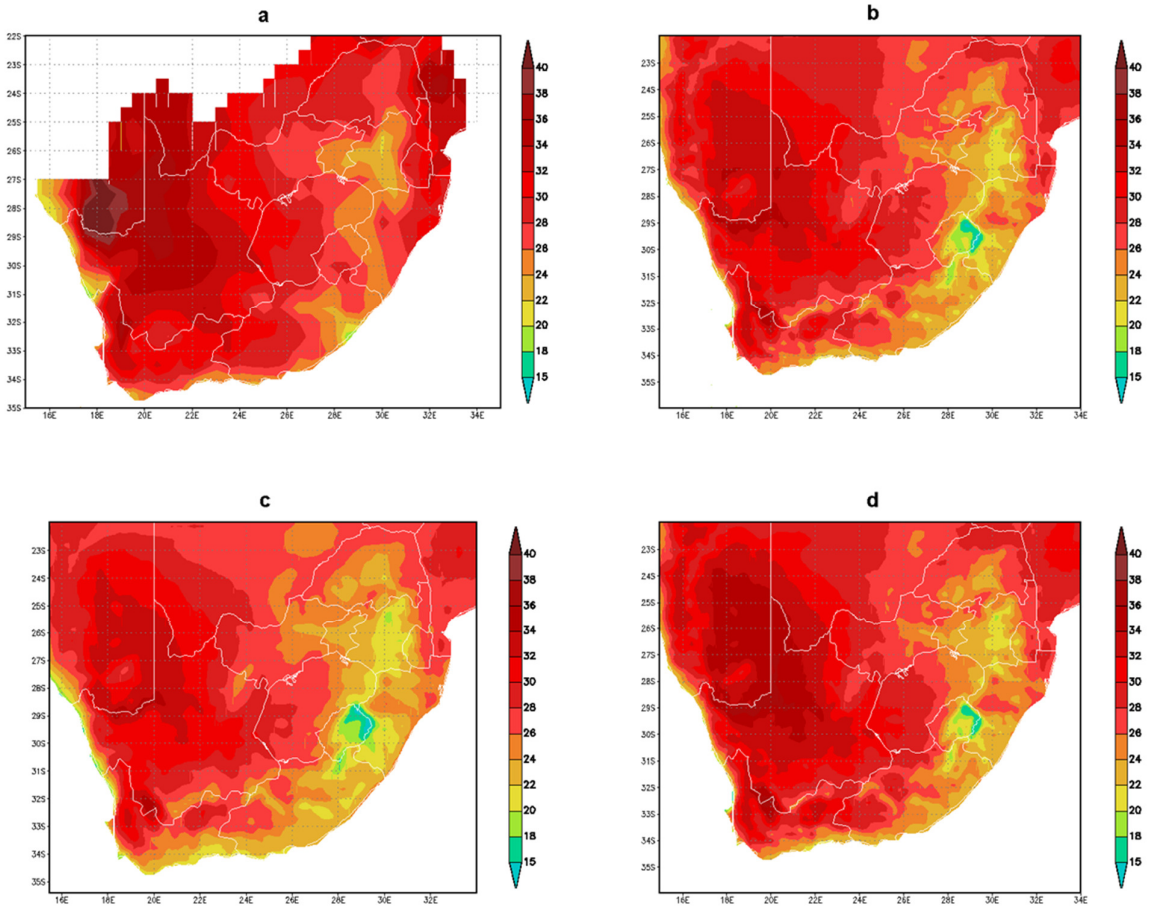

Figure 5.5:

January 2008 averaged maximum temperatures measured in ℃ from (a) observations, (b) 15km Unified Model (UM) without Data Assimilation (DA), (c) 12km UM without DA and (d) 12km UM with DA.

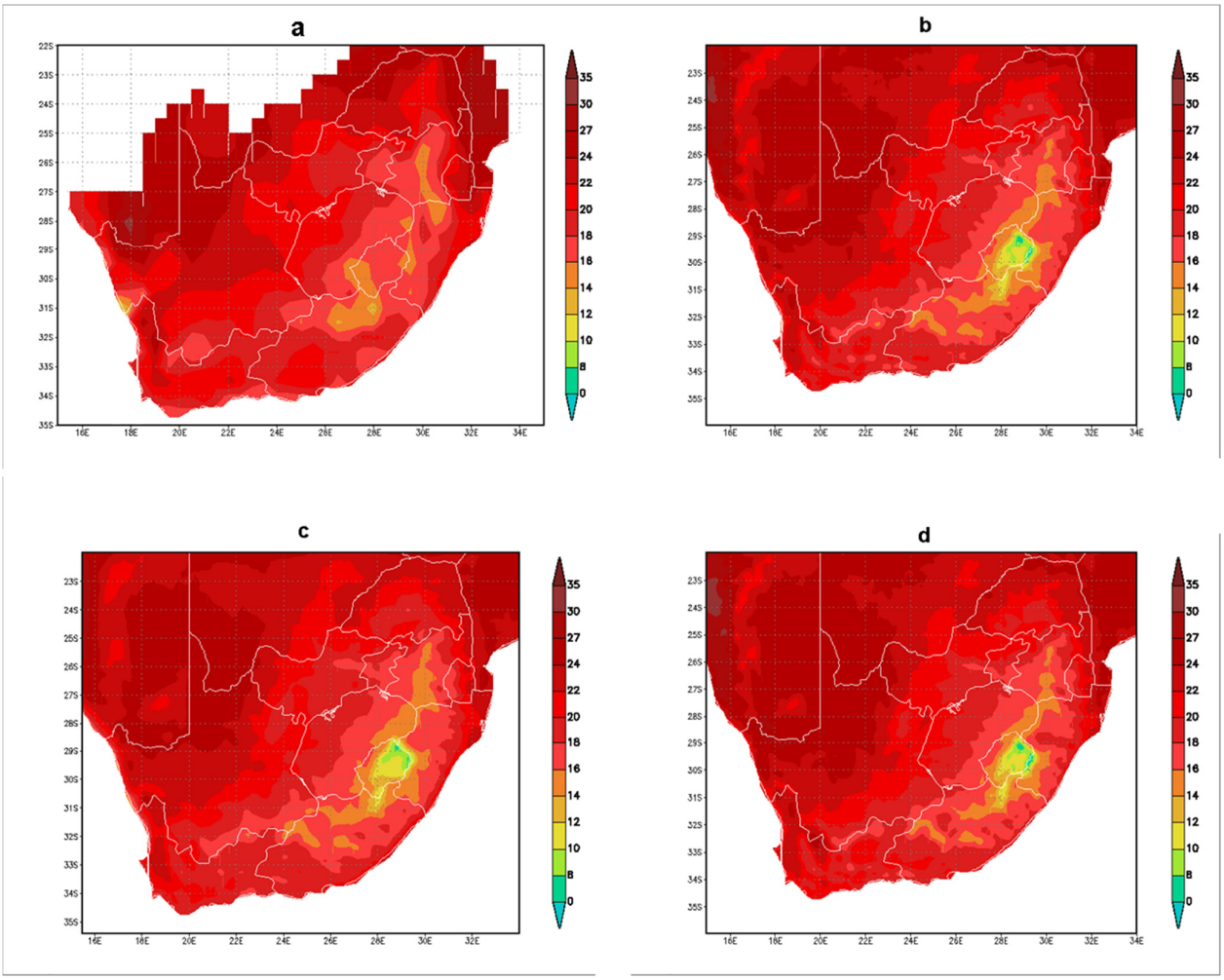

Figure 5.6:

April 2008 averaged maximum temperatures from (a) observations, (b) 15km Unified Model (UM) without Data Assimilation (DA), (c) 12km UM without DA and (d) 12km UM with DA.

Average maximum temperatures for July 2008 are illustrated in figure 5.7. July observed temperatures range from 12^{0}C to 18^{0}C over the central parts of South Africa, and from 18^{0}C to 22^{0}C over the eastern coastline; they then decrease westwards until the higher lying areas and then start to increase again. A similar pattern to the observed is evident from the three model configurations; the difference is that over the eastern coastline and adjacent interior, the three configurations show much cooler temperatures (12^{0}C -14^{0}C) than observed. The three configurations of the UM simulated maximum temperatures below 10^{0}C over the eastern interior of South Africa; this feature is not evident from the observed. Over a small area in the southern parts of the Northern Cape Province and the northern parts of the Western Cape Province; the observed maximum temperatures are below 10^{0}C, and the

15km UM simulation without DA captured this feature very well. A general under-estimation of maximum temperatures throughout the country is evident from the three model configurations, but the extent of the under-estimation is less for the 12km UM simulation with DA as compared to the 12km and 15km UM simulations without DA .

Average maximum temperatures for October 2008 are demonstrated in figure 5.8. October observed maximum temperatures range from 18^0C to over 22^0C over the central interior of South Africa and range from 24^0C to 26^0C over the northern parts of the Northern Cape Province, western parts of the North West Province as well as western and northern parts of Limpopo Province. The 12km UM simulation with DA captured this feature very well except over the southern half of the Northern Cape Province where much cooler maximum temperatures than observed are evident. Maximum temperatures below 8^0C are observed over a small area in the southern parts of the Northern Cape Province, and the 15km UM simulation without DA managed to capture this feature; whereas the other two configurations failed to capture such a feature. The observed maximum temperatures over eastern and southern coastlines as well as adjacent interior range from 10^0C to 14^0C and all three configurations used failed to capture this feature.

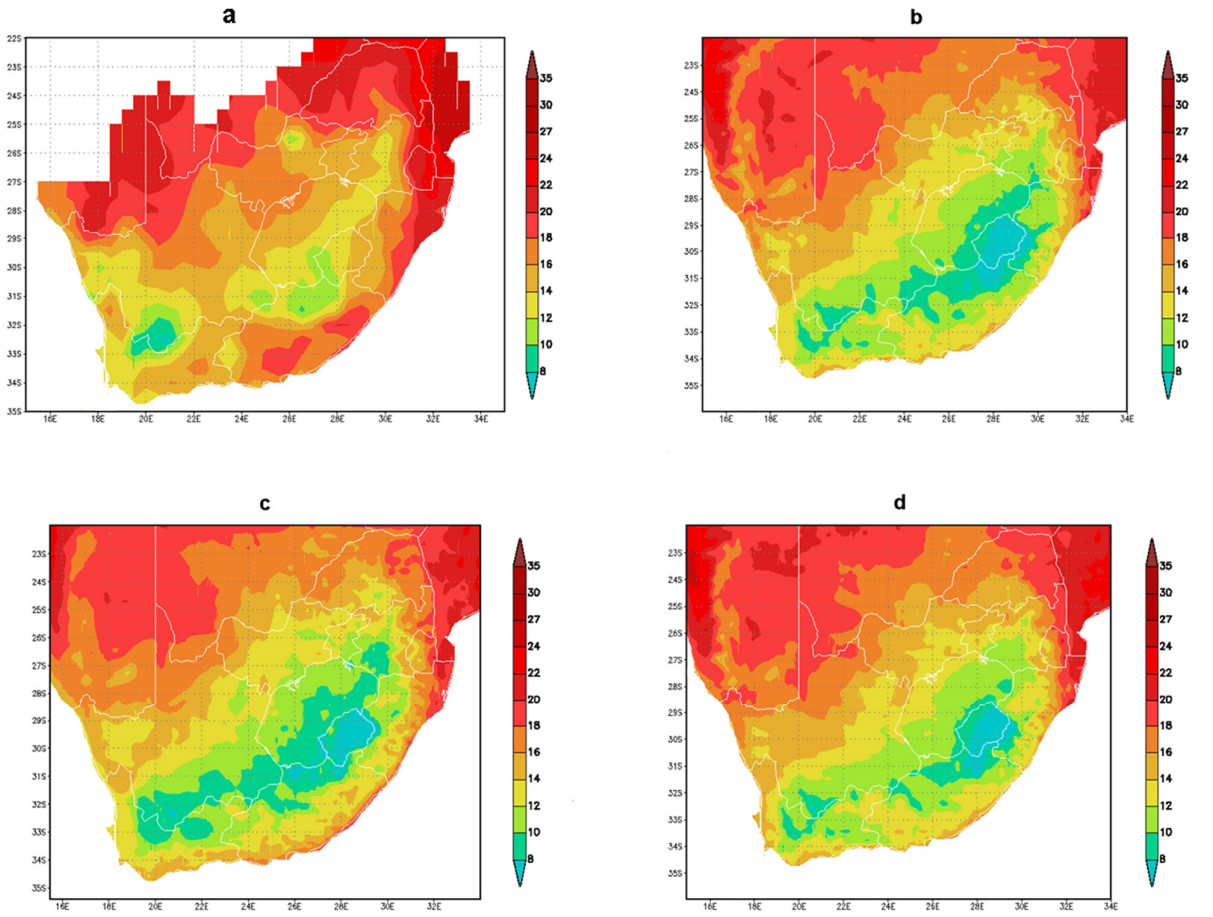

Figure 5.7:

July 2008 averaged maximum temperatures measured in ℃ from (a) observations, (b) 15km Unified Model (UM) without Data Assimilation (DA), (c) 12km UM without DA and (d) 12km UM with DA.

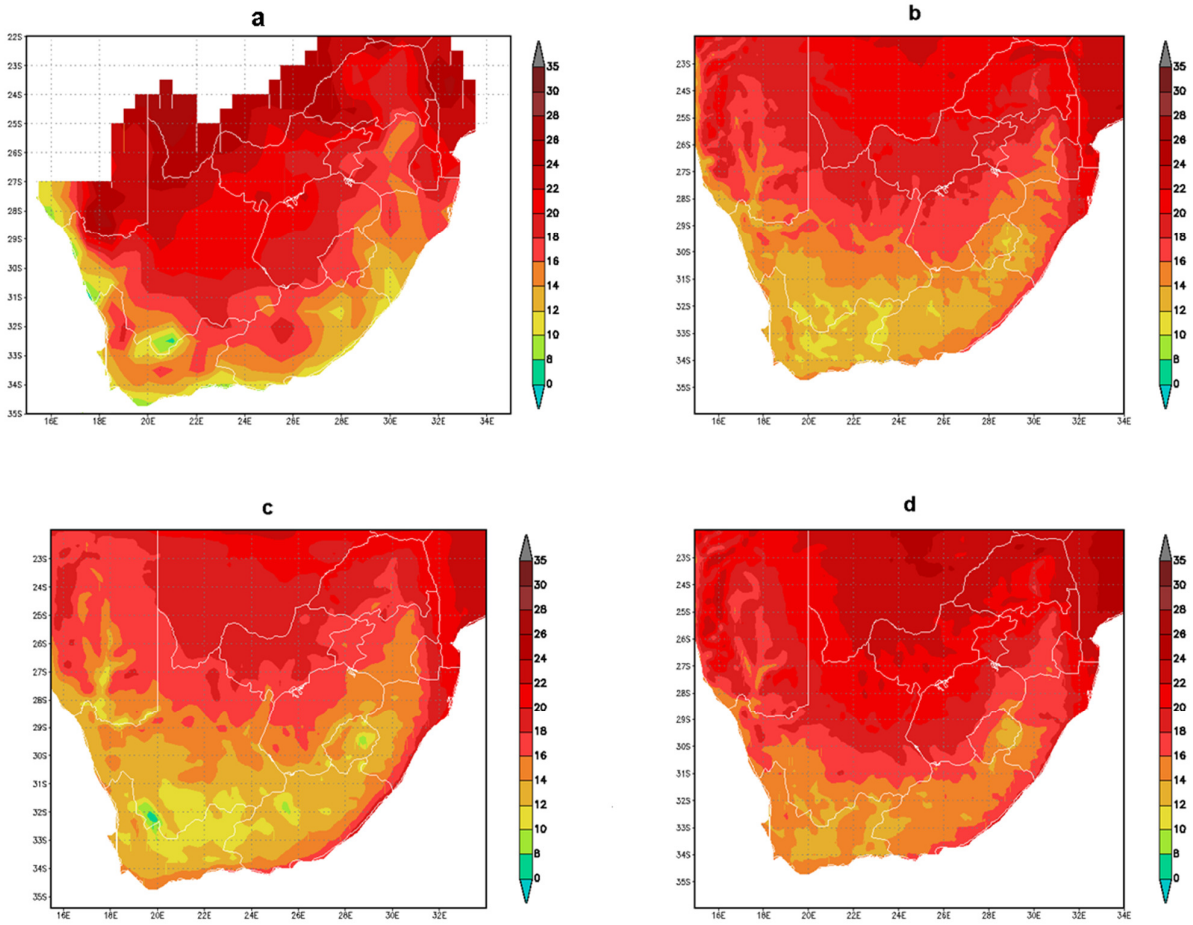

Figure 5.8

October 2008 averaged maximum temperatures measured in ℃ from (a) observations, (b) 15km Unified Model (UM) without Data Assimilation (DA), (c) 12km UM without DA and (d) 12km UM with DA.

5.3 VERIFICATION SCORES FOR CONTINUOUS VARIABLES

Different point stations across the South African domain were selected and grouped together according to their altitude AMSL (Table 3.2). The Mean Error (ME), Mean Absolute Error (MAE) and Root Mean Square Error (RMSE) for the monthly average of daily maximum and minimum temperature for the different groups of stations were investigated and the results are discussed.

5.3.1 MINIMUM TEMPERATURES

The ME scores of minimum temperatures from the three UM configurations are displayed in figure 5.9. A general underestimation of minimum temperatures for all the groups used in most of the months is evident from all three configurations. Even though the lowest ME score of -0.02 in group 4 was simulated by the 15km UM simulation without DA during the month of May, on average the 12km UM simulation with DA had the lowest ME scores. The 12km UM simulation without DA had the largest ME scores for all groups in most of the months. This implies that even though the UM under-estimates minimum temperatures, the 12km UM simulation with DA outperforms the 12km and 15km UM simulations without DA. The worst performance is evident from the 15km UM simulation without DA in all groups for all months used in the study.

The MAE results from minimum temperatures simulated by the three UM configurations are demonstrated in figure 5.10. For each group of stations, the same pattern is evident from the three configurations in simulating minimum temperatures. The differences lie in the range of MAE scores for the three simulations. The minimum MAE scores in all groups are found in the 12km UM simulation with DA, and the highest MAE scores where from the 12km UM simulation without DA. It is seen that the UM simulation with DA gives more accurate results than the 12km and 15km UM simulations without DA in simulating minimum temperatures over South Africa.

The RMSE results from minimum temperatures simulated by the three UM configurations are shown in figure 5.11. The three UM configurations show a similar pattern in simulating minimum temperatures for individual groups of stations, for example, a minimum in June for groups 3 and 8, a minimum in April for group 2 and December for group 5. The lowest minimum RMSE is evident in group 4 and was simulated by the 12km UM simulation with DA. The maximum RMSE for all the groups range from 1.38 to 2 and were all simulated by the 12km UM simulation without DA. It is clearly indicated by the results that the 12km UM simulation with DA outperformed the 12km and 15km UM simulations without DA.

Figure 5.9:

Mean Error (ME) verification scores of daily minimum temperatures during 2008 for the three Unified Model (UM) configurations.

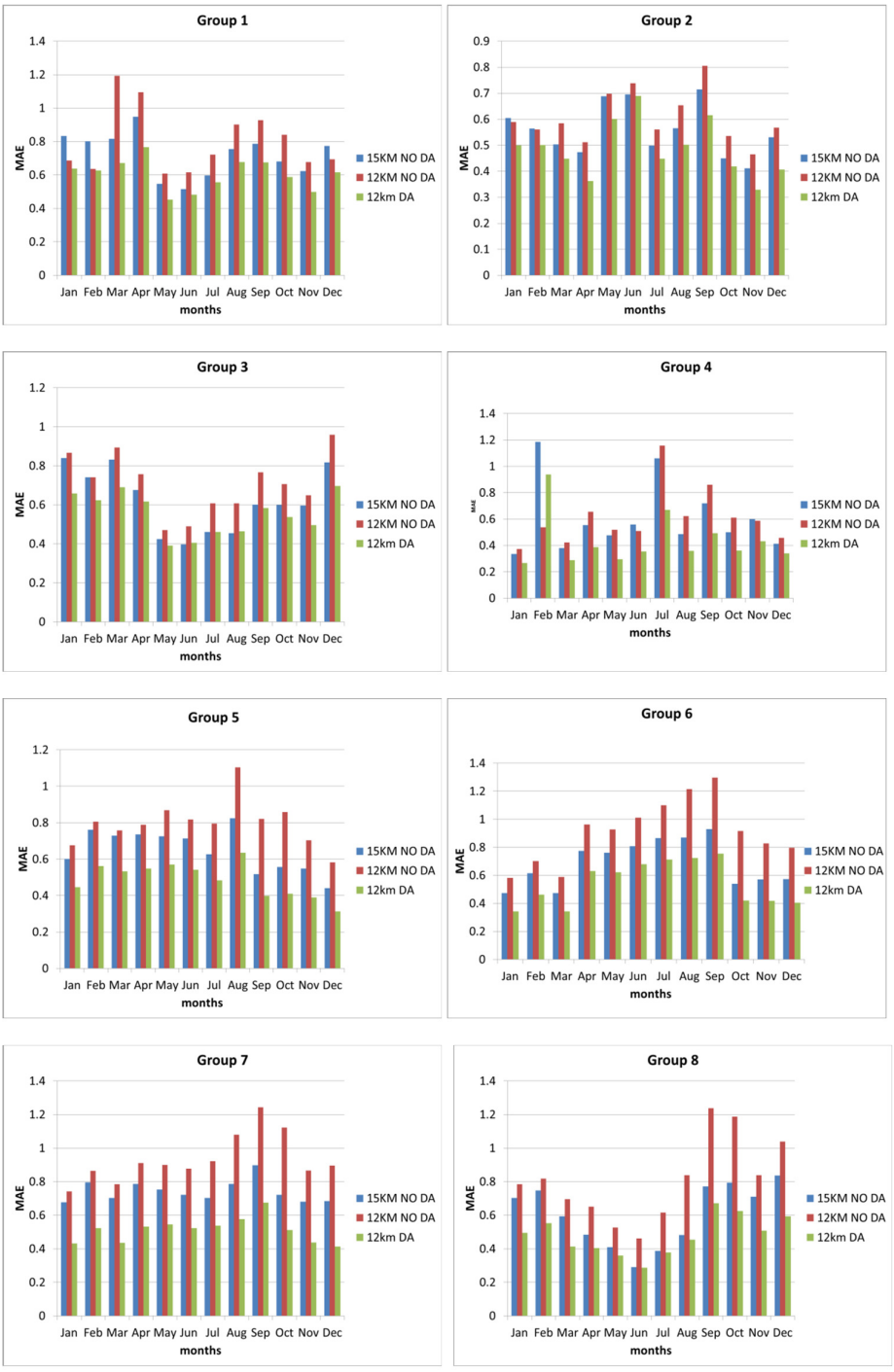

Figure 5.10:

Mean Absolute Error (MAE) verification scores of daily minimum temperatures during 2008 for the three Unified Model (UM) configurations.

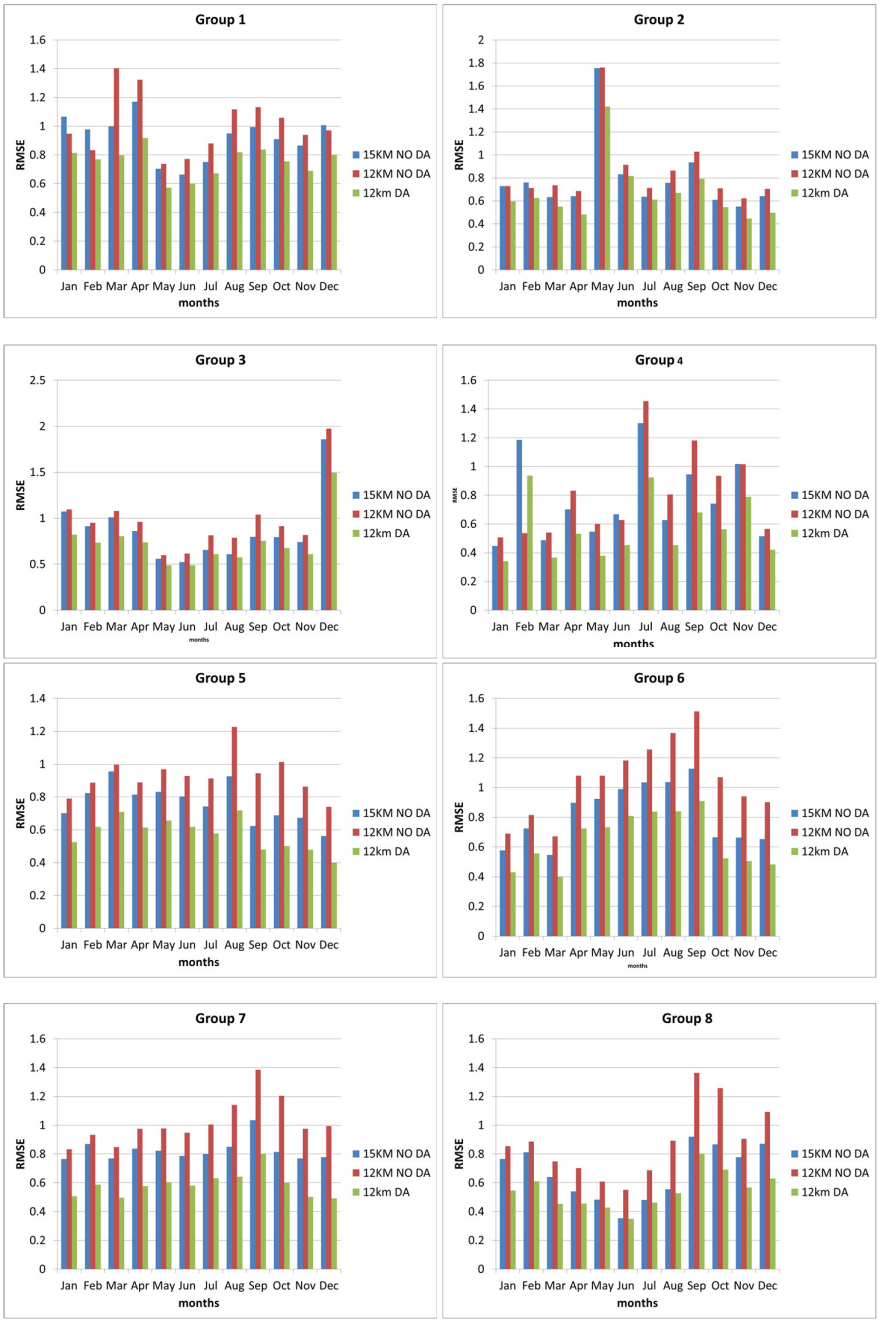

Figure 5.11:

Root Mean Square Error (RMSE) verification scores of daily minimum temperatures during 2008 for the three Unified Model (UM) configurations.

5.3.2 MAXIMUM TEMPERATURES

The ME results from maximum temperatures simulated by the three UM configurations are Illustrated in figure 5.12. Results show both similarities and differences between the three UM configurations. Underestimation of maximum temperatures for all months in all groups is evident from the three configurations. The three configurations follows the same pattern in simulating maximum temperatures, the lowest ME scores are found during the summer months and the highest ME scores are found during winter months, with the exception of group 2 having its highest ME in December. The 12km UM simulation with DA outperformed the other configurations in simulating maximum temperatures in all groups, hence the ME scores. On the other hand the 12km UM simulation without DA had the highest ME scores for all the months, in all the groups. This suggests that out of the three configurations; the 12km UM simulation with DA is the most reliable tool for simulating maximum temperatures and the 12km UM simulation without DA is the least reliable.

The MAE results from maximum temperatures simulated by the three UM configurations are shown in figure 5.13. Results show both similarities and differences between the three UM configurations. For each group of stations, the three configurations show the same pattern in simulating maximum temperatures. The differences lie in the range of MAE scores for the three simulations. The maximum MAE scores in all groups were found in the 12km UM simulation with DA, and the highest MAE scores where from the 12km UM simulation without DA. It is seen that the UM simulation with DA gives more accurate results than the 12km and 15km UM simulations without DA in simulating maximum temperatures.

The RMSE results from maximum temperatures simulated by the three UM configurations are illustrated in figure 5.14. The three UM configurations show a similar pattern in simulating maximum temperatures for individual groups of stations, for example, the lowest RMSE score is found in February for groups 2, 6 and 7, and in December for groups 1 and 8. Group 3 had the lowest RMSE score in March and groups 4 and 5 had lowest RMSE scores in April and June respectively. The lowest RMSE scores were from the 12km UM simulation with DA and they range from 0.2 to 0.7 whilst the range for the highest RMSE scores, simulated by the 12km UM simulation without DA is 2.3 to 4. This confirms the previous scores indicating that the 12km UM simulation with DA gives more accurate results than the 12km and 15km UM simulations without DA in simulating maximum temperatures.

In summary results from objective verification suggests a general under-estimation of both minimum and maximum temperatures by the three configurations of the UM throughout the entire period. The maximum temperatures were mostly accurate and reliable during the summer months, whereas for the minimum temperature the period at which they are more accurate and reliable differs for different groups of stations. It was further proven that the simulation of minimum and maximum temperatures is sensitive to the location of the station used. For almost all the months used, group 8 was the least accurate for both maximum and minimum temperatures, proving that stations at the escarpment have the worst MAE scores (DeConing, 2001). Group 1 also had the least accurate minimum temperatures and group 2's maximum temperatures were one of the least accurate, groups 5 , 6 and 7 are in higher lying areas and error was also higher in regions but lower than in group 8. Errors in these could be attributed to the differences in the local features between the model and real data caused by the adjacent oceans. Topography may also affect the performance of the model in simulating temperatures closer to the coasts as well as over the escarpment. Group 3 and 4 are more of inland stations but at a lower altitude, and had the most accurate and reliable scores. The 12km UM simulation with DA outperformed the 12km and 15km UM simulations without DA for most of the months and for all groups used in the study. It was also shown that simulations from the 12km and 15km UM without DA were similar but the 15km UM simulation without DA outscored the 12km UM simulation without DA in most of the months for all the groups used in the study.

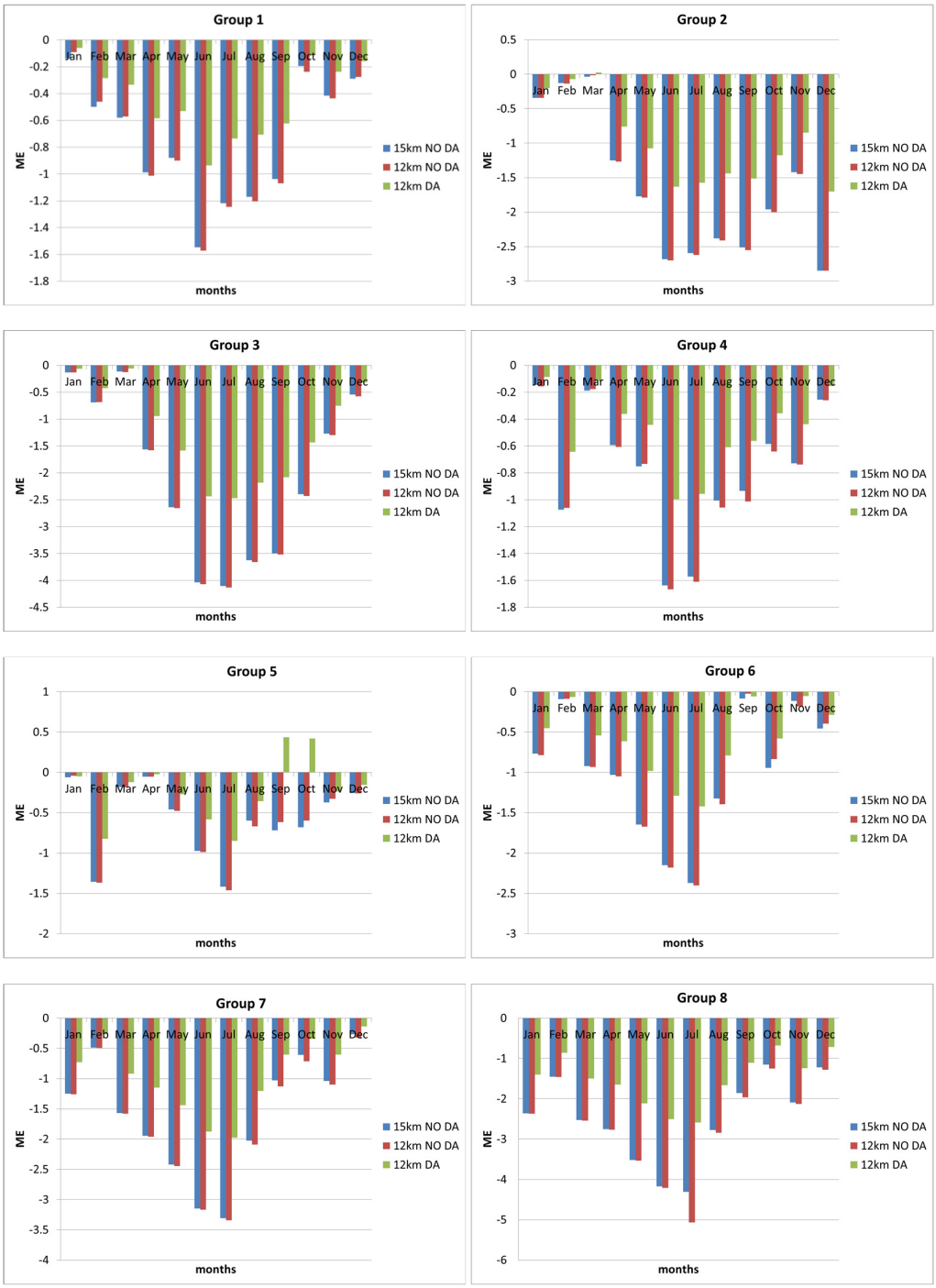

Figure 5.12:

Mean Error (ME) verification scores of daily maximum temperatures during 2008 for the three Unified Model (UM) configurations.

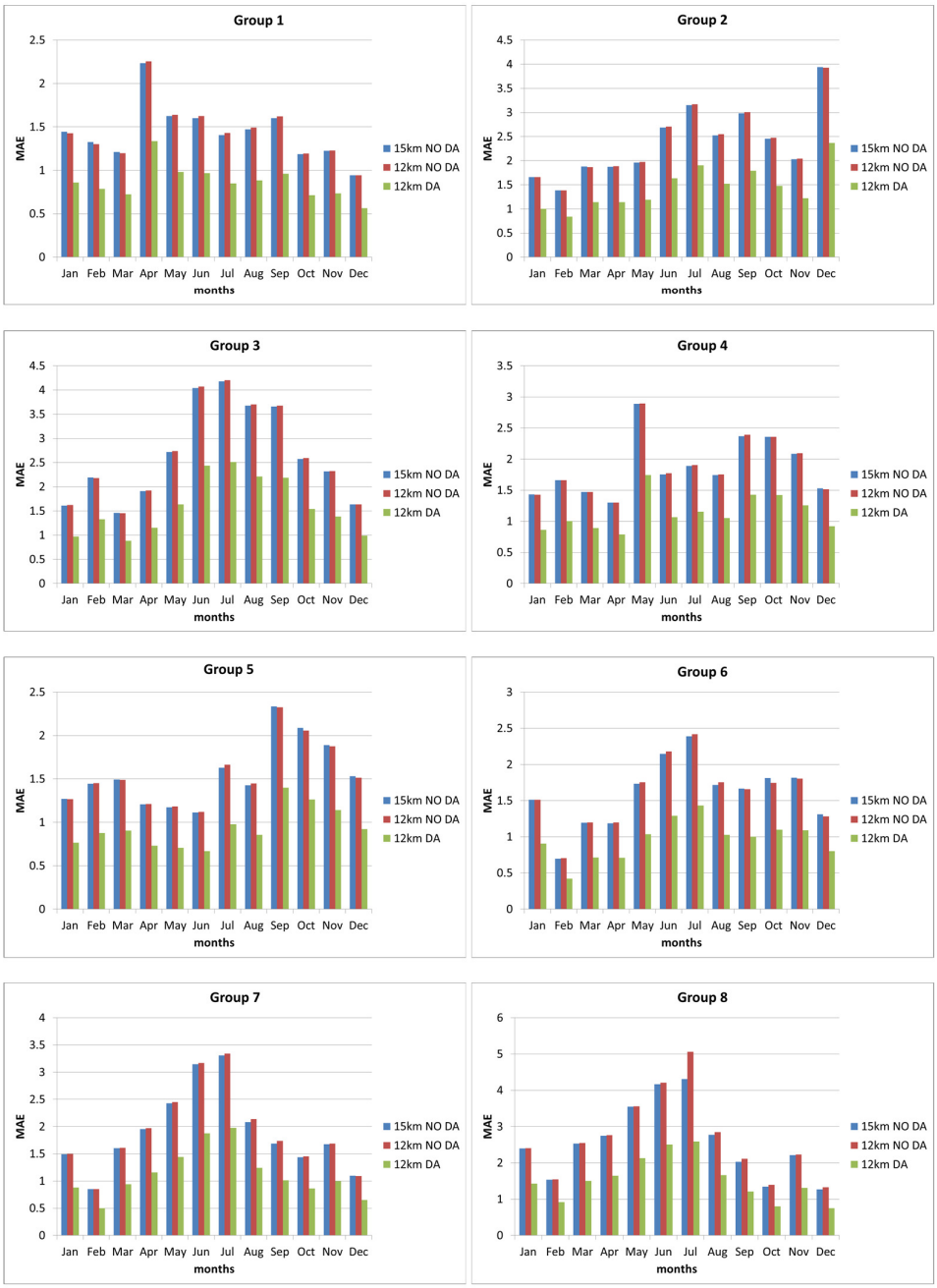

Figure 5.13:

Mean Absolute Error (MAE) verification scores of daily maximum temperatures during 2008 for the three Unified Model (UM) configurations.

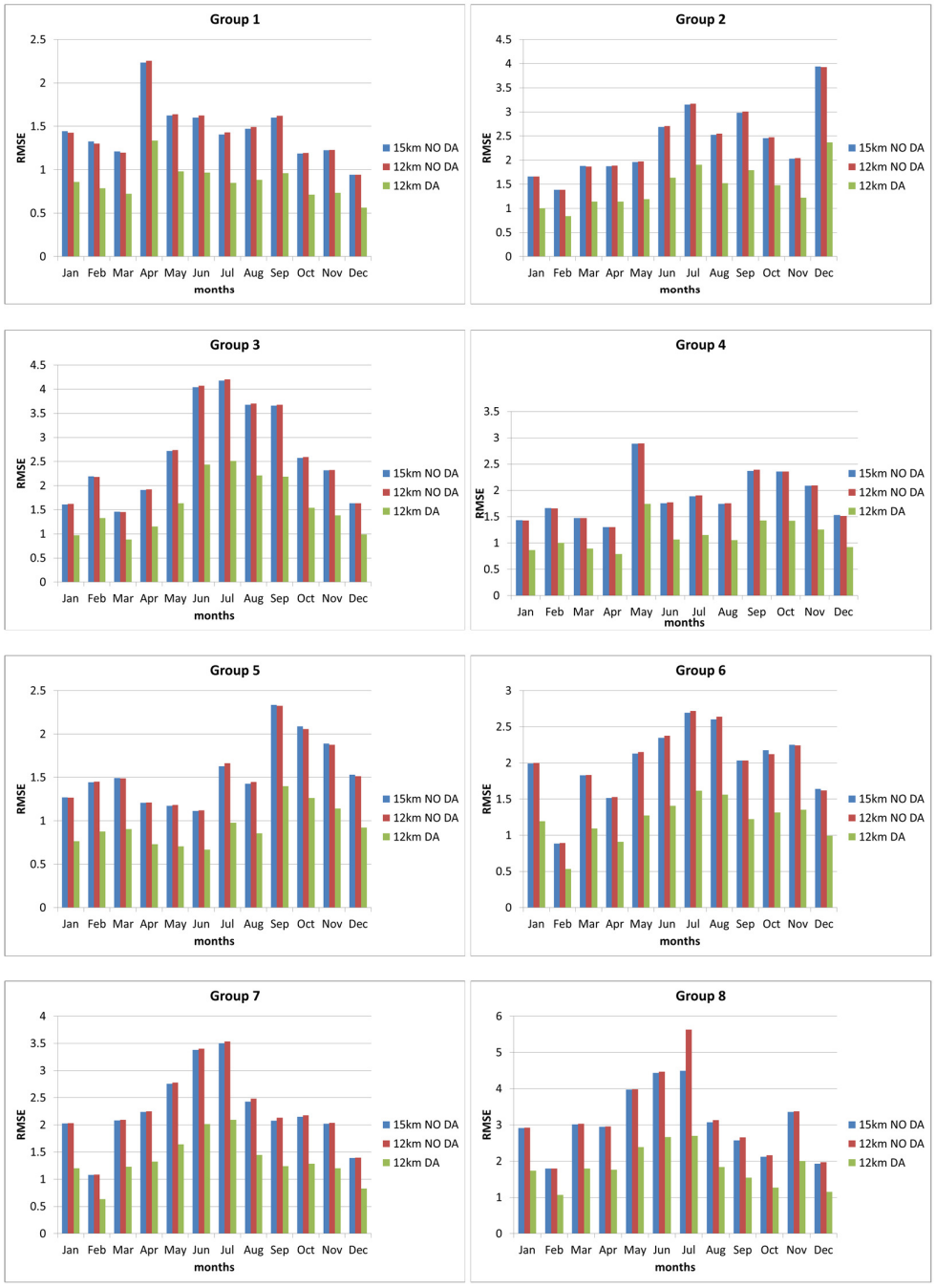

Figure 5.14:

Root Mean Square Error (RMSE) verification scores of daily maximum temperatures during 2008 for the three Unified Model (UM) configurations.

5.4 SUMMARY

Verification of minimum and maximum temperatures for three configurations of the UM were presented in this chapter. The verification was done subjectively using eyeball verification and objectively using verification of continuous scores described in chapter 3. Both the subjective and objective verification of minimum and maximum temperatures from the three model configurations of the UM suggests that 12km UM simulation with DA gives reliable and accurate results than the 12km and 15km UM simulations without DA; It was further shown that although there was no significant difference between the 12km and the 15km UM without DA, the 15km UM simulation without DA, proved to me more reliable and accurate than the 12km UM simulation without DA in simulating minimum and maximum temperatures over South Africa and this may be attributed to the fact that the domain of the 15km resolution is also smaller compared to the two 12km resolution disallowing the model time to drift away from the forcing fields.

CHAPTER 6

DISCUSSIONS AND CONCLUSION

The research documented in this dissertation was inspired by the need to verify the performance of the UM in simulating and predicting weather over South Africa. To achieve this aim, two objectives were addressed. The first objective was to compare model outputs from three model configurations of the UM. The second objective was to verify the model outputs from the three model configurations of the UM against observations. The UM configurations used were, 12km horizontal resolution with DA, the 12km resolution without DA and the 15km resolution without the DA.

Verification of rainfall as well as minimum and maximum temperature for the year 2008 was therefore done to achieve this. For rainfall verification the model was subjectively verified using the eyeball verification for the entire domain of South Africa, followed by objective verification of categorical forecasts for rainfall regions grouped according to standardized monthly rainfall totals obtained by cluster analysis and finally objective verification using continuous variables for selected stations over South Africa. Minimum and maximum temperatures were subjectively verified using the eyeball verification for the entire domain of South Africa, followed by objective verification of continuous variables for selected stations over South Africa, grouped according to different altitudes above mean sea level (AMSL).

It was shown that the three UM configurations overestimates rainfall over the central and eastern parts of the country; this could be attributed to the fact that rainfall over the central and eastern parts of the country is of convective origin, where as rainfall over the south western parts of the country is due to frontal systems. The overestimation of rainfall by the UM particularly over the eastern parts of the South Africa is consistent with the results of Engelbrecht et al. (2002). The results from subjective verification further suggest that all three model configurations, underestimates minimum and maximum temperatures throughout the country. The extent of underestimation is more pronounced on minimum temperatures especially over the south eastern interior of South Africa.

Objective rainfall verification of categorical variables showed similarities between the three configurations of the UM in simulating rainfall for smaller thresholds. All three model configurations are successful in simulating rainfall for smaller rainfall threshold; this was shown by high PC scores, extremely small BIAS and FAR scores for rainfall thresholds of 0.1mm and 0.5mm. Differences between the three configurations are more obvious when considering rainfall thresholds of 2mm and beyond. All three model configurations showed difficulty in simulating rainfall of higher thresholds. This suggests that the UM may be missing the precise location of a rainfall event, according to Accadia et al. (2005) mesoscale models may have success in predicting a general weather situation, but may miss the timing, intensity and exact position of the rainfall event. The 12km UM simulations with DA showed higher PC scores and lesser BIAS and FAR scores than the 12km and 15km UM simulations without DA.

Results from objective verification of continuous variables, demonstrated low ME (minimum and maximum temperatures), MAE (both rainfall, minimum and maximum temperatures) and RMSE (both rainfall, minimum and maximum temperatures) scores for the 12km UM simulation with DA; and high ME, MAE and RMSE scores for the 12km and 15km UM simulations without DA.

In summary, both the subjective and objective verification of the three model configurations of the UM (for both rainfall as well as the minimum and maximum temperatures) suggests that 12km UM simulation with DA gives better and reliable results than the 12km and 15km UM simulations without DA. This is in agreement with previous studies (Benjamin et al., 1991;Stauffer et al., 1991; Stauffer and Seaman, 1994 Seaman et al., 1995; Warner et al., 1997; Kalnay, 2003; Yussouf and Stenrud, 2010), which demonstrated that employing DA in NWP models may improve the model's performance.

It was further shown that although there was no significant difference between the model outputs from the 12km and the 15km UM without DA, the 15km UM simulation without DA, proved to me more reliable and accurate than the 12km UM simulation without DA in simulating minimum and maximum temperatures over South Africa, on the other hand the 12km UM simulation without DA is more reliable and accurate than the 15km UM simulation without DA in simulating rainfall over South Africa. This result is consistent with sensitivity studies done by Gallus (1999) indicating that the response to change in horizontal resolution depends on the phenomena being simulated.

The one-year period (2008) used in this study; may not be sufficient enough to give conclusive results, but it does however give an idea on the performance of the UM in simulating and predicting weather over South Africa. Future work, with a longer period and more model configurations of the UM is recommended.

REFERRENCES

Accadia C, Mariani S, Casaioli M, Lavagnini A and Speranza A, 2005: Verification of Precipitation Forecasts from Two Limited-Area Models over Italy and Comparison with ECMWF Forecasts Using a Resampling Technique. Wea. Forecasting., **20,** 276-300.

AMS statement, 2001: Seasonal to Interannual climate prediction. *Bull .Amer. Meteor. Soc.*, **82**, 701-703.

Anthes, R.A., Kuo,Y.H , and Gyakum, J.R. , 1983: Numerical Simulations of a Case of Explosive Marine Cyclogenesis. *Mon. Wea. Rev.*, **111**, 1174-1188.

Austin, J., Butchart, N. and Swinbank, R., 1997: Sensitivity of ozone and temperature to vertical resolution in a GCM with coupled stratospheric chemistry. *Quart. J. Roy. Meteor. Soc.,* **123,** 1405–1431.

Banitz E, 2001: Evaluation of short-term weather forecasts in South Africa. *Water SA.*, **27**, 489-498.

Benjamin, S., Brewster, K., Brummer, R., Jewett, B., Schlatter, T., Smith T., and Stamus, P., 1991: An isentropic three-hourly data assimilation system using ACARS aircraft observations. *Mon. Wea. Rev.*, **119,** 888-906.

Bornemann, J., Lean, H. W., Wilson, C. A. and Clark, P. A. , 2005: A new high resolution operational model for the UK. *Met Office NWP technical report* **423**.

Brooks, H.E., Doswell III, L.A., and Maddiox, R.A., 1992: On the use of Mesoscale and cloud scale models in operational forecasting. *Wea. Forecasting,* **7**, 120-132.

Butchart, N. and Austin, J., 1998: Middle Atmosphere Climatologies from the Troposphere–Stratosphere Configuration of the UKMO's Unified Model. *J. Atmos Sc.,* **55**, 2782-2809.

Das, H.P., Doblas-Reyes, F.J., Garcia ,A., Hansen, J., Mariani, L., Nain, A. S.,Ramesh, K., Rathore, L.S., and Venkatarama, S., 2010 : Weather and Climate Forecasts for

Agriculture: In WMO 2012, Guide to Agricultural Meteorological Practises, *WMO*, 134,799pp.

Case, J.L., Manobianco, J., Lane, J. E., Immer, C.D. and Merceret, F.J., 2004: An Objective Technique for Verifying Sea Breezes in High-Resolution Numerical Weather Prediction Models. *Wea. Forecasting,* **19**, 690-705.

Charney, J. G., Fjortoft, R. and von Neumann, J., 1950: Numerical Integration of the Barotropic Vorticity Equation. *Tellus*, **2** , 237 -257.

Chen, C.S., Chen, Y.L., Liu, C.L., Lin, P.L and Chen, W.C., 2007: Statistics of Heavy Rainfall Occurrences in Taiwan. *Wea. Forecasting,* **22**, 981-1002.

Coiffier, J., 2004: Weather forecasting technique considered as a sequence of standard processes from the forecaster's point of view. *Preprints WMO Workshop , Toulouse*, 26–29 October 2004 *, WMO, Geneva, Switzerland.*

Colle, B.A. and Mass, C. F., 2000: The 5–9 February 1996 Flooding Event over the Pacific Northwest: Sensitivity Studies and Evaluation of the MM5 Precipitation Forecasts. *Mon. Wea. Rev.*, **128**, 593-617.

Colle, B.A, Mass, C.F. and Smull, B. F., 1999: An Observational and Numerical Study of a Cold Front Interacting with the Olympic Mountains during COAST IOP5. *Mon. Wea. Rev.*, **127**, 1310-1334.

Colle, B.A., Mass, C. F. and Ovens, D. 2001: Evaluation of the Timing and Strength of MM5 and Eta Surface Trough Passages over the Eastern Pacific. *Wea. Forecasting,* **16**, 553-572.

Colle, B.A., Olson, J.B. and Tongue, J.S., 2003: Multi Season Verification of the MM5 Part II: Evaluation of High Resolution Precipitation Forecasts over North Eastern United States. *Wea. Forecasting*, **18**, 458 – 480.

Coiffier, J., 2004: Weather forecasting technique considered as a sequence of standard processes from the forecaster's point of view. *Preprints WMO Workshop , Toulouse*, 26–

29 October 2004 *, WMO, Geneva, Switzerland.*

Cotton, W.R. and Pielke, R.A., 1976: Weather Modification and Three Dimensional Mesoscale Model. *Bull. Amer. Meteor. Soc.*, **57**, 788 – 796.

Cullen, M.J. and Davies, T., 1991: A conservative split-explicit integration scheme with fourth-order horizontal advection. *Quart. J. Roy. Meteor. Soc.,* **117,** 993–1002.

Daley, R. and Puri, K., 1980: Four-Dimensional, Data Assimilation and the Slow Manifold. *Mon. Wea. Rev.*, **108**, 85-99.

Dando, P.,2004: Unified Model Documentation Paper version 3.0, *Met Office Fitzroy Road Exeter, Devon EX1 3PB, United Kingdom,460.*

Davies, T., Cullen, M. J. P., Malcolm, A. J., Mawson, M. H., Staniforth, A., White, A. A. and Wood, N., 2005: A new dynamical core for the Met Office's global andregional modeling of the atmosphere. *Quart. J. Roy.Meteor. Soc.,* **131**, 1759–1782.

De Coning E, 1997: Isentropic Analysis as a Forecasting Tool in South Africa. Unpublished M.Sc. Thesis, Univ. of Pretoria, S. Afr.

Done, J.M., 2002: Predictability and Representation of Convection in a Mesoscale Model,. *Phd Thesis, University of Reading.*

Dudhia 1993: A nonhydrostatic Version of the Penn State NCAR Mesoscale Model:Validation Tests and simulation of an Atlantic Cyclone and Cold Front. pp1493.

du Plessis, L. A., 2002: A review of effective flood forecasting, warning and response system for application in South Africa. *Water SA,* **28**, 129–137.

Dyson LL and van Heerden J, 2002**:** A model for the identification of tropical weather systems over South Africa. Water SA., **28**, 249-258.

Edwards, J. M., and Slingo, A., 1996: Studies with a flexible new radiation code. Part I: Choosing a configuration for a large-scale model. *Quart. J. Roy. Meteor. Soc.,* **122,** 689–719.

Engelbrecht F.A., Rautenbach C.J. deW., McGregor J.L. and Katzfey J.J. (2002). January and July climate simulations over the SADC region using the limited area model DARLAM. *Water SA,* **28**, 361–374.

Essery, R., Best, M. and Cox, P., 2001: MOSES 2.2 technical documentation. *Hadley Centre Tech Rep.*, 30, 31 pp.

Fisher, M., 2002: Assimilation Techniques (4): 4dVar. *Meteorological Training Course Lecture Series, ECWMF,* pp9.

Frank, W. M., 1993: A hybrid Parameterization with multiple closures in the representation of cumulus convection in Numerical Models. *Meteorological Monographs*. **24**, .151-154.

Gallus, W.A., 1999: Eta Simulations of three extreme precipitation vents: Sensitivity to Resolution and Convective Parameterization, *Wea. Forecasting*, **14**, 405 –426.

Gallus, W.A., 2002: Impact of Verification Grid-Box Size on Warm-Season QPF Skill Measures, *Wea. Forecasting*, **17**, 1296 -1302.

Gaudet, B. and Cotton, W.R., 1998: Statistical Characteristics of a Real-Time Precipitation Forecasting Model**,** *Wea. Forecasting,* **13**, 966-982.

Ginis, I., Richardson, R.A. and Rothstein, L.M., 1997: Design of a Multiply Nested Primitive Equation Ocean Model, *Mon. Wea. Rev.*, **126**, 1054 – 1079.

Giorgi, F. and Mearns, L.O., 1991: Introduction to special section: Regional Climate modelling revisited. *J Geophys .Res.*, **104**. 6335 -6352.

Gregory, J. H., Keyser, D. and Bosart, L .F.,1996: The Ohio Valley Wave-Merger Cyclogenesis Event of 25–26 January 1978. Part II: Diagnosis Using Quasigeostrophic Potential Vorticity Inversion, *Mon. Wea. Rev.*, **124**, 2176–2205.

Gregory, D., and Rowntree, P. R., 1990: A mass-flux convection scheme with representation of cloud ensemble characteristics and stability-dependent closure. *Mon. Wea. Rev.*, **118**, 1483–1506.

Harnack, R.P., Apffel, K., Cermak III, J. R., 1999: Heavy Precipitation Events in New Jersey: Attendant Upper-Air Conditions, *Wea. Forecasting* **14**, 933-954.

Hamill, T.M., 1999: Hypothesis Tests for Evaluating Numerical Precipitation Forecasts, *Wea. Forecasting,* **14**, 155-167.

Harris, L .M. and Durran, D.R., 2010: An Idealized Comparison of One-Way and Two-Way Grid Nesting, *Mon. Wea. Rev.*, **138**, 2174 – 2187.

Harrison, M.S.J., 1984: A generalized classification of South African rain-bearing synoptic systems, *Int. J. Climatol* , **4**, 547-560.

Holton, J.R., and Hakim, G.,J., 2012: Introduction to Dynamic Meteorology, *Academic Press.*, pp 552.

Janjić, Z.I., 1994: The Step-Mountain Eta Coordinate Model: Further Developments of the Convection, Viscous Sublayer, and Turbulence Closure Schemes. *Mon. Wea. Rev.*, **122**, 927–945.

Jankov, I., Gallus Jr, W.A., Seagul, M., Shaw, B. and Koch, S.E., 2005: The Impact of Different WRF Model Physical Parameterisation and Their Interaction on Warm Season MCS Rainfall, *Wea. Forecasting*, **20**, 1048 – 1060.

Ji, Y. and Verneker, A.D., 1996: Simulation of the Asian Summer Monsoons of 1987 and 1988 with a regional model nested in a Global GCM. *J. Climate.*, **12**, 3335-3342.

Joubert, A.M., Katzfey, J.J., McGregor, J.L. and Ngunyen, K.C., 1999: Simulating midsummer climate over southern Africa using a nested regional climate model. Journal of Geophysical research, **104**, 19015 – 19025.

Jury, R.M., 2002: The Economic Impacts of Climate Variability in South Africa and

Development of Resource Prediction Model., *J. Appl. Meteor.*, **41**., 46-55.

Kalnay, E., 2003: Atmospheric Modelling, Data Assimilation and Predictability. *Cambridge University Press, UK.*

Kendon, E.J., Jones, R.G., Kjellstrom, E. and Murphy, J., 2010: Using and Designing GCM-RCM Ensemble Regional Climate Projections. *J. Climate*, **23**, 6485-6503.

Kgatuke, M.M., Landman, W.A., Beraki, A. and Mbedzi, M.P., 2008: The internal variability of the RegCM3 over South Africa. Int. J. Climatol., **28**, 505 – 520.

Kruger, A.C., 2004: Climate of South Africa: Climate Controlls. *WS44, South African Weather Service, Pretoria, South Africa.*

Kruger, A.C., 2007: Climate of South Africa: Precipitation.*WS47, South African Weather Service, Pretoria, South Africa.*

Kruger, A.C., 2008: Climate of South Africa: Surface Temperature.*WS48, South African Weather Service, Pretoria, South Africa.*

Kruger, A.C. and Shongwe, S., 2004: Temperature Trends in South Africa: 1960 – 2003. Int. J. Climatol, **24**, 1929 – 1945.

Kruzinga, S. and Murphy, A.H., 1983: Use o an Analogue Procedure to formulate objective probabilistic temperature forecasts in the Netherlands. Mon. Wea. Rev., **111**, 2244-2254.

Landman, W.A. and Mason, S.J., 1999: Changes in the association between Indian Ocean sea-surface temperatures and summer rainfall over South Africa and Namibia. Int. J. Climatol., **19**, 1477 – 1492.

Lean, H.W., Clark, P. A., Dixon, M., Roberts, N .M., Fitch, A. Forbes ,R. and Halliwell ,C.,2008: Characteristics of High-Resolution Versions of the Met Office Unified Model for Forecasting Convection over the United Kingdom. Mon. Wea. Rev.,**136**, 3408-3424.

Leoncini,G., Pielke,R.A. and Gabriel, P. , 2008 : From Model-Based Parameterizations to Lookup Tables: An EOF Approach. *Wea. Forecasting*, **23**, 1127-1145.

Lindesay, J.A. and Jury, M.R., 1991: Atmospheric circulation controls and characteristics of a flood event in central. South Africa*. Int. J.Climatol.* **11** 609-627.

Lock, A. P., Brown, A. R., Bush, M. R., Martin, G. M., and Smith ,R. N. B., 2000: A new boundary layer mixing scheme. Part I: Scheme description and single-column model tests. Mon. Wea. Rev., **128**, 3187–3199.

Louw Limpopo Droog,al Reen dit Elders. Beeld 2004 Feb 24.

Ma, Y., Huang, X. Mills, G. A. and Parkyn, K., 2010: Verification of Mesoscale NWP Forecasts of Abrupt Cold Frontal Wind Changes. *Wea. Forecasting,* **25**, 93-112.

Malcom, A.J. and Roberts, N.M., 2005: Towards an operational 1km model. *Technical Document British Crown,United Kingdom,pp5.*

Marshall, C.H., Crawford, K.C., Mitchell, K.E. and Stenrud, D.J., 2003: The Impact of Land Surface Physics in the Operational NCEP Eta model on simulating the diurnal cycle: Evaluation and testing using Oklahoma Mesonet Data. *Wea. Forecasting*, **18**, 748 – 768.

Mason, S.J., 1998: Seasonal forecasting of South African rainfall using a non-linear discriminant analysis model. *Int. J. Climatol*, **18**, 147-164.

Mass, C., Ovens, D., Westrick, K. and Colle, B., 2002: Does increasing horizontal resolution produce better forecasts? The results of two years of real-time numerical weather prediction in the Pacific Northwest. *Bull.Amer.Meteor.Soc.,* **83**, 407-430.

Matarira, C.H. A. and Jury, M.R., 1992: Contrasting atmospheric structure during wet and dry spells in Zimbabwe. *Int. J. Climatol*, **12**, 165-171.

McGregor, J.L., 1996: Semi-Lagrangian Advection on Conformal-Cubic Grids. *Mon. Wea. Rev.*, **124**, 1311-1322.

McGregor, J.L., Wash, K.J. and Katzfey, J.J., 1993: Nested Models for Regional Climate Studies. *John Wiley and sons*, 367 – 385.

Mesinger, F., Janjic, Z. Nickovic, S., Gavrilov, D., and Deaven, D., 1988: The Step-mountain Coordinate: Model description and performance for cases of Alpine lee cyclogenesis and for a case of an Appalacian redevelopment. *Mon. Wea. Rev.*,**116**, 1493-1518.

Moeng, C.H., Sulivan, P.P., Khairoutdinov, M.F. and Randall, D.A., 2010: A mixed scheme for subgrid-scale fluxes in cloud-resolving Models. *J. Atmos Sci.*, **67**, 3692-3705.

Molinari, J., and Dudek, M., 1992: Parameterization of convective precipitation in mesoscale numerical models: A critical review. Mon. Wea. Rev, **120**, 326 – 344.

Moran, J.M. and Morgan, M.D., 1994: Meteorology: The Atmosphere and Science of Weather. *4th Ed. MacMillan Publishing Company, New York*, 517pp co.

Murphy, A.H., 1991: What is a good forecast: An Essay on the nature of Goodness in weather forecasting. *Wea. Forecasting*, **6**,281-293.

Murphy, A.H., 1992: Notes and Correspondence: Climatology Persistence, and Their Linear Combination as Standards of Reference in Skill Scores. *Wea. Forecasting*, **7**, 692-698.

Murphy, A.H., 1993: Notes and Correspondence: On Summary Measures of Skill in rare event forecasting based on contingency tables. *Wea. Forecasting, **8**,* 400-402.

Murphy, J., 1999: An Evaluation of Statistical and Dynamical Techniques for Downscaling Local Climate. J. Climate., **12**, 2256 – 2284.

Nurmi, V.P. A., Nurmi, P., Seitz, D., Michaelides, S., Athanasatos, S., and Papadakis, M. ,2012: Economic value of weather forecasts on transportation – Impacts of weather forecast quality developments to the economic effects of severe weather. *EWENT report D5.2* .

Orlanski, I. and Katzfey J. J., 1987: Sensitivity of Model Simulations for a coastal cyclone. *Mon. Wea. Rev.*, **115**, 2792-2821.

Park, S. K. and Zupanski, D., 2003: Four-dimensional variational data assimilation for mesoscale and storm-scale applications. *Meteorology and Atmospheric Physics*, **82**, 173 -208.

Pielke, R.A., 1976: Foreword: *Mon. Wea. Rev.*, ***104,*** 1465-1465.

Ploshay, J.J. and Lau, N., 2010: Simulation of the Diurnal cycle in Tropical Rainfall and Circulation during Boreal Summer with a High-Resolution GCM. *Mon. Wea. Rev.*, **138,** 3434-3453.

Qian, J.H., Giorgi, I.F. and Fox-Roobinovitz, M., 1999: Regional Stretched Grid Generation and its application to the NCAR RegCM. J. *Geophys. Res.* **104**.

Reason, C.J.C., Keibel, A., 2004: Tropical Cyclone Eline and Its Unusual Penetration and Impacts over the Southern African Mainland. *Wea. Forecasting*, **19**, 789–805.

Rife, D.L. and Davis, C. A., 2005: Verification of Temporal Variations in Mesoscale Numerical Wind Forecasts, *Mon. Wea. Re*v., **133**, 3368-3381.

Riphagen, H. A., Bruyere, C. L. ,Jordaan, W., Poolman, E.R. and Gertenbach, J., 2002 : Experiments with the NCEP Regional Eta Model at the South African Weather Bureau, with Emphasis on Terrain Representation and Its Effect on Precipitation Predictions, *Mon. Wea. Rev.*, **130**, 1246-1263.

Richter N and Taljaard J. “Stormreen ruk Suid-Kaap”. Die Burger 2004 Dec 23.

Robertson, A.W., Lali, U., Zebaik, S.E. and Goddard, L., 2004: Improved Combination of

Multiple Atmospheric GCM Ensembles of Seasonal Prediction. *Mon. Wea. Rev.*, **132**, 2732-2744.

Roeber, P.J., Schultze, D.M., Colle, B.A. and Stenrud, D.J., 2004: Toward Improved Prediction: High Resolution and Ensenmble Modelling System in Operation. *Wea. Forecasting,* **19**, 936 – 944.

Sapa. "Residents Flee as Rising Waters Wash Away Homes". Pretoria News 2003 Nov 28.

Sapa. "Ravaging Floods". Sowetan 2006 Nov 15.

Scaife, A.A., Butchart, N., Warner, C. D. and Swinbank, R., 2002: Impact of a Spectral Gravity Wave Parameterization on the Stratosphere in the Met Office Unified Model. *J. Atmos Sci,* **59**, 1473-1489.

Schmidli, J. B., Chow, F.K., de Wekker, S.F.J., Doyle, J., Grubisic, V., Holt, T., Jiang, Q., Lundquist, K.A., Sherridan, P., Vosper, S., Whiteman, C.D., Wyszogrodzki, A.A. and Zangl, G., 2011: Intercomparison of Mesoscale Model Simulations of the Daytime Valley Wind System. *Mon. Wea. Rev.*, **139**, 1389–1409.

Schulze, B.R., 1965: Climate of South Africa-Part 8: *General Survey. WB 28, Republic of South Africa*, 330 pp.

Schulze, G.C., 2007: Atmospheric Observations and Numerical Weather Prediction. *S A Journal of Science*, **103**, 318-322.

Schulze, R.E., 1997: South African atlas of Agrohydrology and Climatology, Report TT82/96, 273 Pretoria Water Research Commission.

Schulze, R.E. and Maharaj, M., 2007: Rainfall Seasonality. In: Schulze RE (Ed) 2007, South African atlas of Climatology and Agrohydrology .WRC Pretoria, RSA, Report 1489/1/06.

Schulze, R.E., Maharaj, M., Warburton, M.L., Gers, C.J., Horan, M.J.C., Kuns, R.P. and Clark, D.J., 2008: South African atlas of Climatology and Agrohydrology. WRC Pretoria, RSA, Report 1489/1/08.

Seaman, N.L., Stauffer, D.R. and Lario-Gibbs, A.M., 1995: A Multi-scale Four-Dimensional Data Assimilation System Applied in the San Joaquin Valley during SARMAP. Part I: Modeling Design and Basic Performance Characteristics. *J.Appl. Meteor.*, **34**, 1739-1761.

Seth, A., and Giorgi, P., 1998: The Effects of Domain Choice on Summer Precipitation Simulation and Sensitivity in a Regional Climate Model, *J. Climate, 11***,** 2698-2712.

Skamarock, W.C., 2004: Evaluating Mesoscale NWP Models using Energy Spectra, *Mon. Wea. Rev*, **132**, 3019-3032.

Snook, J. and Pielke, R.A., 1995: Diagnosing a Colorado Heavy Snow Event with a Non-hydrostatic Mesoscale Numerical Model Structured for Operational Use, *Wea. Forecasting*, **10**, 261-285.

South African Weather Service, 2006: *Annual Report 2005/06.* Pretoria.

South African Weather Service, 2011: *Annual Report 2010/11.* Pretoria.

Stanski, H.R., Wilson, L.J. and Burrows, W.R., 1989: Survey of Common Verification Methods in Meteorology. *World Weather Watch Technical Report*, **8**,WMO.geneva.

Stauffer, D.R. and Seaman, N.L., 1994: Multi-scale Four-Dimensional Data Assimilation. *J.Appl. Meteor, **33**,* 416-434.

Stauffer, D.R., Seaman, N.L. and Binkowski, F.S., 1991: Use of Four-Dimensional Data Assimilation in a Limited-Area Mesoscale Model Part II: Effects of Data Assimilation within the Planetary Boundary Layer. *Mon. Wea. Rev*., **119**, 734-754.

Stein, U. and Alpert, P., 1993: Factor Separation in Numerical Simulations**.** *J. Atmos Sci.,* **50**, 2107-2115.

Stenrud, D.J., 2007: Parameterisation Schemes: Keys to Understanding Numerical Weather Prediction Models. *Cambridge University Press*. 459pp.

Strydom I and Arendse A. "Death in the Cape of Storms". Pretoria News 2001 Jul 9.

Su, H., Shuyi, S. C. and Bretherton, C.S., 1999: Three-Dimensional Week-Long Simulations of TOGA COARE Convective Systems Using the MM5 Mesoscale Model. *J. Atmos. Sci*. , **56**, 2326-2344.

Taljaard, J.J., 1994: Atmospheric Circulation Systems, Synoptic Climatology and Weather Phenomena of South Africa. Part 1: Controls of the weather and climate of South Africa. *Tech. Pap.* **27**, SA Weather Service , Pretoria, 45pp.

Taljaard, J.J., 1996: Atmospheric Circulation Systems, Synoptic Climatology and Weather Phenomena of South Africa. Part 5: Temperature phenomena in South Africa. *Tech Pap.* **31**, SA Weather Service , Pretoria 53pp.

Teixeira, M.S. and Satyamurty, P., 2007: Dynamical and Synoptic Characteristics of Heavy Rainfall Episodes in Southern Brazil**.** *Mon. Wea. Rev*., **135**, 598-617.

Tennant, W., 2008: Experience with UM/VAR at the South African Weather Service. *Preprints 4th WMO Workshop on the Impact of Various Observing Systems on Numerical Weather Prediction 19-21 May 2008, WMO, Geneva, Switzerland.*

Thiel G and Gosling M. "Rain and wind lash Cape Communities". The Star 2003 Mar 25.

Tustison, B., Harris, D. and Foufoula-Georgiou, E., 2001: Scale issues in verification of precipitation forecasts. *J. Geophys. Res.,* **106,** 11775–11784.

Tyson, P.D. and Preston-Whyte RA, 2000: The Weather and Climate of Southern Africa. *Oxford University Press*. Cape Town South Africa.

Von Lieres V. "Fruit Growers Expect Minimal Flood Damage". Business Report 2003 Mar 26.

Wang, W. and Seaman, N. L., 1997: A Comparison Study of Convective Parameterization Schemes in a Mesoscale Model. *Mon. Wea. Rev.*, **125**, 252-278.

Warner, C.D., Scaife, A.A. and Butchart, N., 2005: Filtering of Parameterized Nonorographic Gravity Waves in the Met Office Unified Model. *J. Atmos Sci.,* **62**, 1831-1848.

Warner, T.T., 2011: Quality Assurance in Atmospheric Modeling. *Bull. Amer. Meteor. Soc.*, ***92***, 1601-1610.

Warner, T.T., Peterson, R.A. and Treadon, R.E., 1997: A Tutorial on Lateral Boundary Conditions as a Basic and Potentially Serious Limitation to Regional Numerical Weather Prediction. *Bull. Amer. Meteor. Soc.*, **78**, 2599-2617.

White, A. A., and Bromley, R. A., 1995: Dynamically consistent, quasi-hydrostatic equations for global models with a complete representation of the Coriolis force. *Quart. J. Roy. Meteor. Soc.,* **121**, 399–418.

Williams, K.D., and Brooks, M.E., 2008: Initial Tendencies of Cloud Regimes in the Met Office Unified Model. *J. Climate.,* **21**,833-840.

Wilson, D. R., and Ballard, S. P., 1999: A micro-physically based precipitation scheme for the UK Meteorological Office Unified Model. Quart. J. Roy. Meteor. Soc., **125**, 1607–1636.

WMO, 2000: Guidelines on Performance Assessment of Public Weather Services*. TD No 1023.*

Wu, X. Liang, X. and Park, S., 2007: Cloud-Resolving Model Simulations over the ARM SGP. *Mon. Wea. Rev.*, **135***, 2841-2855.*

Younger, P.M., Gadian, A.M. and Beven, K.J., 2006: High resolution modeling of the conditions over the Brue catchment using the UK Met Office Unified Model. *European GeoSciences* U*nion* , **8**.

Yussouf, N. and Stenrud, D.J., 2010: Impact of Phased-Array Radar Observations over a Short Assimilation Period: Observing System Simulation Experiments Using an Ensemble Kalman Filter. *Mon. Wea. Rev.*, **138,** 517- 538.

Zavala, V.M., Constantinescu, E. M. and Anitescu, M., 2009: Economic Impacts of Advanced Weather Forecasting in Energy System Operations, *National Science Foundation, Pennslavia State University* .